Republic of Iraq
Ministry of Higher Education and Scientific Research
University of Babylon
College of Science for Women
Department of Chemistry

Removal of orange G dye using prepared GO/ZnO nanocomposite as a photo catalyst under solar light Irradiation

A Thesis

Submitted to the Council of the College of Science for Women, University of Babylon in Partial Fulfillment of the Requirements for the Degree of Master of Science in Chemistry

By

Hiba Razaq Kazem Alwan

B.Sc. Babylon University 2019

Supervised

Assist.Prof. Dr. Hazim Yahya Al-gubury

2022 A.D **1444 A.H**

بسم الله الرحمن الرحيم

﴿ يَا أَيُّهَا الَّذِينَ آمَنُوا إِذَا قِيلَ لَكُمْ تَفَسَّحُوا فِي الْمَجَالِسِ فَافْسَحُوا يَفْسَحِ اللَّهُ لَكُمْ ۖ وَإِذَا قِيلَ انشُزُوا فَانشُزُوا يَرْفَعِ اللَّهُ الَّذِينَ آمَنُوا مِنكُمْ وَالَّذِينَ أُوتُوا الْعِلْمَ دَرَجَاتٍ ۚ وَاللَّهُ بِمَا تَعْمَلُونَ خَبِيرٌ ﴾

صدق الله العلي العظيم

سورة المجادلة : الآية «11 »

Supervisor's Certification

I, certify that this research entitled **"Removal of orange G dye using prepared GO/ZnO nanocomposite as a photo catalyst under solar light Irradiation "** was prepared by **"Hiba Razaq Kazem "** under my supervision at the Department of Chemistry/ College of Science for women /University of Babylon as a partial fulfillment of the requirements for the Degree of Master in Science / Chemistry.

Signature:

Name: Dr. Hazim Yahya Mohammed Ali

Scientific Degree: Assistant Professor

Address: University of Babylon / College of Science for women /Department of Chemistry

Date: / 8 / 2022

Recommendation of Head of Chemistry Department

According to the available recommendation , I forward this thesis for Discussion

Signature of Chemistry Department

Name: Dr. Hazim Yahya Mohammed Ali

Scientific Degree : Assistant Professor

Address : Head of Chemistry Department

University of Babylon / College of Science for Woman

Date: / 8 / 2022

Certification of the Examining Committee

We certify that we have read this thesis entitled " **Removal of orange G dye using prepared GO/ZnO nanocomposite as a photo catalyst under solar light Irradiation** " And as examining committee examined the Master student " **Hiba Razaq Kazem** " in its content, we find that it is adequate to award her degree of Master in Chemistry with degree (Excellence).

Committee Chairman
Signature:
Name: Dr. Ayad F. Alkaim
Scientific order: Prof.
Address: University of Babylon/ College of Science for women / Chemistry department
Date: / /2022

Committee Member
Signature:
Name: Dr. Alaa K Hashim Al-Khalaf
Scientific order: Prof.
Address: University of Al-Qasim Green/ College of Environmental of Sciences
Date: / / 2022

Committee Member
Signature:
Name: Dr. Asmaa Hashim Hammadi
Scientific order: Asst. Prof.
Address: University of Babylon/ College of pharmacy
Date: / / 2022

Committee Member (Supervisor)
Signature:
Name : Dr. Hazim Yahya Mohammed Ali
Scientific order: Asst. Prof.
Address: University of Babylon/ College of Science for women / Chemistry department
Date: / / 2022

Date of Examination : /8/2022
Deanship Authentication of college of Science for Women
Approved for the College committee of graduate studies

Committee Member
Signature:
Name: Dr. Abeer Fauzi Murad
Scientific order: Prof. Dr
Address: Babylon University / College of science for women
Date: / / 2022

University of Babylon
College of Science for Girls

Dedication

To the greatest Prophet Mohammad (may Allah bless him and grant him peace).

To my family …

To my friends …

To everyone who supports me and encourages me even with a smile

Acknowledgements

Praise be to Allah, and praise be to Allah for His blessings and countless gifts, through which the paths of life shine forth through His grace.

I extend my sincere thanks, appreciation and gratitude to my supervisor, Dr. Hazim Yahya Al-gubury, for the advice, directions and continuous moral support to complete this work. Thank you from the heart.

Sincere thanks are due to the Prof . Dr . Ayad Alkaim , Dr . Sadiq A. karim , Dr. Ali talib for their help in this work .

All thanks to the professors of the Department of Chemistry.

All thanks to my family, friends and colleagues for the support and encouragement.

Hiba

Summary

This work contains two major parts:

The first part include preparation of graphene oxide (GO) by modified hummer method , preparation zinc oxide (ZnO) nanopartical by sol-gel method and preparation of GO/ZnO nanocomposite by sonocatalysis method. Study the characteristic of nanocomposite using various techniques such as X-ray diffraction (XRD) , Fourier transform infrared (FTIR) , Energy dispersive X-ray spectroscopy (EDX) , Scanning electron microscopy (SEM) , Specific surface area (BET) and Thermo gravimetric analysis (TGA) . The particle size of synthesized GO/ZnO nanocomposite was calculate using scherer equation (23.769nm) .

The second part include study of photo catalytic activity of prepared nanocomposite, by using orange G dye. The rate of photocatalytic degradation process is affected by different parameters such as initial concentration of dye, effect of mass of catalyst , initial pH of solution, effect of temperature , effect of light intensity , effect of CH_3OH and H_2O_2 . All experiments was performed under optimum condition from (0.15 g / 100 mL) of GO/ZnO nanocomposite, (10mL/min) air flow rate . The best removal percentage of orange G dye (97.33%) . The effect of dye concentration has been studied the optimum value of orange G dye (10mg/L) dye . The light intensity 9mW/cm^2. pH=8.74, temperature 25°C and at laboratory conditions for orange G dye. Activation energy for the photo degradation process was calculated using arrhenius equation .they were equal to (35.35 KJ/mol) .Enthalpy and entropy of activation and free energy of activation can be estimated according to eyring equation . Thermodynamic parameters (ΔH, ΔS) for orange G dye were calculated (32.88 kJ/mol and - 0.164 kJ/mol.k)

respectively, from the results the reaction is endothermic with low randomness. ΔG (81.75 kJ/mol) was calculated and the reaction is non-spontaneous.

Contents

Table of Contents

Chapter One : Introdution

Contents

Chapter two: Experimental Part

Contents

Contents

Contents

Chapter Three: Results and Discussion

Contents

List of Tables

Chapter two: Experimental Part

Contents

Chapter Three: Results and Discussion

Contents

List of Figures

Chapter One: Introduction

Contents

Chapter Two: Experimental Part

Chapter Three: Results and Discussion

Contents

Contents

Contents

Contents

Directory of Abbreviations

Abbreviation	Description
Å	Angstrom
Atm	Atmosphere
Abs	Absorbance
BET	Brauner Emeet Teller
C	Concentration
cal	Calculated
CB	Conduction band
$^{\circ}C$	Centigrade
cm	Centimeter
Comm.	Commercial
CVD	Chemical Vapor Deposition
DI-H_2O	Deionized water
D.W	Distal water
Eg	Energy gap
e^-_{CB}	Negative electron conduction band
Etc	et cetera
Exp	Experimental
Eq	Equation
SEM	Scanning Electron Microscopy
FTIR	Fourier Transform Infrared Spectroscopy
G	Gram
h^+_{VB}	Positive hole valance band
K	Kelvin
log	logarithm
mA	Milliampere

Contents

Mg	Milligram
Min	Minute
mL	Milliliter
MPa.	Mega pascal
mW	Milliwatt
Nm	Nanometer
NMs	Nanomaterial
NPs	Nanoparticles
PPM	Part per million
Pre.	Prepard
PVS	physical vapor synthesis
T	Temperature
t	Time
UV	Ultraviolet
UV–vis	Ultraviolet–visible
V	Volume
VB	Valance band
W	Weight
XRD	X-ray diffraction
ZnO NPs	Zinc Oxide Nanoparticles
hν	The photon energy
λ	Wavelength
α	Alfa
k	Adsorption rate constant
θ	Bragg's angle of the peak
β	Full width at half- maximum intensity of the diffraction peaks
ω	Frequency
e^-/ h^+ pair	Electron- hole pair
D	Average crystal size
PDE	Photo degrade efficient
AOPS	Advance oxidation processes
Fcc	Face centred cubic
Hcp	Hexagonal closed pack
ROS	Reactive oxygen species

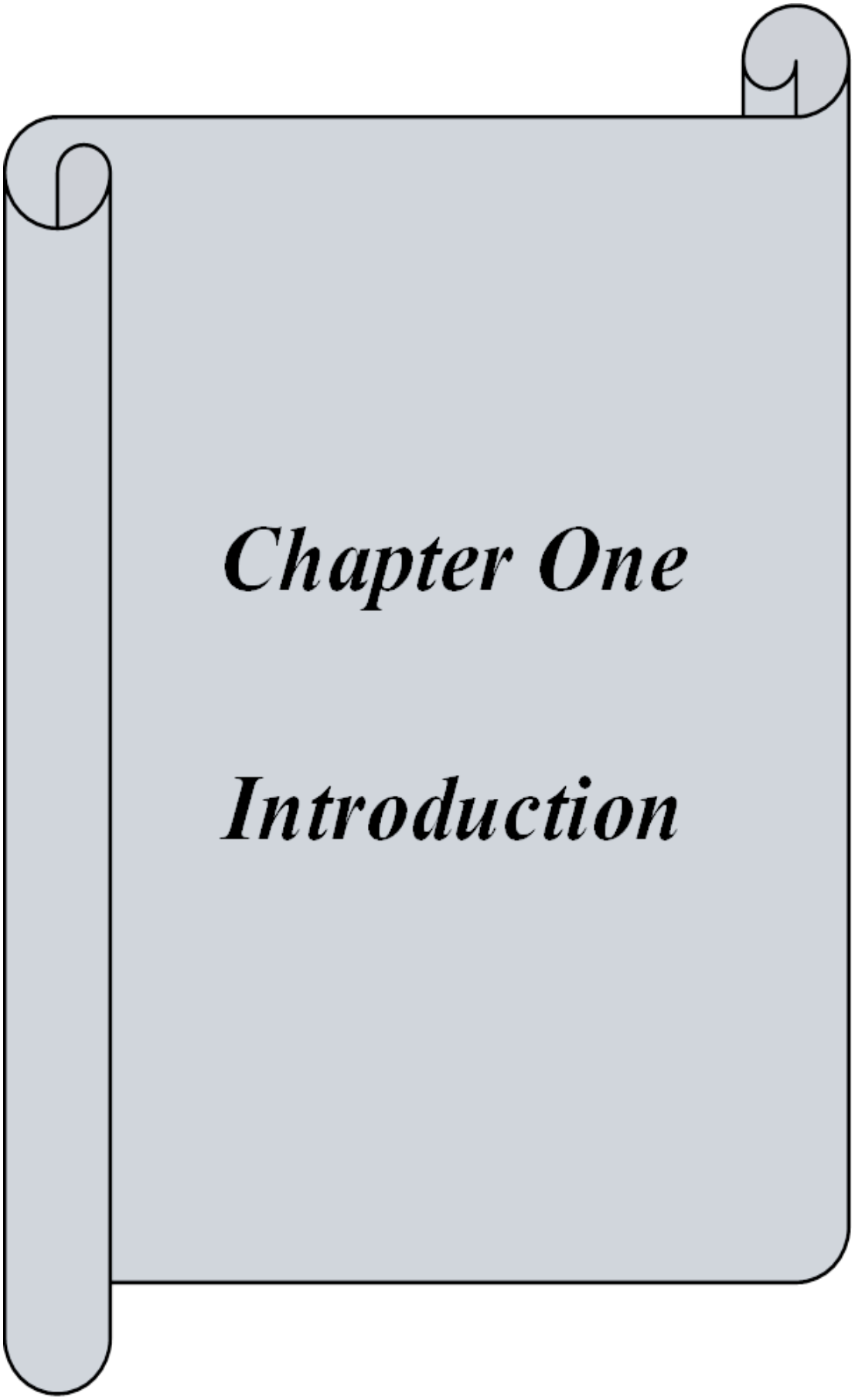
Chapter One
Introduction

1- Introduction

1-1 General Introduction

The discharge of colored effluent into streams not only alters their natural aesthetic, but also interferes with the transmission of sunlight into streams, reducing photosynthesis. Wastes from the dye industry, the pulp textile industry, and the paper sector are all highly colored. The presence of even trace amounts of dyes in water reduces light penetration through the water surface, preventing photosynthesis by aquatic plants. Various dyes are teratogenic, carcinogenic, mutagenic, and poisonous to humans, microorganisms, and various fish species. As a result, the removal of water wastes is crucial for the environment (Aljeboree et al., 2020).The removal and decrease of pollutants such as heavy metals (HM), toxic organic dyes and solvents, pesticides, and the separation of oil or other toxic pollutants from water are all examples of environmental remediation employing biopolymers (Almutairi et al., 2021).

1-2 Nanotechnology

The principles in "nano-technology" were first used in a discussion delivered by physics professor Richard Feynman at an American Physical Society meeting at Caltech on December 29, 1959, even before the phrase was in the lexicon. This presentation was the catalyst for the development of nanotechnology as a field of study.Albert R. Hibbs suggested to Feynman that his micromachines may be used in medicine. Professor Norio Taniguchi of Tokyo Science University coined the term"nanotechnology" in a 1974 study. In the late 1970s and 1980s, Eric Drexler promoted molecular nanotechnology's promise. In 1981, scanning tunneling microscopy was developed. Engines of Creation (Eric

Drexler), the first book about nanotechnology, was released in 1986. (Adya et al., 2020).Nanotechnology and nanoscience refers to the improvement, advancement or application of atomic/molecular structures with at least one dimension that is in the nanoscale range (1~100 nm) with variable composition, hape/morphology, size, or surface properties (Nasrollahzadeh et al., 2020). A nanomaterial is defined as a material with at least one exterior dimension at the nanoscale, according to the International Organization for Standardization. Nanoparticles can be classed based on their shape or chemical composition, in addition to their tiny size. Carbon-based nanomaterials come in a variety of shapes and sizes, depending on their chemical makeup. (Rhazouani et al., 2021).

1-2-1 Synthesizes of nanoparticles

For the preparation of metallic nanoparticles, many methods are used, which are divided into two categories: bottom up methods and top down approaches.

1- Top-down : the destructive technique is used in this procedure. Starting with a bigger molecule, it is divided into smaller units, which are subsequently turned into appropriate NPs. Grinding/milling, chemical vapor deposition (CVD), physical vapor deposition (PVD), and other decomposition processes are examples of this technology (Khan et al., 2019).

2- Bottom-up: the approach to nanoparticle synthesis is based on the production of nanoparticles from smaller molecules, such as the combining of atoms, molecules, or tiny particles. In this approach, the nanoparticles' nanostructured building components are first created, then combined to make the finished nanoparticle.

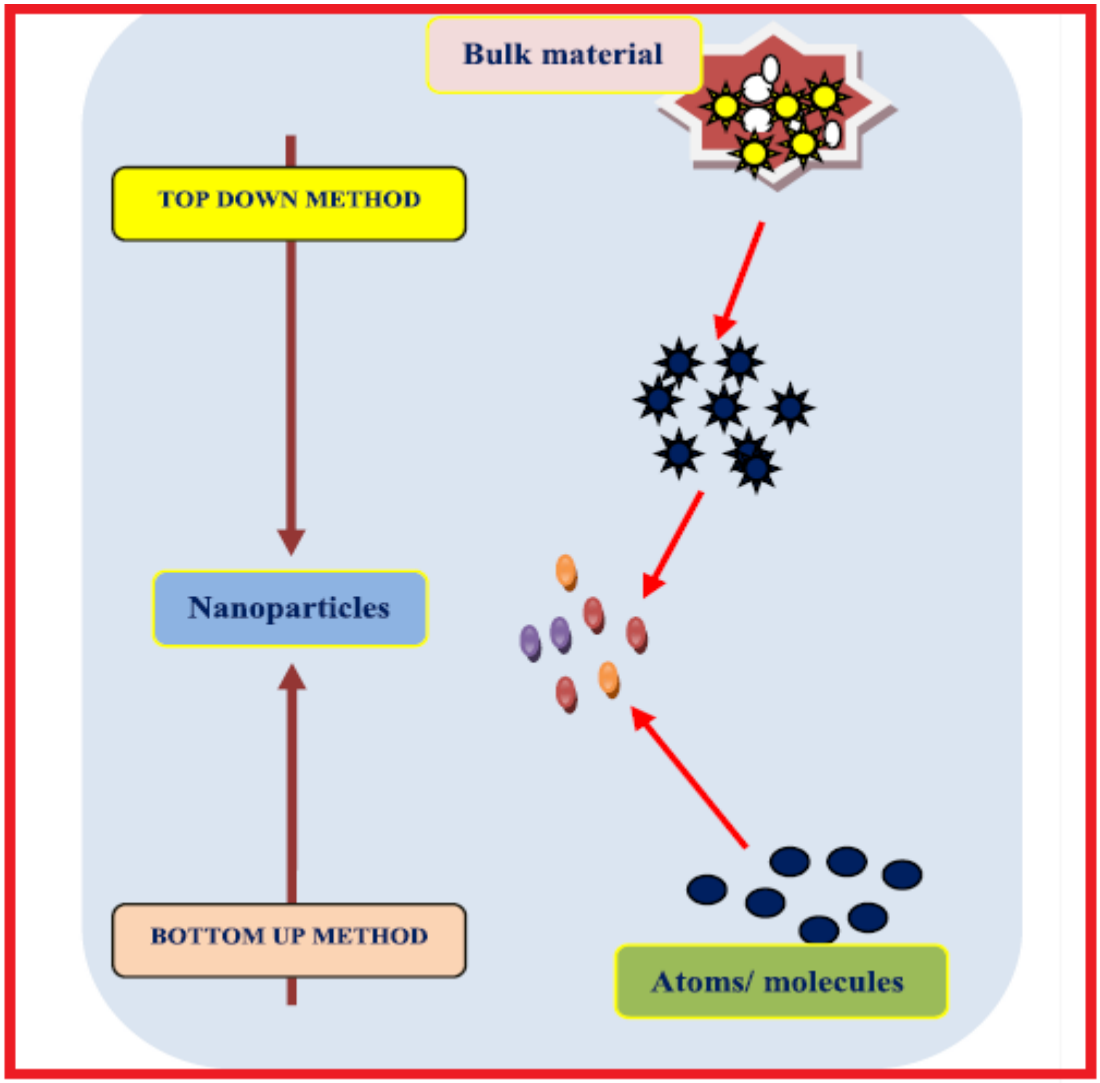

Fig.(1-1) : An overview of top down and bottom up method (Jamkhande et al ., 2019).

1-2-2 Application of nanotechnology

1- Water Treatment.

2- Food Additives (Niculescu et al., 2022).

3- Applications in Drugs and Medications.

4- Application in Energy.

5- Application in Agriculture.

6- Diagnostic Application of nanoparticle (Jadhav et al., 2021).

1-2-3 Classification of Nanomaterials

nanomaterial classification based on their dimensionality

1-2-3-1 Zero-dimensional nanomaterials

All three dimensions of these materials are nanoscale size (i.e., less than 100 nm). Graphene quantum dots, carbon quantum dots, fullerenes, inorganic quantum dots, magnetic nanoparticles, and noble metals are only a few examples (Wang et al., 2020).

1-2-3-2 One-dimensional Nanostructures

a scale smaller than 100nm, nanomaterials have two exterior dimensions. The micrometer (Lz > 100nm) is the last dimension. Nanotubes, nanofibers, and nanowires belong to this group (Erol et al., 2018).

1-2-3-3 Two-dimensional Nanostructures

These materials have two dimensions of >100 nm each. They have plate-like structures and thin layers of at least one atomic layer thickness. Graphene, graphene oxide, and reduced graphene oxide, layered double hydroxides, transitionmetal dichalcogenides, transitionmetal oxides, black phosphorus, graphitic carbon nitride, hexagonal boron nitride, antimonite, boron nanosheets, and tin telluride nanosheets (Li et al., 2022).

1-2-3-4 Three-dimensional Nanostructures

These structures, such as nanocomposite, which consists of many phases on the premise that one of the solid phases is transitioning to the nanoscale, reveal nanoscale properties as a consequence of their internal nanoscale dimensions but have no exterior dimension in the nanoscale (Lee et al., 2018).

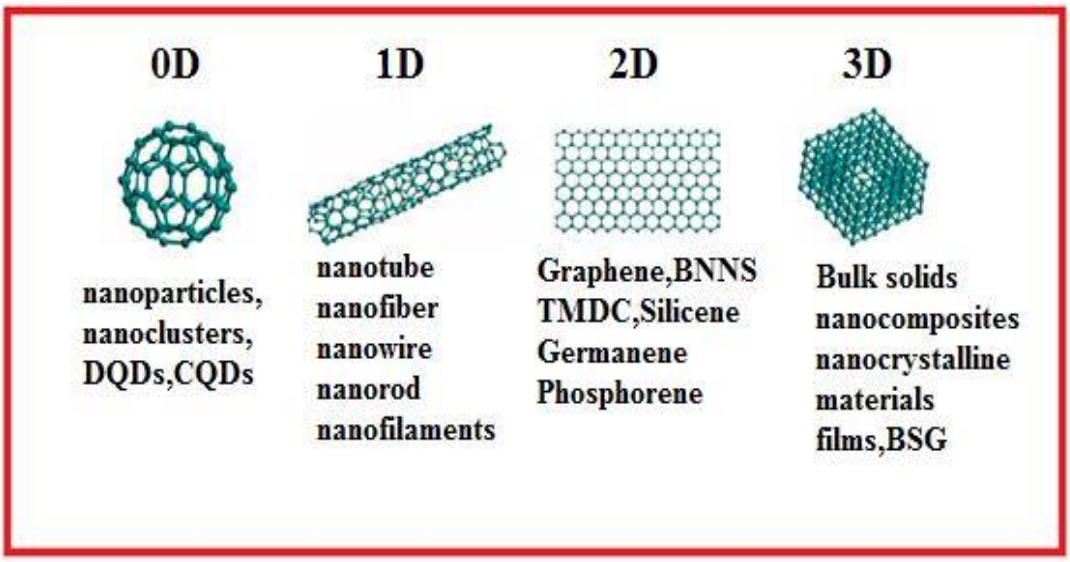

Fig .(1-2) : Classification of nanomaterials depending on the dimensions (Barhoum et al., 2022).

1-3 ZnO nanopartical

Zinc oxide (molecular formula ZnO) is widely regarded as one of the most widely used inorganic nanomaterials. It's a white powder that's almost insoluble in water (Paul et al., 2019). Many enzymes, including as carbonic anhydrase, carboxypeptidase, and alcohol dehydrogenase, become inactive without zinc, but cadmium and mercury, both members

of the same group of elements, are toxic. It was also taken into account the toxicity of nanoparticles that produce damaging ions. Zinc oxide reacts with acids and alkalis to form Zn^{2+} ions because it is amphoteric.

$$\mathbf{ZnO + 2HCl \rightarrow ZnCl_2 + H_2O} \quad \textbf{(1-1)}$$

$$\mathbf{ZnO + 2NaOH \rightarrow Na_2ZnO_2 + H_2O} \quad \textbf{(1-2)}$$

$$\mathbf{ZnCl_2 \rightarrow Zn^{2+} + 2Cl^-} \quad \textbf{(1-3)}$$

(Siddiqi et al., 2018). In humans, zinc is required for the activity of enzymes.We have about (2-3 g) of zinc in our bodies, with a daily requirement of (10-15 mg) . Zinc oxide nanoparticles are used as a dietary supplement because they are easily absorbed by the body due to their small particle size. Zinc has been found to have an impact on a number of physiological processes (Darshita et al., 2021).

1-3-1 Crystal Structures of ZnO

Zinc oxide (ZnO) is an II-VI semiconductor with a broad direct band gap of 3.37 eV and a significant exciton binding energy of around 60 meV at 300 K. (i.e. in the near-UV range). The figures for ZnO band gap energy provided in literatures are not always the same due to the existence of various degrees of oxygen vacancies in the ZnO samples. ZnO can crystallize in three different forms depending on the conditions: hexagonal wurtzite, cubic zinc blende, and rock-salt structure.

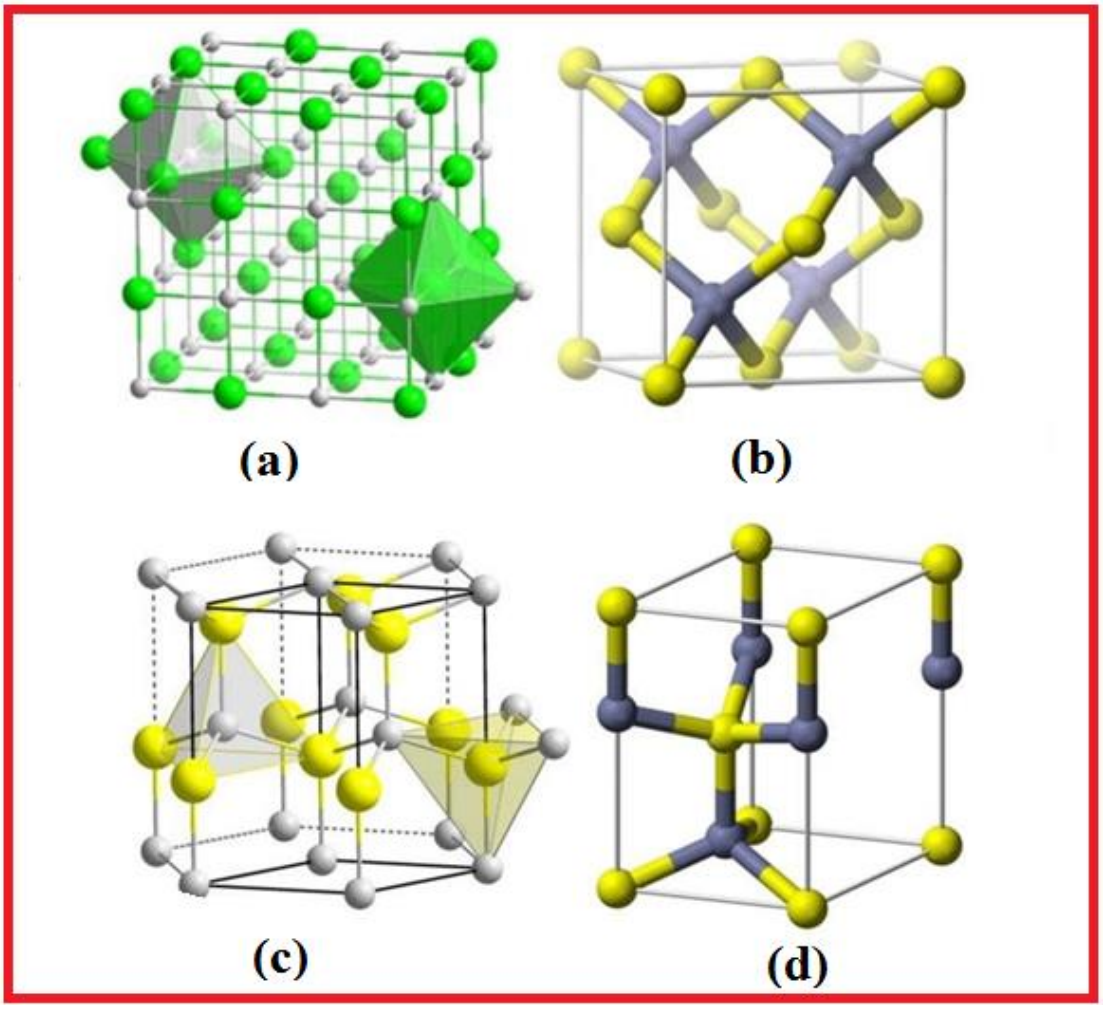

Fig.(1-3) : Stick and ball representation of ZnO crystal structures: (a) the rock-salt structure; (b) the cubic zinc blende unit cell ; (c) the wurtzite structure ; (d) the wurtzite structure unit cell.

The hexagonal wurtzite structure of ZnO is the most thermodynamically stable and, as a result, the most common of the three. Under normal conditions, ZnO preferentially crystallizes as wurtzite. The ions in the wurtzite structure are tetrahedrally coordinated, much like in the zinc blende structure (Figure 1-3 (b)), however instead of the fcc-type lattice in the zinc blende structure, each type of ions forms a separate hexagonal closed pack (hcp)-type lattice (Zhou et al., 2017).

1-3-2 Applications of zinc oxide nanoparticles

The uses of ZnO have changed significantly over time. ZnO also has many specialized applications, the most important of which are

1-3-2-1 Ceramics and concrete :

Ceramics, particularly the tile sector, is the second major application of ZnO. The French and American ZnO processes are both suitable. ZnO has a high heat capacity, thermal conductivity, and temperature stability, as well as a low coefficient of expansion, which are all desired features in the manufacture of ceramics.

1-3-2-2 Pigments and coatings :

Zinc Oxide (ZnO) is an essential white inorganic pigment in niche applications, although being mostly replaced by TiO_2. Zinc oxide pigments are referred to as 'zinc white,' 'Chinese white,' or 'zinc flowers,' with the phrase 'zinc white' now reserved for ZnO pigment manufactured using the French technique. The pigment is available in two forms: dry and oil paste (Moezzi et al., 2012).

1-3-2-3 Medical applications :

Zinc Oxide structure are used in a wide variety of medicinal and biological applications. Mirzaei and Darroudi gave an outstanding presentation on green ZnOS synthesis and biological applications. They offered a full description of the green polymers, plants, and bacteria used in ZnOS synthesis, as well as an explanation of how ZnOSs are used in anti-cancer therapies.

1-3-2-4 Sensing applications :

Because of their excellent binding ability with biomolecules, enhanced electrochemical potential, and sensing features, ZnOSs are considered an excellent candidate for the fabrication of biosensors, electrochemical sensors, and gas sensors in their various nano dimensions, i.e. nanoparticles, nanorods, nanosheets, nanolayers, etc. (Noman et al., 2022).

1-3-2-5 The Textile Industry :

Commercialization of nanotechnological goods has a lot of potential in the textile industry. Water repellent and self-cleaning textiles, in particular, hold a lot of promise for military applications when there isn't much time for laundry under harsh conditions. Self-cleaning and water resistant textiles are also very useful in the business environment for preventing unwanted stains on garments. Another key issue to consider is protecting the body from the harmful UV rays of the sun.

1-3-2-6 Photocatalysis :

In recent years, there has been a lot of research on photocatalysis. By using oxidation or reduction reactions on the catalyst's surface, an electron-hole pair is created below the intensity of light in this process. An organic pollutant can be oxidized directly by a photogenerated hole or indirectly by a reaction with distinctive reactive groups (ROS), such as the hydroxyl radical OH, created in solution, in the presence of a photocatalyst (Kołodziejczak-Radzimska et al., 2014).

1-4 Graphene Oxide

Graphene is a one-atom thick hexagonal carbon lattice with a vast surface area, great thermal and electrical conductivity, and mechanical strength.Because pure graphene has no imperfections, it has a low chemical reactivity and is inert in organic solvents. Fabrication of graphene at high temperatures, on the other hand, produces imperfections but degrades its structure. These structural flaws, on the other hand, serve as active locations for electron transport and, as a result, stimulate electrostatic interactions (Shahriari et al., 2021). When graphite is oxidized in protonated fluids, graphite oxide is formed, which is made up of many stacked layers of graphene oxide (GO). GO has a hexagonal carbon structure similar to graphene, but it also contains oxygen-based functional groups such as hydroxyl (OH), alkoxy (C–O–C), carbonyl (C=O), carboxylic acid (COOH), and others. Apart from the simplicity of production, these oxygenated groups have a number of advantages over graphene, including increased solubility and the ability to surface functionalize, both of which have opened up new possibilities for application in nanocomposite materials. (Smith et al., 2019) . Because of its unique and excellent qualities, graphene oxide (GO) is currently an emerging novel substance in the world of science and technology. Due to its unusual two-dimensional lamellar structure and large surface area, as well as full surface accessibility and edge reactivity, the water-soluble derivative of graphene oxide is highly valued and continues to be extensively explored by scientists all over the world (Kamakshi et al.,2018).

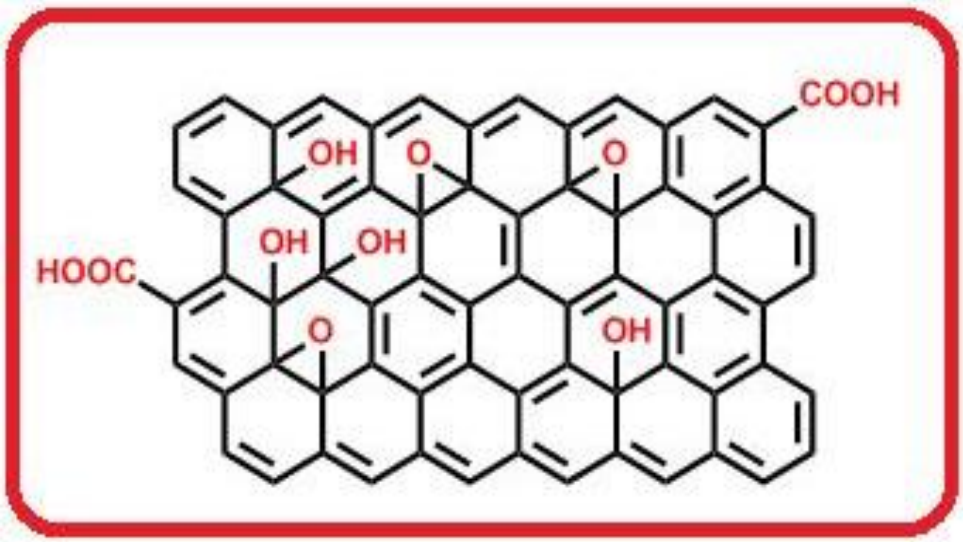

Fig.(1-4) : The schematic structure of graphite oxide (GO) (Song et al., 2014).

1-5 Dyes

Due to the large amounts of water needed in dyeing processes, the textile sector is one of the largest producers of liquid effluent pollutants. Furthermore, the different effluent properties in terms of pH, dissolved oxygen, organic and inorganic chemical content are determined by the different processing stages and types of synthetic dyes used during this conversion(Saratale et al., 2011). Textile dyes are one of the most common kinds of organic compounds that are causing water contamination. Azole dyes make up the majority of the dyes now on the market, with anthraquinone dyes following in second.UV and visible light irradiation have no effect on them. They are also resistant to aerobic degradation and can be transformed to carcinogenic aromatic amines in anaerobic or in vivo settings (Madhavan et al ., 2010). Azo dyes are the most common synthetic colorants used in everyday life, particularly in textile processing. Azo dyes are distinguished by the presence of one or more azo bonds (–N=N–) in combination with aromatic systems and

auxochromes (–OH, $–SO_3$, and so on). Poisonous, mutagenic, carcinogenic, and non-biodegradable textile effluents have been discovered, posing a public health danger. Traditional methods for eliminating azo dyes from the aquatic environment include physical, chemical, and biological processes such as adsorption, coagulation, photo-catalysis, ozonation, and biosorption. However, these tried-and-true procedures have proven to be costly, time-consuming, and ineffective (Cai et al., 2016). Azo dye compounds have a wide range of applications in the industry, including photodynamic therapy, photosensitivity, and biological activity due to their use in anti-inflammatory, antibacterial, and antifungal treatments (Karim et al., 2019).

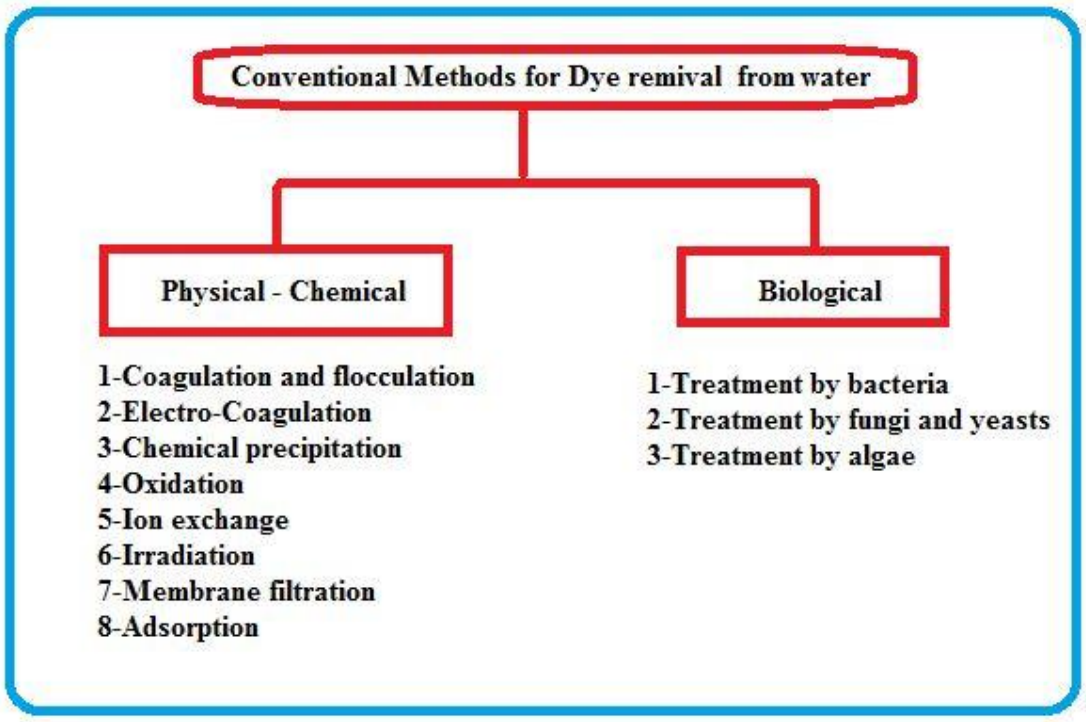

Fig.(1-5): Treatment methods for the removal of dyes from wastewater effluent (Saratale et al., 2011).

1-5-1 Classification of dyes

There were just a few natural dyes available prior to the invention of synthetic colors. Since the annual global output of dyes has increased, the classification of dyes has become necessary. At several tens of millions of tonnes, they are thought to exist (Benkhaya et al., 2020).

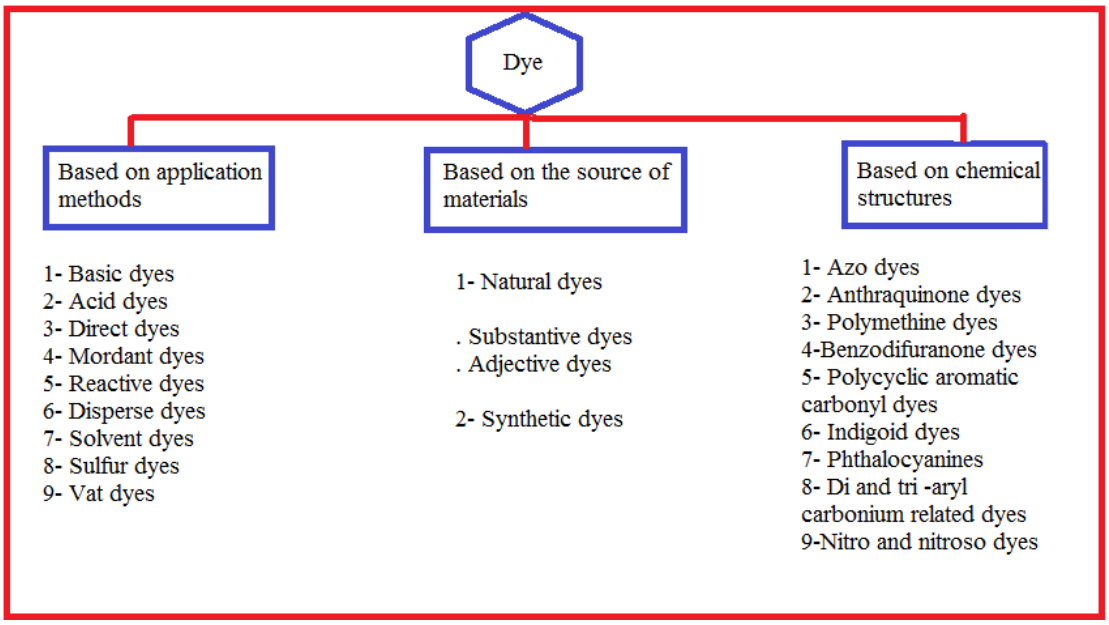

Fig. (1-6) : Schematic diagram for classification of dyes according to their chemical structure and method of application (Benkhaya et al.,2020).

1-6 Orange G dye

The azo dye is a type of dye that is used to make Orange G is an azo dye, which is a type of dye. Disodium salt of 7-hydroxy-8-[(E)-phenyldiazenyl] naphthalene-1,3-disulfonic acid In OG dye, one azo group is connected to an aromatic ring. Because of its molecular structure, it is chemically stable.The chemical formula is $C_{16}H_{10}N_2Na_2O_7S_2$. (Rana et al., 2021). This dye was chosen because it

has a variety of functional groups, such as (sulfonate, aryl , hydroxyl , and azo groups) (Meetani et al ., 2011).

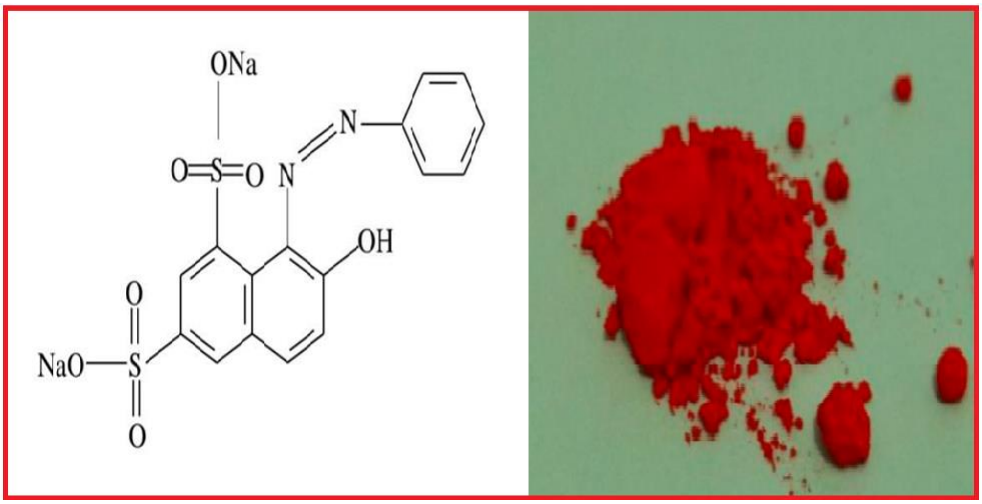

Fig.(1-7) : Structures of orange G dye

1-7 Principles of Heterogeneous Photocatalysis

Heterogeneous reactions have risen in prominence among the various types of chemical reactions in recent years. Heterogeneous reactions, particularly in industrial fields, necessitate solid catalysts. Indeed, heterogeneous environments are used in 80 percent of commercial catalytic processes today. Among numerous forms of heterogeneous reactions, the mechanism of surface reactions on a solid substance has been extensively studied. Heterogeneous reactions in other systems, on the other hand, have not been investigated in depth from a macroscopic perspective due to technical constraints. In liquid–liquid heterogeneous materials, for example, phase separation is difficult, and optical spectroscopic investigation is difficult due to the substantial light scattering generated by heterogeneity (Masuda et al., 2020).Using semiconductor oxides, metal oxides, and solar lamps, heterogeneous

photo catalytic methods have been employed to remove organic and inorganic pollutants from carbon dioxide and water in the last decade. Zinc oxide is one of the most important semiconductors because it is a highly stable, inexpensive metal oxide that is both nontoxic and environmentally benign (Al-Gubury et al., 2018).

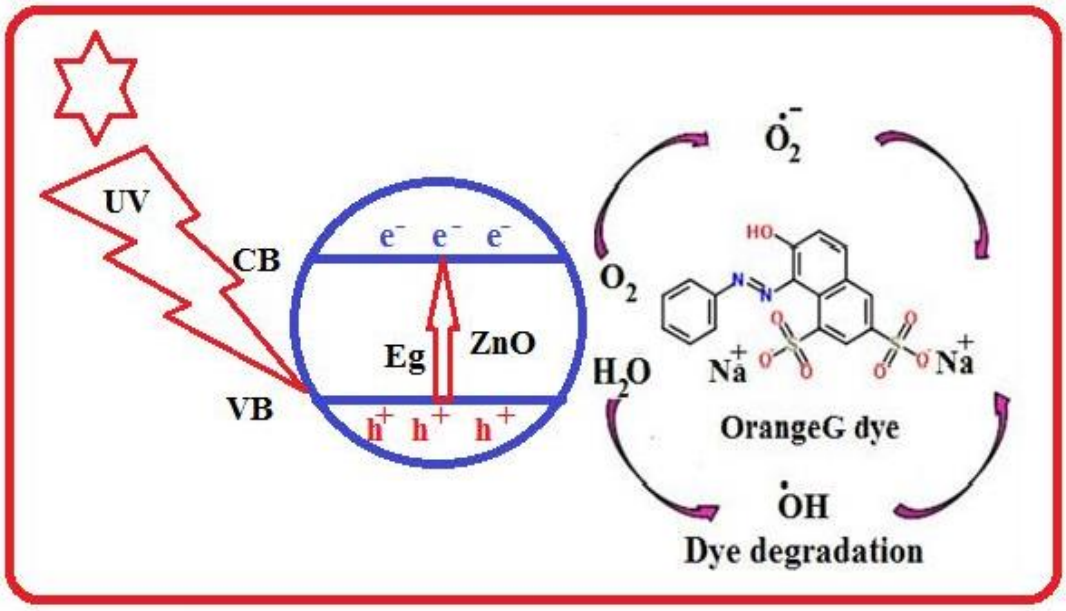

Fig.(1-8) : A schematic diagram illustrating the principle of photocatalysis .

$$ZnO + hv \rightarrow ZnO\,(e^- + h^+) \qquad (1\text{-}4)$$

The holes in the valance band can be oxidize directly the pollutant

$$h^+ + \text{dye} \rightarrow \text{dye}^{\cdot +} \rightarrow \text{degradation of the dye} \qquad (1\text{-}5)$$

or generate high reactive hydroxyl radicals (OH·) by decomposition of watre

$$h^+ + H_2O \rightarrow H^+ + OH^{\cdot} \qquad (1\text{-}6)$$

or reaction with hydroxyl ions (-OH) in water, are involved in an oxidation reaction .

$$h^+ + OH^- \longrightarrow OH^{\cdot} \quad (1\text{-}7)$$

Photo electrons produced in the conduction band on the catalyst surface, on the other hand, can convert adsorbed oxygen into superoxide anions when they engage in a reduction reaction (Karthikeyan et al., 2020) (Rong et al., 2016).

$$e^- + O_2 \rightarrow O_2^{\cdot -} \quad (1\text{-}8)$$

$$2e^- + O_2 + 2H^+ \rightarrow H_2O_2 \quad (1\text{-}9)$$

$$e^- + H_2O_2 \rightarrow OH^- + OH^{\cdot} \quad (1\text{-}10)$$

$$OH^{\cdot} + \text{dye} \rightarrow \text{intermediates} \rightarrow CO_2 + H_2O \quad (1\text{-}11)$$

(Dhatwalia et al., 2022) (Rajamanickam et al., 2016).

1-8 Improving Surface Properties of Zinc Oxide nanoparticle

Zinc oxide (ZnO) is a potential material for UV sensing because it is a safe wide-band semiconductor with a high binding energy of excitons at ambient temperature. However, pure ZnO has low sensitivity and weak responsivity, making it unsuitable for practical applications. As a result, many attempts have been made to increase the performance of ZnO UV sensors, such as adding various chemicals. Controlling band gap, defect states, carrier concentration, carrier mobility, and lifespan UV sensing of materials may all be improved with the use of additives and dopants. This enables increased sensitivity in the construction of devices. Semiconducting, metallic, non-metallic, and polymeric additives are common. Carbonaceous species have been shown to efficiently separate

photo-generated excitons on the surface of ZnO and reduce the rate of electron-hole recombination by forming an electrical field in the charge space near hetero-interfaces. When a hybrid nanostructure was spray coated on ZnO nanorods, it was found to have a strong response to UV radiation. On the other hand, graphene oxide (GO) is a unique and innovative carbonaceous material whose composites have shown considerable improvements in UV sensitivity, possibly due to its high active surfaces and great carrier mobility, among other unique features. The effect of GO confinement on the stability and dispersion of ZnO nanoparticles is significant; on the other hand, ZnO nanoparticles on the GO can operate as a chemical trap to prevent graphene agglomeration. As a result, GO and ZnO are both promising candidates for making practical nanocomposites (Alamdari et al., 2019). photocatalytic degradation of organic dye utilizing GO/ZnO photocatalyst mechanism :

$$\mathbf{GO\text{-}ZnO + hv \rightarrow ZnO_{CB}\,(e^-) + ZnO_{VB}\,(h^+)} \quad \textbf{(1-12)}$$

$$\mathbf{ZnO_{CB}\,(e^-) + GO \rightarrow ZnO_{CB} + GO\,(e^-)} \quad \textbf{(1-13)}$$

$$\mathbf{GO\,(e^-) + O_2 \rightarrow GO + {\cdot}O_2^-} \quad \textbf{(1-14)}$$

$$\mathbf{ZnO_{VB}\,(h^+) + H_2O \rightarrow ZnO_{VB} + {\cdot}OH} \quad \textbf{(1-15)}$$

$$\mathbf{Orange\ G + {\cdot}O_2^- + {\cdot}OH \rightarrow CO_2 + H_2O + Intermediates} \quad \textbf{(1-16)}$$

The pace of electron-hole (e^- and h^+) pair creation and the availability of adequate contact between the dye and the catalyst determine the catalyst's photodegradation efficacy. Orange G dye is initially adsorbed on the surface of the GO/ZnO photocatalyst. Visible light illumination excites the GO/ZnO nanohybrid. When photon energy exceeds band-gap energy (hv > Eg), holes in the valence band (VB) and electrons in the conduction band (CB) are created in GO containing ZnO. The photoinduced

electrons from the CB of ZnO are captured by the GO nanosheets in the catalyst structure, thereby increasing the photo-generated charge separation efficiency. When photoinduced electrons-holes react with O_2 and H_2O/·OH in the solution, strong active oxidizing species ($\cdot O_2$ super oxide radical anion and · OH/hydroxyl radicals) are produced. The two types of oxidizing reactive radicals ($\cdot O_2$ / ·OH) can then destroy orange G molecules adsorbed on the catalyst surface, producing CO_2, water (H_2O), and intermediates (Puneetha et al., 2021).

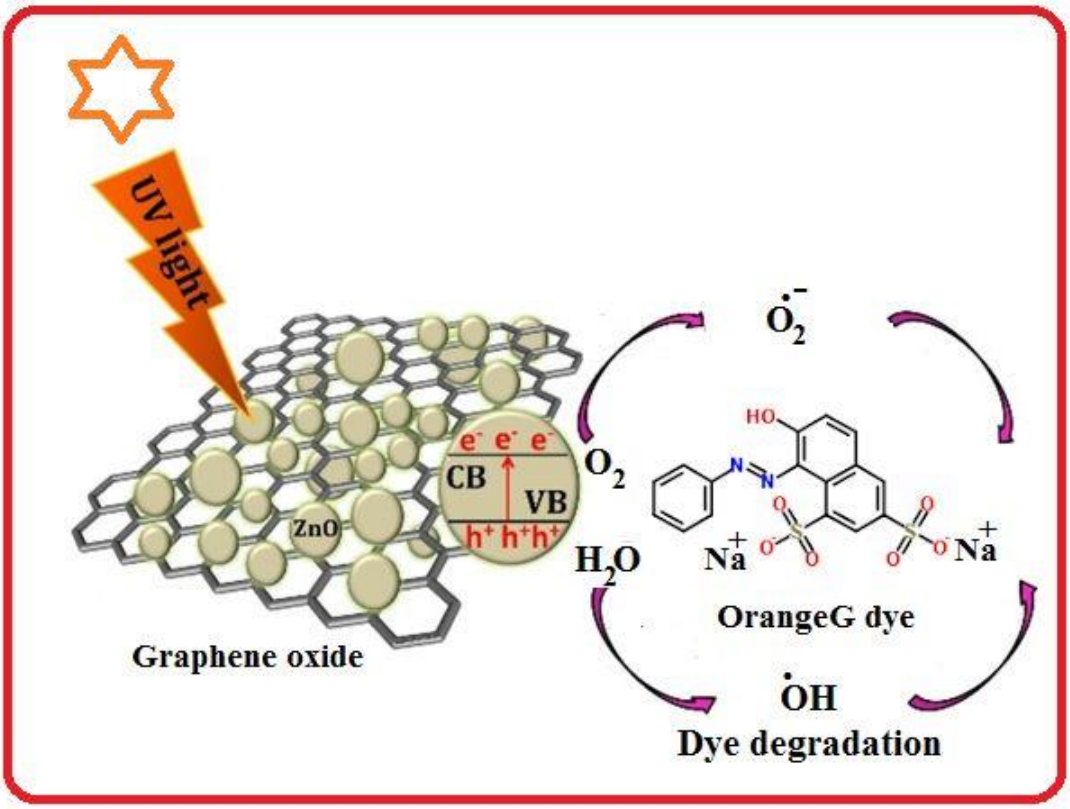

Fig.(1-9) : Schematic diagram for proposed charge transfer on the surface of GO/ZnO nanocomposite under solar light.

1-9 Advance Oxidation Process(AOPs)

AOPs are technologies that are used to oxidize a variety of organic pollutants in dirty water in order to produce clean water for human use, such as drinking and other domestic uses (Sharma et al., 2018). Antibiotic breakdown is aided by advanced oxidation processes (AOPs), which has piqued researchers' curiosity. Because of its low cost and high removal efficiency, the Fenton process has been widely employed for wastewater treatment (Yu et al., 2018). The so-called Advanced Oxidation Processes (AOPs) are a group of technologies that are comparable but not identical and are based primarily (but not only) on the generation of highly reactive hydroxyl radicals . Photocatalysis, both heterogeneous and homogeneous, Fenton and Fenton-like processes, ozonation, ultrasound, microwaves, and g-irradiation, electrochemical processes, and wet oxidation processes are all examples of AOPs (Dewil et al., 2017) (Khan et al., 2020). AOPs are used to successfully remove pollutants in plants that produce drinking water, in wastewater treatment systems to remove biorecalcitrant micro-pollutants, and in disinfection techniques (including photo-assisted ones).These reactions are based on the generation of potent reactive species (typically radicals) capable of attacking and mineralizing nearly all oxidizable compounds (Marco et al., 2021).

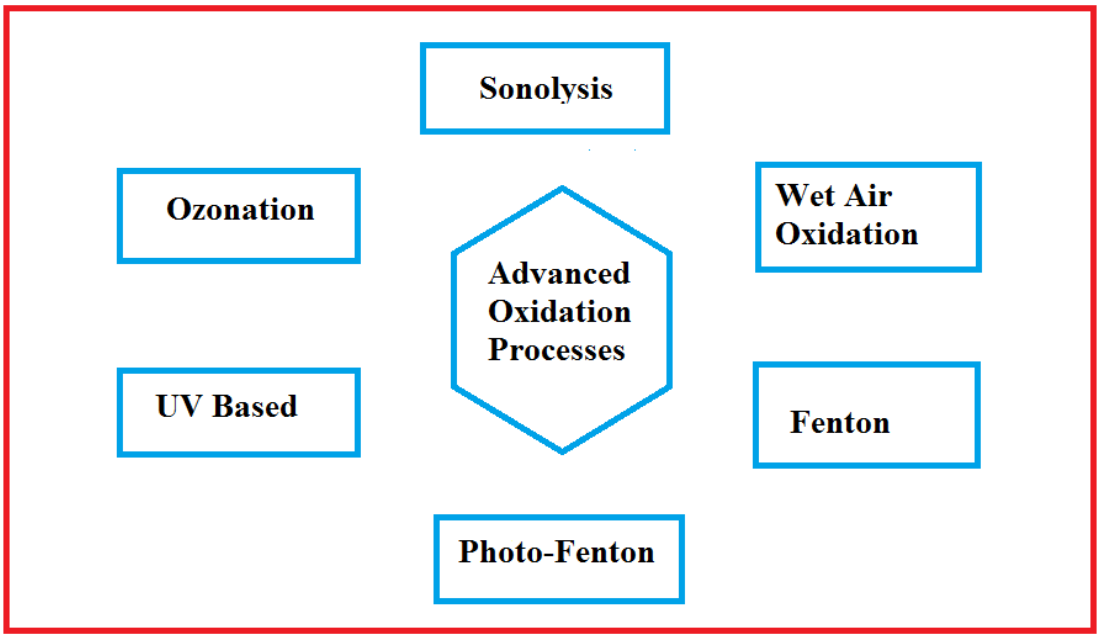

Fig.(1-10)：Classification of Advanced Oxidation.

1-10 Literature Review

(Jiang et al., 2011) succeeded in developing a method for synthesizing graphite oxide/TiO_2 composites as a highly efficient photocatalyst by in situ depositing TiO_2 nanoparticles on graphene oxide nanosheets via liquid phase deposition, followed by a 200 C calcination treatment. The photocatalytic activity of ascomposites was influenced by post-calcination temperature, graphene oxide content, and solution pH.

(Xiang et al., 2012) allows researchers to investigate recent advances in the design and production of graphene-based semiconductor photocatalysts using a variety of methodologies, such as in situ growth, solution mixing, hydrothermal, and/or solvothermal approaches. Photocatalytic capabilities of the resulting graphene-based composite systems are also examined in connection to environmental and energy applications such photocatalytic pollution degradation, photocatalytic hydrogen generation, and photocatalytic disinfection.

(Zhou et al., 2012) under a pH of 11 adjusted by ammonia water, the hydrothermal approach was effectively used to synthesize reduced graphene oxide (RGO) and fabricate ZnO–RGO hybrid (ZnO–RGO) with zinc nitrate hexahydrate and graphene oxide (GO) as raw materials. Hydrothermal conditions with ammonia provided thermal and chemical factors to synthesize RGO during the reduction of GO. X-ray diffraction (XRD), X-ray photoelectron spectroscopy (XPS), scanning and transmission electron microscopy, and photoluminescence spectra are also used to describe it.

(Pop et al., 2012) the hydrothermal technique was used. The purpose of this research was to look at the thermal properties of graphene, such as its specific heat and thermal conductivity

(from diffusive to ballistic limits), as well as the impact of substrates, defects, and other atomic alterations. uccessfully make a reduced-calorie meal.

(Chen et al., 2013) in this study, a ZnO/graphene oxide (ZnO/GO) composite material was synthesized using an improved two-step approach, with ZnO nanoparticles thickly coated on GO nanosheets and studied using IR, XRD, TEM, and UV–vis techniques.

(Ameen et al., 2013) a nanohybrid of zinc oxide (ZnO) and graphene oxide (GO) was produced by a chemical process and used as a photocatalyst for the photodegradation of crystal violet (Cv) dye in these studies. The (Cv) dye is likewise degraded to a considerable degree (by 95%) .

(Zhang et al., 2014) a two-fold enhancement method was used in this work to minimize electronhole recombination and increase photocatalytic efficiency. First, the effect of adding graphene oxide (GO) on the photocatalytic activity of ZnO was carefully examined. Also, because of its high capacity for dye adsorption and charge separation, GO has been recommended as a way to boost ZnO's photocatalytic activity. Second, Pd nanoparticles were used to adorn ZnOGO, resulting in ZnOGOPd nanocomposites that are typically superior photocatalysts .

(Kashinath et al., 2015) for the first time, success was reported employing a microwave-assisted hydrothermal technique to synthesize ZnO-GO nanocomposite using $ZnCl_2$ and NaOH as precursors. In this paper, a microwave aided facile hydrothermal approach was used to examine the synthesis, interaction, kinetics, and mechanism of hybrid Zinc Oxide-Graphene Oxide (ZnO-GO) nanocomposite. In addition, the ZnO-GO nanocomposite improves and performs as a steady photo-

response degradation performance of Brilliant Yellow under UV light exposure compared to pure GO and ZnO nanoparticles. Optical investigations using UV-Vis and Photo Luminescence reveal that the band gap of nanocomposite has increased, resulting in improved photodegradation performance.

(Rabieh et al., 2016) this paper outlines a green approach for hydrothermally synthesizing hierarchical ZnO-reduced graphene oxide (ZnO-RGO) nanocomposites as an effective photocatalyst for the photodegradation of blue B dye. Scanning electron microscopy (SEM), X-ray diffraction (XRD), energy dispersive spectroscopy (ESD), and UV–Vis spectroscopy hybridizing with RGO sheets were also used to evaluate the samples.

(Alshamsi and Ali , 2016) a kinetics of the production of reduced graphene oxide utilizing an aqueous solution of Hibiscus Sabdarriffa L was explored in this work. Effects of treatment duration, pH, reaction temperature, and extract concentration were studied as experimental parameters. The synthesis of pseudo RGO was further aided by a high pH value, a high reaction temperature, and a large volume of extract. In addition, the results reveal that synthesized RGO has the superior conductivity and spectrum response qualities when compared to GO.

(Kashinath et al., 2016) the photo deterioration of Brilliant Blue under UV-Vis light exposure was studied using a zinc oxide-graphene oxide (ZnO-GO) anocomposite synthesized by a simple, low-temperature wet chemical technique aided by microwave irradiation. XRD confirms that the lattice constants and band gap energy of ZnO have changed when compared to pure nano-sized ZnO particles. The photo degradation of Brilliant Blue was accomplished under UV-Vis light radiations after the

graphene oxide sheets were anchored/tailored with ZnO particles. The findings show that graphene oxide hybridized with ZnO can produce efficient photocatalytic activity, and that the degree of photocatalytic activity enhancement is strongly influenced by the bonding of ZnO nanowires and GO. They also assert that the optical, structural, and morphology of pure ZnO and ZnO-GO nanostructures should be investigated.

(Wu et al., 2016) a ternary ZnO/reduced graphene oxide (rGO)/polyanline (PANI) nanocomposite was produced and employed as a photocatalyst in this work, including TEM, SEM, X-Ray diffraction, FTIR, and Raman characterization. When compared to pure ZnO, the degradation of methyl orange dye photocatalyst demonstrates an improved photocatalytic performance with a maximum degradation efficiency of about 100% within 60 minutes under UV light irradiation (15 percent). The rGO, which significantly improves the capacity to transfer photoexcited electrons and the specific surface area of the material, the PANI, which boosts light absorption and dye adsorption, and the synergistic impact among ZnO, rGO, and PAN are all credited with this improvement.

(Kumaresan et al., 2017) the hydrothermal technique was used to make ZnO nanoparticles using zinc chloride and ammonium hydroxide as raw materials in this study. The structure and crystalline nature of produced nanoparticles were studied using the X-ray diffraction method. Reflection is also important. Spectroscopy research indicated that the optical band gap of ZnO varies somewhat depending on particle size. The influence of pH of the precursor solution on the generated ZnO nanoparticles resulted in nanoneedle, hexagonal disk, porous nanorods, and nanoflower architectures, as seen by field emission scanning electron

microscopy pictures. The produced ZnO nanoparticles' photocatalytic activity was further tested for Rhodamine B (RhB) dye, which demonstrated 94 percent degradation and high stability over five cycles.

(Giovannetti et al., 2017) TiO_2 is one of the most commonly investigated and used photocatalysts for environmental cleanup, according to this study. However, due to its 3.2 eV band gap, it is most active when exposed to UV light, while it has a low efficiency when exposed to visible light. The integration of carbon nanomaterials, such as graphene, in order to generate carbon-TiO_2 composites, is a promising area for TiO_2 activation in the visible light region of the whole solar spectrum. The creation of graphene-based TiO_2 photocatalysts has sparked renewed interest in recent years. In addition, the current brief overview discusses recent improvements in TiO_2 photocatalyst coupling with graphene materials, with the goal of expanding TiO_2's light absorption from UV to visible wavelengths.

(Moorthy et al., 2017) the hydrothermal approach was employed to synthesize the nanocomposite in this study, and the particles were analyzed using characterisation techniques such as XRD, UV-Vis, FTIR, FESEM, and TEM. Also, several ways can be used to eliminate organic and inorganic contaminants, the best of which is photocatalysis activity. Two of the dyes utilized in this project were Methylene Blue (MB), Methylene Violet (MV), Methylene Orange (MO), and Bromophenol Blue (BB). These dyes have high photocatalytic properties, which allow them to destroy pigments in visible light.

(Zaaba et al., 2017) this work was successful in extracting GO from graphite flakes using a modified hummer's approach, which differs from the traditional hummer's method. The acetone-GO (A-GO) and ethanol-

GO (E-GO) were then spin-coated onto silicon wafers and IDE (E-GO). Several square microns of GO were obtained, according on the SEM results. Furthermore, because of the big agglomerates and contact between the flakes in the E-GO sample, the currentvoltage pattern showed that E-GO created more current flow than A-GO. Meanwhile, FTiR analysis of GO reveals that both samples include hydroxyl, epoxy, carboxyl, and carbonyl functional groups. Furthermore, the interlayer spacing of A-GO sample is slightly higher than E-GO sample, owing to the lower diffraction peak of A-GO.

(Raliya et al., 2017) under visible light, the degradation of an azo dye, methyl orange (MO), was evaluated in simulated wastewater with various oxide nanoparticles acting as photocatalysts. For adsorptive and photocatalytic removal of the dye, titanium dioxide (TiO_2), zinc oxide (ZnO), and graphene oxide (GO) were produced, characterized, and used. The ideal conditions for dye removal were determined by varying factors such as the starting concentration of MO and the size of the nanoparticle photocatalyst. Finally, photocatalytic performance of nanocomposites comprising the three components (GO–TiO_2–ZnO) was investigated.

(Jayachandiran et al., 2018) in this study, the researchers were successful in preparing ZnO and rGO/ZnO nanocomposite as electrode materials for supercapacitor applications. The ultrasonic-assisted solution approach was employed to make the rGO/ZnO nanocomposite, which is a simple and cost-effective method. XRD, FESEM, TEM, and confocal Raman are also used to characterize it. The XRD pattern confirmed the crystal structure of ZnO and the nanocomposite's development.The generated rGO/ZnO nanocomposite is a superior electrode material for suparcapacitor application, according to these findings.

(Ravi et al., 2018) in this study, we succeeded in synthesizing a reduced graphene oxide-based zinc oxide (ZnO/RGO) nanocomposite (NC) using a simple and environmentally friendly hydrothermal technique. To explore its structure, morphology, and thermal stability, it was also analyzed using XRD, FESEM, EDS, TGA, FTIR, and UV-DRS. The effects of pH, dye concentration, and catalyst dose were also investigated in order to optimize.

(Shanmugasundaram et al., 2018) the hydrothermal technique was used to prepare hierarchical mesoporous zinc oxide (ZnO) and reduced graphene oxide-zinc oxide (ZnOrGO) composites for the degradation of organic contaminants in natural water resources in this study. The crystal structure and phase purity of the materials were also studied by powder x-ray diffraction, micro-Raman, and X-ray photoelectron spectroscopy investigation. Ultra violet-diffused reflectance and photoluminescence spectroscopy analyses were also used to study the optical characteristics of the as-prepared materials. The egradation kinetics of methylene blue (MB) dye in aqueous solution under normal solar light illumination were used to assess the photocatalytic activity of the as-prepared materials.

(Shukla et al., 2019) the simple production of graphene-supported palladium (Pd) nanoparticles anchored zinc oxide nanorods (PdZnO/G) by the sol-gel ethod is described in this paper. The hexagonal wurtzite crystal structure (with P63mc phase) of Pd-ZnO/G nanorods was further confirmed by X-ray diffraction (XRD) pattern, which is comparable to ZnO structure. Graphene-supported Pd nanoparticles anchored on ZnO nanorods increased the average crystallite size of ZnO nanorods, according to X-ray diffraction data. The successful attachment of Pd nanoparticles on the surface of ZnO/G nanorods was disclosed using field emission scanning electron microscopy (FESEM). The distinct oxidation

states and surface compositional features of nanorods were obtained using X-ray spectroscopy (XPS). The presence of palladium, carbon, and oxygen in the Pd-ZnO/G structure was confirmed using energy dispersive spectroscopy. After graphene and palladium doping, the optical absorption shifted towards the low wavelength region for the Pd-ZnO/G structure and the high wavelength region for the ZnO/G nanostructure.

(Peter et al., 2019) the manufacture of visible light-active ZnO photocatalyst through nitrogen and graphene oxide modification, followed by its application to the degradation of brilliant clever green (BG) dye, was a success in this work. X-ray diffraction (XRD), Fourier transform infrared (FTIR), transmission electron microscopy (TEM), UV–vis absorption, and diffuse reflectance spectra (UV–vis DRS) are all used to characterize the material. Modifications to ZnO positive by extending its light absorption capabilities into the visible area dramatically increased its photocatalytic activities under visible light, according to this study.

(Zhang et al., 2019) using zinc oxide (ZnO) as a photocatalyst, graphene (GO) as a dispersant, and poly (vinylidene fluoride) (PVDF) membrane as a carrier, create PVDF/GO/ZnO composite membranes with photocatalytic performance for organic dyes. The addition of GO increased the dispersibility of ZnO in PVDF membranes due to the significant hydrophilicity of the carboxyl group, as evidenced by SEM data. The photocatalytic degradation rate of PVDF/GO/ZnO composite membranes for methylene blue (MB) may reach 86.84 percent under Xenon irradiation (300W).

(Di et al., 2019) using an in situ synthesis approach for photodegradation of methylene blue under visible light illumination, a

new ZnO–GO/CGH composite was synthesized in this study.SEM techniques are also used to characterize it. Methylene blue dye degradation has a high clearance efficiency of 99 percent.

(Abbasi et al., 2020) the magnetic ZnO nanocomposite (GO-Fe_3O_4-ZnO) is synthesized utilizing graphene oxide (GO) as a substrate, and the obtained samples are characterized using XRD and VSM. The produced nanocomposites contain modified GO with Fe_3O_4 cubic structure and hexagonal wurtzite structure of ZnO nanoparticles, according to XRD findings. Based on the results of the VSM. According to the results of the UV–vis spectrophotometer, all of the generated materials can absorb UV irradiation and breakdown the MO. At each concentration and irradiation period, the egradation of (MO) dye utilizing GO-Fe_3O_4-ZnO is greater than that of Fe_3O_4-ZnO.

(Sharma et al., 2020) in this study, an environmentally friendly and solar light-responsive graphene oxide wrapped zinc oxide nanohybrid was made hydrothermally utilizing lemon and honey as chelating and complexing agents, respectively. During the synthesis of GO and ZnO, an eterostructure was created by modifying the reaction conditions. The nanohybrid had remarkable photocatalytic activity for methylene blue degradation (89 percent).

(Lin et al., 2020) the nanocomposites of ZnO and GO with synergistic photocatalytic activities were synthesized using a precipitation approach with GO as the catalyst carrier in this study. X-ray diffraction, X-ray photoelectron spectroscopy, UV-vis spectroscopy, field emission scanning electron microscopy, and transmission electron microscopy were used to characterize the nanocomposites, which also performed photocatalytic activity. The composites' photodegradation efficiency is

97.6%, and the first-order photodegradation reaction rate constant is calculated to be 0.04401 min^{-1}.

(Maruthupandy et al., 2020) chemical precipitation was used to make very pure zinc oxide nanoparticles (ZnO NPs) and graphene-zinc oxide nanocomposites (G-ZnO NCs) in this study. Fourier transfer infrared spectroscopy, X-ray diffraction spectroscopy, Raman spectroscopy, scanning electron microscopy, and transmission electron microscopy (TEM) techniques were used to describe the material. When compared to other dyes examined, the synthesized NCs were extremely effective at removing Rh-B.

(Al-Mamun et al., 2021) using the sol–gel technique followed by heat treatment, nanostructured zinc oxide (ZnO) was doped with silver (Ag) and graphene oxide (GO) nanoparticles to synthesize Ag/GO/ZnO. SEM and FTIR methods were used to characterize the samples. The enhanced photodegradation activity of the Ag/GO/ZnO nanocomposite suggests that it could be used to remediate organic contaminants from textile effluent.

1-11 Aims of the present work

1- prepearation of GO by modified hummer method.

2- prepearation of ZnO nanopartical by sol-gel method.

3- Synthesis of GO/ZnO nanocomposite by sonocatalysis method.

4-Study the characteristic of nanocomposite using XRD, SEM, EDX, FTIR, TGA and BET techniques.

5- Study the photo activity of nanocomposite using orange G dye.

6-Study different parameter such as effect of dye concentration , effect of mass of catalyst , effect of temperature , H_2O_2 , CH_3OH , PH and light intensity.

Chapter Two

Experimental

Part

2. Materials and Methodologies

2.1. Chemical Materials

The chemicals were used as received without any further purification

Table (2-1): Chemicals used and respective suppliers

NO.	Name of substance	Chemical formula	Supplied company	Purity %
1	Graphene Oxide	GO	British Drug Houses (B.D.H	95
2	Zinc Oxide nanoparticle	ZnO	Indian Production	98
3	Graphite powder	C	British Drug Houses (B.D.H	99
4	Sulfuric acid	H_2SO_4	British Drug Houses (B.D.H	98
5	Hydrogen Peroxide	H_2O_2	Indian Production	30
6	Orange G dye	$C_{16}H_{10}N_2Na_2O_7S_2$	Indian Production	90
7	Ethanol	CH_3CH_2OH	Merck Germany	98
8	Zinc acetate dihydrate	$ZnC_4H_6O_4$	British Drug Houses (B.D.H	99
9	Sodium hydroxide	NaOH	CDH) Central Drag House	97
10	Hydrochloric acid	HCl	Sigma -Aldrich	35
11	Sodium nitrate	$NaNO_3$	British Drug Houses (B.D.H	98
12	Potassium Permanganate	$KMnO_4$	British Drug Houses (B.D.H)	99

2.2. Instruments Analysis

Table (2-2): Instruments used in this study

No.	instrument	Company	Position of instrument
1	Furnace	Furnace Size - Tow Gallenkamp , South of Korea	Babylon University / Collage of Science for women /Chemistry Department
2	Centrifuge	CL008 , JANETZI – T5, Belgium	Babylon University / Collage of Science for women /Chemistry Department
3	Dried oven	LDO – 060e , Labphy , Korea	Babylon University / Collage of Science for women /Chemistry Department
4	Fourier-Transform Infrared	SpactraIR-2, Perkin Elmer Instrument, USA	Babylon University / Collage of Science for women /Chemistry Department

5	Hotplate Magnetic Stirrer	LMS-1003, HANNA instruments ,Lapphy England	Babylon University / Collage of Science for women /Chemistry Department
6	pH meter	HI 83141 , Hanna, Romania	Babylon University / Collage of Science for women /Chemistry Department
7	Energy dispersive X-ray spectroscopy	EDX,Zeiss,germany	Tehran University, IRAN
8	Scanning electron microscopy	SEM, Zeiss , Germany	Tehran University, IRAN
9	Sensitive electronic balance	3003- Denver instrument , Germany	Babylon University / Collage of Science for women /Chemistry Department
10	Ultrasonic path	405 power sonic , Hwashin , korea	Babylon University / Collage of Science for women /Chemistry Department

11	Surface area analyzer (BET)	NanoSORD , Haskarsazan ,Iran	Tehran University, IRAN
12	UV-visible spectrophotometer Single beam	UV mimi-1240 , shimadzu , Japan	Babylon University / Collage of Science for women /Chemistry Department
13	X- Ray Diffractometer	XRD6000, Shimadzu, Japan	Ministry of Sciences and Technology, IRAQ
14	Thermo gravimetric analysis (TGA)	DTG-60 , Shimadzu, Japan	Babylon University / Collage of Science for women /Chemistry Department
15	Oven	Memmert,Germany	Babylon University / Collage of Science for women /Chemistry Department

2 .3. Photocatalytic Reactor Set up

Figure.(2-1) shows the photocatalytic degradation system has been used to carry out all experiments.

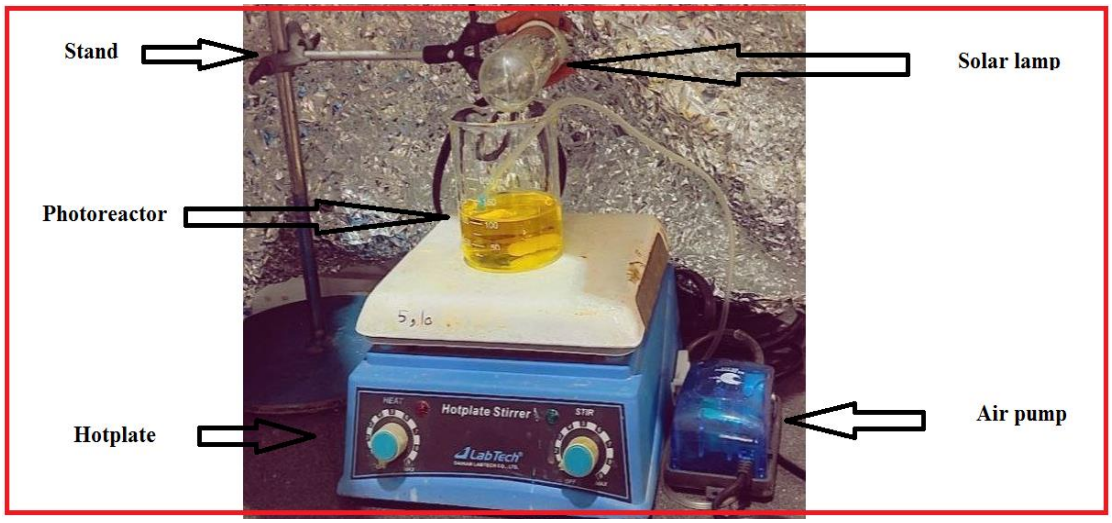

Fig.(2-1) : Optical photo for main parts of the Photocatalytic degradation system .

2- 4 Methodologies

2– 4–1 Photocatalytic degradation experiment:

The photocatalytic degradation experiment was carried out with the use of a photocatalytic reactor system, which included all of the major components illustrated in Figure.(2-1). The photocatalytic activity of the produced GO/ZnO nanocomposite was studied using dye. Under solar light, photocatalytic degradation of dye in aqueous solution was completed using GO/ZnO composites as photo catalyst. There are two pieces to a photo reactor. The first was employed to cool the suspension solution with the help of the cooling water that passed through it. The second component contains a suspension solution with a capacity of (100 mL) for degrading the dye. Using distilled water, a (100mg/L) stock solution of dye solutions was created. Stirring produced a suspension

solution combination for concentrating dye. By adding (0.15 g) of GO/ZnO nanocomposite to (100 mL) of dye and stirring, a suspension mixture was created. A benchtop solar light source was used to irradiate the respective suspension solution mixture. Every 10 minutes, about 2-3 mL of sample was taken with a syringe and centrifuged at 3000 rpm for 10 minutes, after which the dye absorbance was measured with a UV–Vis spectrophotometer.

2-4-2 Preparation of graphene oxide (GO) by modified hummer method

In an Erlenmeyer flask, mix (115 mL) of sulfuric acid (H_2SO_4), (2.5 g) of sodium nitrate ($NaNO_3$), and (5 g) of graphite powder well for (30 min) in an ice bath at (0 $^{\circ}$C). Then slowly add (15 g) of potassium permanganate ($KMnO_4$) to the mix and stir for (15 minutes), until the color changes from violet to dark green. Then, for (30 minutes), heat the mixture to (35 $^{\circ}$C) while stirring. Slowly pour (230mL) of distilled water into the mixture (it's potentially explosive). The color of the mixture turns nutty brown after (15 minutes) in a (98 $^{\circ}$C) . Finally, to finish the process, add (400 mL) of distilled water, followed by (50 mL) of hydrogen peroxide (H_2O_2). Filter the solution and wash the precipitate seven times with hydrochloric acid (1:10), followed by washing with distilled water. The precipitate was then dried at (80 $^{\circ}$C) in an oven (Kashinath et al., 2016) .

2– 4–3 Preparation of zinc oxide (ZnO) nanopartical by sol-gel method

To prepare zinc oxide, dissolv (2.24 g) of zinc acetate solution in (20 mL) of distilled water for (15 minutes) using a stirrer.And (1.15 g) of NaOH is dissolved in (20 mL) of distilled water for (15 minutes) using a stirrer.The drops of NaOH solution were added to the Znic acetate solution during stirring, resulting in a milky dye. Without stirring, the mixture was heated for (3 hours) at (80 °C). Centrifuge after cooling, washing with distilled water and ethanol overnight and drying at(60 °C). Finally, at a temperature of (400 °C) the remains are incinerated in a furnace (Hasnidawani et al., 2016).

2– 4–4 Preparation of GO/ZnO nanocomposites by sonocatalysis method

(3g) of graphene oxide (GO) in (150 mL) of distilled water and (0.75 g) of zinc oxide (ZnO) in (50 mL) of distilled water separately and put in an ultrasonic bath for (30 min). The GO and ZnO solutions were mixed in an ultrasonic bath for (45 minutes). Transfer the mixture to a magnetic stirrer for (60 minutes), then place in a dry oven at (60 °C) overnight (Ahmad et al., 2014).

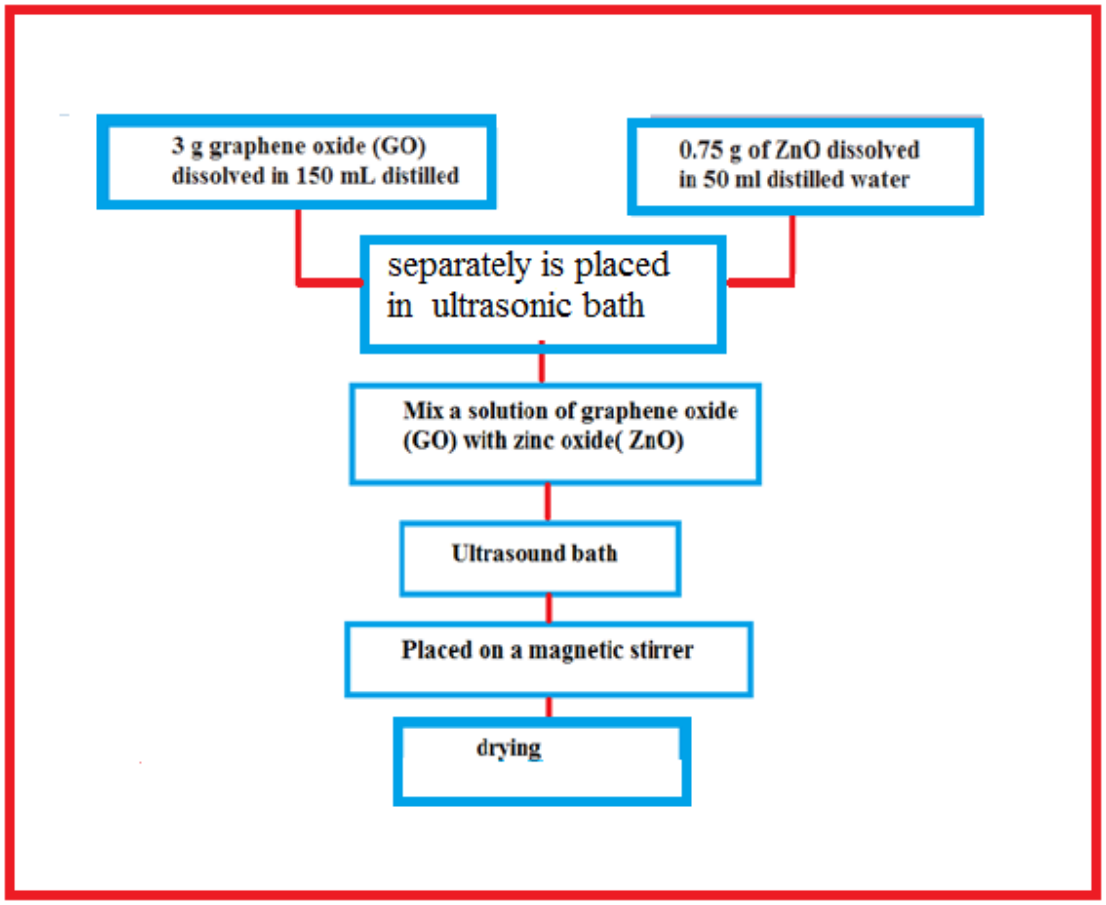

Fig.(2-2): Synthesis scheme of GO/ZnO nanocomposites using sonocatalysis process.

2-5 Characterizations of prepared GO/ZnO nanocomposite

Several techniques were used to characterize the synthesized GO/ZnO nanocomposite, including X-ray diffraction (XRD), scanning electron microscope (SEM), Brunauer–Emmett–Teller (BET), Fourier transform infrared spectroscopy (FTIR), thermo gravimetric Analysis (TGA) , Energy dispersive X-ray spectroscopy (EDX) .

2- 5-1 X-rays Diffraction Patterns (XRD)

An X-ray diffractometer was used to investigate the crystalline quality of the ZnO, GO and GO/ZnO nanocomposite, particle size, phase

composition, and average spacing layers/rows of atoms. The study was performed with a Shimadzu XRD6000. With 45 Cu K radiation (λ =1.54056 A°) at 40kV, 30mA, a rate of 5 degrees per minute, and a range of 2 degrees, the measuring conditions were set (3- 60). The lattice planes of a crystal are divided by d. Braggs' law describes the length of the reflected X-wave beam (λ), the spacing between the atomic planes (d), and the angle of diffraction (θ) as follows:

$$n\lambda = 2d \sin\theta \qquad (2\text{-}1)$$

Using Scherer's equation and the full width at half maximum (FWHM) of the strong peak, the size of the synthesized GO/ZnO nanocomposite crystallite was determined:

$$D = \frac{k\lambda}{\beta\cos\theta} \qquad (2\text{-}2)$$

D is the usual crystal size, while k is a nearunity form factor. The value for homogeneous shape is 0.94, whereas the value for heterogeneous shape is 0.89. =0.154 nm is the X-ray wavelength of (Cuk), and is the whole width at half-maximum intensity of the diffraction peaks (FWHM). (Meva et al., 2019) (Farghali et al., 2016).

2.5.2 Scanning Electron Microscope (SEM) :

The scanning electron microscopy examination was carried out on a ZESS EVO-50 SEM machine. By depositing a little amount of the sample on the grid, removing excess material using blotting paper, and drying the film on the SEM grid under a mercury lamp for 5 minutes, thin films of the sample were formed on a carbon coated tape. SEM analysis was used to determine the structure of the reaction products that were generated (Mishra et al., 2015).

2-5-3 Brunauer–Emmett–Teller (BET)

The surface area of GO/ZnO nanocomposites was determined using BET surface area analysis. was investigated by using nitrogen adsorption-desorption isotherm (Oppong et al., 2021).

2.5.4 Fourier Transform Infrared Spectroscopy (FTIR)

The functional groups on ZnO, GO and GO/ZnO was determined using a Jasco FTIR-460 plus spectrophotometer and Fourier Transform Infrared spectroscopy (FT-IR) in the wave number range of (4000-400 cm^{-1}). KBr wafers are wafers constructed of KBr (Kumar et al., 2022).

2-5-5 Thermo Gravimetric Analysis (TGA)

Analysis is a destructive analytical technique that analyzes the contents of a sample using high-temperature pyrolysis. Carbon-based materials are frequently heated to (30-1000°C) in an inert or oxidizing environment. This approach measures the change in mass of a sample (percent) as a function of time for a specific temperature or temperature gradient applied to the sample (Kong et al., 2021).

2-5-6 Energy Dispersive X-ray spectroscopy (EDX)

The produced sample (GO/ ZnO) were analyzed using energy dispersive spectroscopy (EDX) to verify chemical compositions.EDX is a semiquantitative, micro-chemical analysis technique that is commonly used for determining the composition of various structures (Anjum et al., 2021) .

2-6 Adsorption activity of the synthesized GO/ZnO nanocomposite.

Several studies were conducted to test the adsorption capabilities of the generated GO/ZnO nanocomposite, including the removal of dyes from their aqueous solutions by adsorption on the surface of the created GO/ZnO nanocomposite. The influence of solution pH, temperature, light intensity, H_2O_2, CH_3OH, mass catalyst, and concentration on the adsorption process was examined .
Equation (2- 4) was used to calculate the percentage of degradation, where A_0 is the initial dye concentration and A_t is the dye concentration after treatment (Gharagozlou et al., 2018).

$$\text{PDE \%} = (A_0 - A_t)/A_0 \times 100 \qquad (2\text{-}3)$$

2-7 Parameters effecting on photocatalytic degradation process :

2-7-1 . Effect of the mass of GO/ZnO on the photocatalytic degradation of orange –G dye

GO/ZnO concentrations of (0.01, 0.03, 0.06,0.15, and 0.7 g/100mL) were used to investigate the effects of different catalyst concentrations. In all studies, the orange G dye concentration was (10 mg/L) , (pH= 8.7) , temperature (25 $^{\circ}$C) . The results of photocatalytic degradation of orange G dye with a catalyst dose of (0.0 1g/100mL) in the presence of a UVC lamp and sunlight after (80 minutes). The results show that the photocatalytic activity of orange G dye was lowest when the catalyst concentration was (0.01 g/100mL) (Krishnan et al., 2020).

2-7-2 . Effect of the Initial Concentration substrate on photocatalytic degradation process using constant mass of coupled of GO/ZnO .

Various studies were carried out with varying initial substrate concentrations of orange G (10, 20, 30, 40, and 50) mg/L and a constant mass of (0.15 g/100mL) of GO/ZnO nanocomposites , (pH=8.7) ,temperature(25°C).A 125-watt tungsten lamp is used in the photocatalytic degradation process (Chiu et al., 2019) (Oun et al., 2017).

2-7-3 Effect of pH on the photocatalytic degradation process using GO/ZnO nanocomposites

The effect of pH on dye degradation is influenced by a number of factors. The ionization state of the surface, catalyst particle size, dye type and amount of substrate adsorption on the catalyst surface are all factors to consider. The degradation reactions were carried out at pH levels of (3.7, 5.6, 8.7, and 10.3) respectively using HCl and NaOH (0.1M) and a constant mass of (0.15 g/100mL) of GO/ZnO nanocomposites, temperature (25°C) and orange G dye concentration was (10 mg/L) (Hayat et al., 2011) .

2-7-4 Effect of light intensity on the photocatalytic degradation process using GO/ZnO nanocomposites

At a constant concentration of (10 mg/L) of aqueous solution of orange G dye and a constant weight of (0.15 g/100mL) of the GO/ZnO catalyst, (pH=8.7) ,temperature (25°C) ,several experiments were carried out with varying light intensities (1, 3, 5, 7 and 9 mW/cm^2) (Samsudin et al., 2015) .

2-7-5 . Effect of the H_2O_2 on the photocatalytic degradation of orange –G dye

A series of studies were carried out in the ranges (0.3,1.5,3,3.9,4.5 % (v/v)) to study the influence of H_2O_2 on dye removal efficiency over nanocomposites at a constant concentration of (10 mg/L) of aqueous solution of orange G dye and a constant weight of (0.15 g/100mL) of the GO/ZnO catalyst , (pH=8.7) ,temperature(25°C) (Gholami et al ., 2016) (Danyliuk et al., 2020).

2-7-6 . Effect of the CH_3OH on the photocatalytic degradation of orange –G dye

At a constant concentration of (10 mg/L) of aqueous solution of orange G dye and a constant weight of (0.15 g/100mL) of the GO/ZnO catalyst, (pH=8.7) ,temperature (25°C) ,a series of studies were carried out in the ranges (3 , 7 , 11 , 17 , 21 % (v/v)) to investigate the influence of CH_3OH on dye removal efficiency over nanocomposites (Salhi et al., 2019).

2-7-7 . Effect of temperature on the photocatalytic degradation process using GO/ZnO nanocomposites

At a constant concentration of (10 mg/L) of aqueous solution of orange G dye and a constant weight of (0.15 g/100mL) of the GO/ZnO catalyst, (pH=8.7) and adjust the temperature of the photocatalytic reaction system from (285, 298, 303, 311) K to see how it affects the photocatalytic performance of the samples when exposed to visible light (Mohammad et al., 2016).

2-8 Measurement of the reaction rate constant

The typical Langmuir-Hinshelwood (L-H) model is used to study the kinetics of dye photodegradation over as-synthesised materials(Krishnakumar et al., 2011) .Eq(2-4) which is expressed as

$$R = \frac{dc}{dt} = \frac{k_f K_a C}{(1+k_a C)} \qquad (2\text{-}4)$$

Where :

R : Rate of reaction, k_f : Rate constant (min^{-1}) , K_a : Langmuir adsorption constant, C : Concentration (mg/L), t : Time (min) The Langmuir–Hinshelwood equation can be modified as :

$$\frac{1}{R} = \frac{1}{(k_f K_a C)} + \frac{1}{k_f} \qquad (2\text{-}5)$$

2-9 Thermodynamic Parameters:

2-9-1 Determination the activation energy:

According to the Arrhenius equation, the activation energy (Ea) is:

$$K = A\, e^{-E_a / RT} \qquad (2\text{-}6)$$

$$\ln K = \ln A - \frac{E_a}{RT} \qquad (2\text{-}7)$$

The equation establishes a link between reaction rate and temperature. The rate constant is denoted by k. The frequency factor is denoted by the letter A. The reaction's Activation Energy is Ea. The gas constant is R (8.314 J mol^{-1} K^{-1}), and The absolute temperature in k is denoted by the letter T (Mohsin et al., 2013)(Kzar et al., 2019) .

2-9-2 Determination enthalpy of activation and entropy of activation

From the plot of the Erying equation , the values of Δ H and ΔS can be computed as follows:

$$\ln\left(\frac{k}{T}\right) = -\frac{\Delta H}{R} \cdot \frac{1}{T} + \ln\left(\frac{K_B}{h} + \frac{\Delta S}{R}\right) \qquad (2\text{-}8)$$

where, K_B＝Boltzmann's constant [1.381×10^{-23}J/K] , T＝ absolute temperature in degrees Kelvin (K), h＝Plank constant [6.626×10^{-34} J·s], k the rate constant, ΔH and ΔS the enthalpy and entropy of activation respectively. (Olajire et al ., 2014).

2-9-3 Determination Free energy of activation

The Gibbs' free energy ΔG may computed using the following formula (Fu et al., 2015).

$$\Delta G = \Delta H - T\Delta S \qquad (2\text{-}9)$$

2-10 Kinetic study of photodegradation :

Different experiments were conducted at the optimum condition, To check the suitability of the model for photocatalytic degradation of orange G dye using GO/ZnO nanocomposite.To ensure the reaction order we tested both pseudo-first- and pseudo-second-order kinetics. The integrated forms of the pseudo-first- and pseudo-second-order models are according to Eq. (2-11) and Eq. (2-12), respectively

$$\ln\frac{A_0}{A_t} = k_1 t \qquad \text{First order} \qquad (2\text{-}10)$$

$$\frac{1}{A_t} = \frac{1}{A_0} + k_2 t \qquad \text{Second order} \qquad (2\text{-}11)$$

where A_0 is the initial Absorbance, A_t is the Absorbance after time t , the pseudo first order kinetics degradation rate constant and was measured using the slope of linear plots ($\ln(A_0/A_t)$ versus t) (Kumar et al ., 2021) (Neto et al., 2021).

Chapter Three

Results and

Discussion

3- Results and Discussion

3-1 Characterization GO/ZnO nanocomposite

3-1-1 X-Ray Diffraction analysis for ZnO nanoparticles

X-ray diffraction technique was used to study crystallinity of synthesized ZnO nanoparticles as a catalyst, and measure the particles size of the synthesized catalyst. XRD analyses of the prepared nanocomposite were carried out using XRD6000, Shimadzu, Japan. The measuring parameters were set with 45 Cu Kα radiation (λ = 1.54056 Å) at 40kV,30mA with a rate of 5deg / min and ran at the 2θ range (3- 90˚). The average crystallite sizes of synthesized ZnO nanoparticles were measured according to the Scherer equation. The calculated value is 28.65 nm . The X-Ray diffraction patterns of zinc oxide are observed in Table (3-1) and Figure. (3-1) , zinc oxide could be indexed to the hexagonal (Ref. Pattern: zinc oxide ,No.98-002-9272),The diffraction peaks at (31.837˚, 34.502˚, 36.334˚, 47.650˚, 56.726˚, 63.012˚, 68.114˚, 69.254˚ and 89.860˚) which are corresponding to the crystallographic planes (010,002,011,012,110,013,112,021,023) respectively. As shown in Figure.(3-1),the distinguishing peaks of synthesized ZnO nanoparticles were detected at 2θ [32.09 ˚,32.73 ˚,34.99 ˚,36.61 ˚,38.06 ˚,48.09 ˚,54.39 ˚,56.99 ˚,63.61 ˚,66.83 ˚,68.45 ˚,69.75 ˚,73.47 ˚,77.51 ˚ and 82.51˚, respectively], which are corresponding to the crystallographic planes (Rajput et al ., 2021) (Irshad et al., 2018) (Maddu et al ., 2021).

Table(3-1): Average crystal size(nm) of ZnO nanoparticles, 2 Theta /deg, FWHM /deg and I/I_0.

Compound	2 Theta /deg	FWHM /deg	I/I_0	Interplanar distance (d)	Average Particle Size/nm
Zinc oxide	36.5619 34.8987 32.0141	0.30090 0.24670 0.28800	100 34 25	2.45571 2.56884 2.79342	28.65

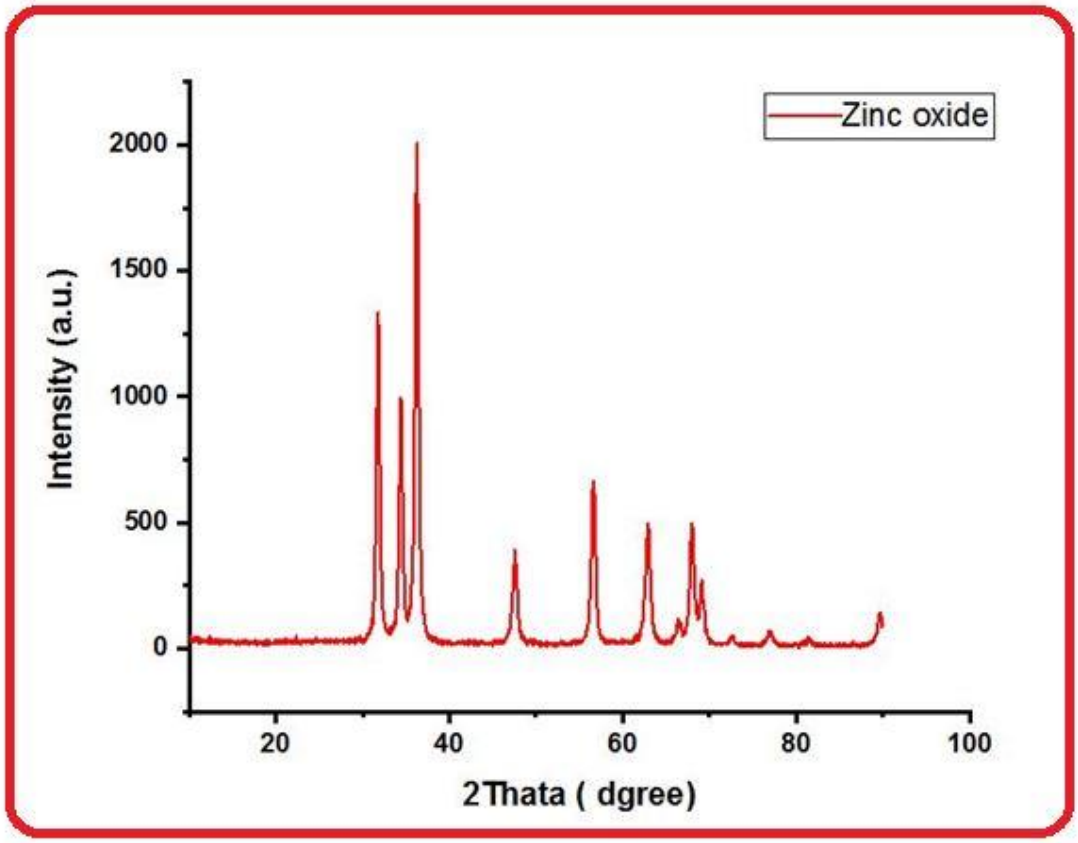

Fig. (3-1) : XRD patterns of ZnO nanoparticles.

3-1-2 X-Ray Diffraction analysis for Graphene oxide

X-ray diffraction technique was used to study the crystallinity of the Graphene oxide, measure the particles size of the synthesized catalyst. All the measurement was performed using XRD6000, Shimadzu, Japan. The measuring parameters were set with 45 Cu Kα radiation (λ = 1.54056 Å) at 40kV, 30mA with a rate of 5deg / min and ran at the 2θ range (3- 90˚). The Graphene oxide show diffraction peaks at (25.45 ˚ , 45.7 ˚) (Aqeel et al., 2019) (Kathiresan et al., 2021) . As shown in Table (3-2) and Figure. (3-2).

Table(3-2):Average crystal size(nm) of GO nanocomposite , 2 Theta /deg, FWHM /deg and I/I_0.

Compound	2 Theta /deg	FWHM /deg	I/I_0	Interplanar distance (d)	Average Particle Size/nm
Graphene oxide	25.5001 23.6537 24.6517	1.35000 0.00000 0.00000	100 85 67	3.49029 3.75839 3.60845	8.41

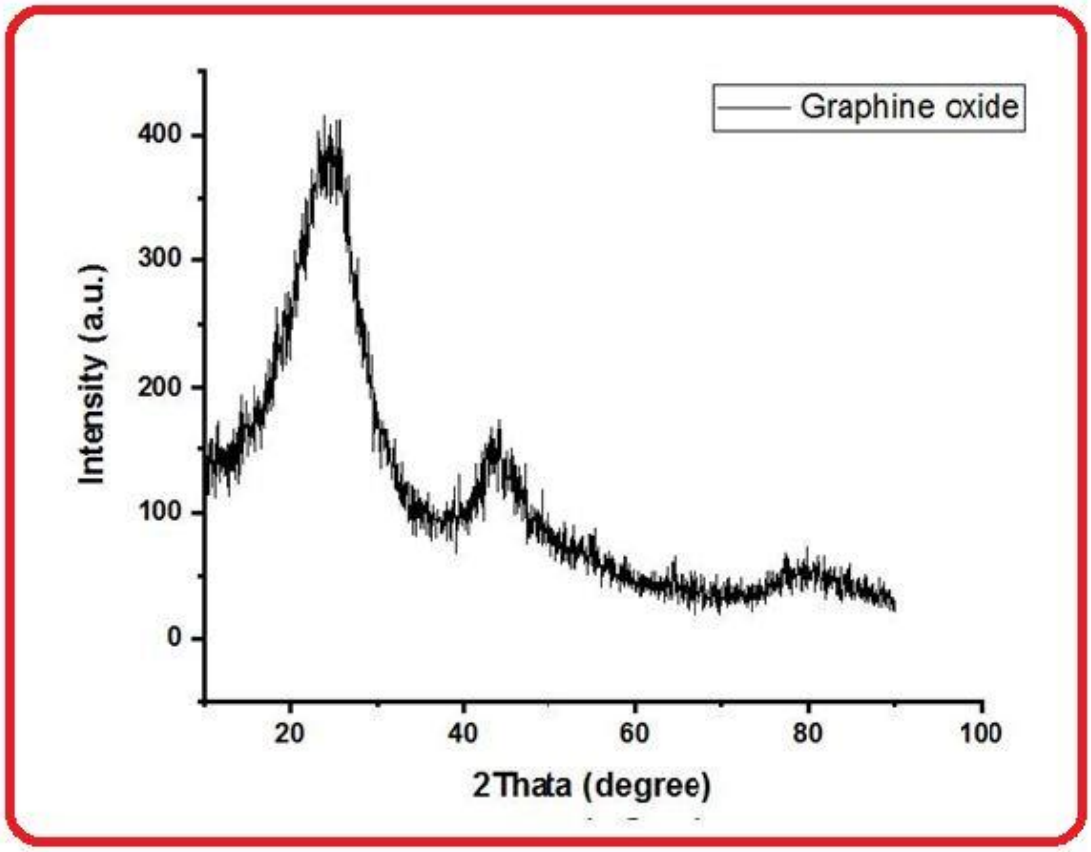

Fig. (3-2) : XRD patterns of Graphene oxide

3-1-3 X-Ray Diffraction analysis for GO/ZnO nanocomposite.

X-ray diffraction technique was used to study the crystallinity of the GO/ZnO nanocomposite as a catalyst, measure the particles size of the synthesized catalyst. All the measurement was performed using XRD6000, Shimadzu, Japan. The measuring parameters were set with 45 Cu Kα radiation (λ = 1.54056 Å) at 40kV, 30mA with a rate of 5deg / min and ran at the 2θ range (3-90˚). The GO/ZnO nanocomposite show diffraction peaks at (25.25 ˚ , 32 ˚, 35.9 ˚, 37.05 ˚ , 45.65 ˚, 48.4 ˚, 58.95 ˚, 62.95 ˚ , 68.15 ˚ and 69.25 ˚) (Munawaroh et al ., 2018) (Mahdavi et al ., 2021). As clear in Table (3-3) and Figure. (3-3).

Table(3-3): Average crystal size(nm) of GO/ZnO nanocomposite 2 Theta /deg, FWHM /deg and I/I_0.

Compound	2 Theta /deg	FWHM/deg	I/I_0	Interplanar distance (d)	Average Particle Size/nm
GO/ZnO nanocomposite	36.4029 31.9255 34.5752	0.37150 0.37160 0.29670	100 60 53	2.46607 2.80097 2.59213	23.769

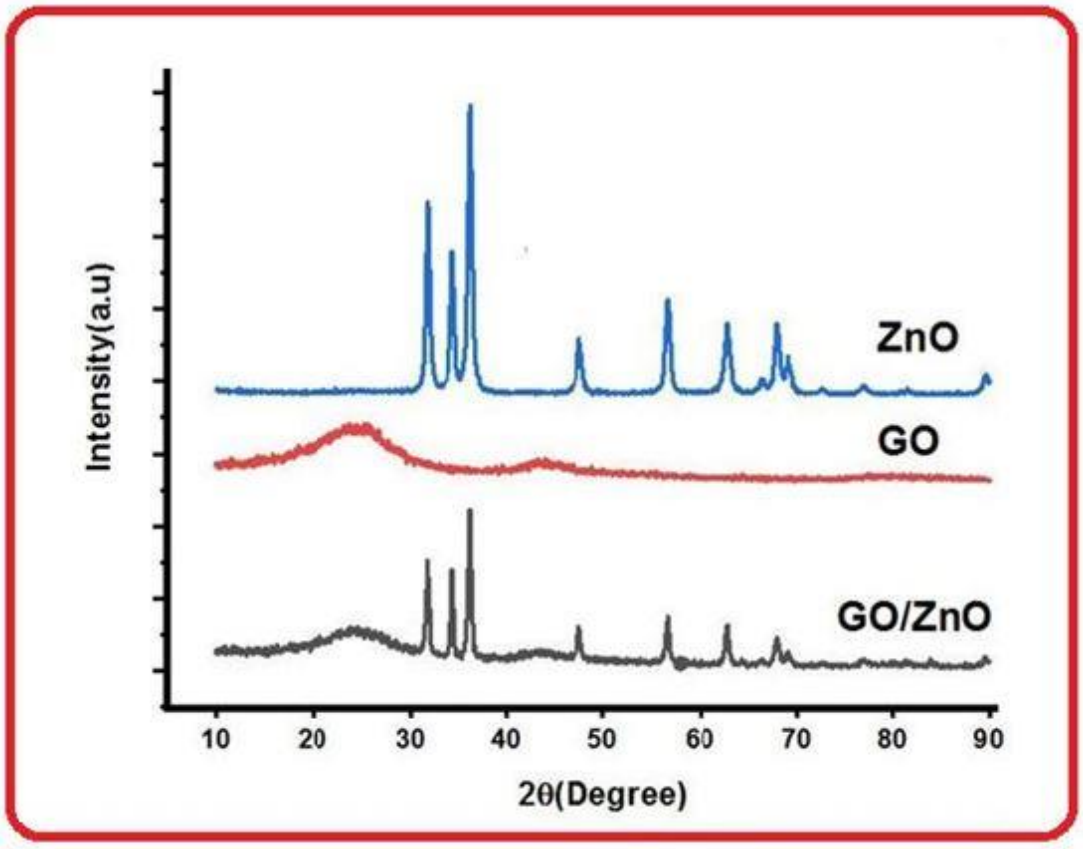

Fig . (3-3) : XRD patterns of GO/ZnO nanocomposite.

3-1-4 Determination the chemical functional groups

Investigate the unknown materials to limiting there identify; it gives good information about the functional group presence in the synthesized nanocomponent.All the information about the component can be determine by passing infrared radiation through a nanocomposite sample. The nanocomposite absorbs the infrared radiation and some of it is transmitted. The catalysts were characterized using the **SpactraIR^{-2},** Perkin Elmer Instrument, USA, at a scanning range of (400 -4000 cm^{-1})The FT-IR spectra was performed to determine the functional groups present in the synthesized zinc oxide (Imran et al., 2020) , synthesized Graphene oxide and the synthesized GO/ZnO nanocomposite respectively.

3-1-4-1- Fourier- Transform Infrared Spectroscopy synthesized Zinc Oxide :

As shown in the Figure.(3-4) FTIR spectra of synthesized zinc oxide consists of the peaks at (444.02,498.75,546.84,607.37,825.45,88018,1029.43,1111.52,1172.86,1376.88,1430.76,2370.23,2921.64,3350 cm^{-1}) . The absorption peak was appear at 3333 cm^{-1} represent to the stretching vibrations of the (OH) groups. The band located at 2895 cm^{-1} represent (CO_2) groups. The peak at 14340 cm^{-1} can be attributed to the (- C-H) bond . The band located (C-OH) at 1034 cm^{-1} , band located (C-C) at 622 cm^{-1} and band located (Zn-O) at 501 cm^{-1} (Margaret et al ., 2021) (Resmi et al., 2021).

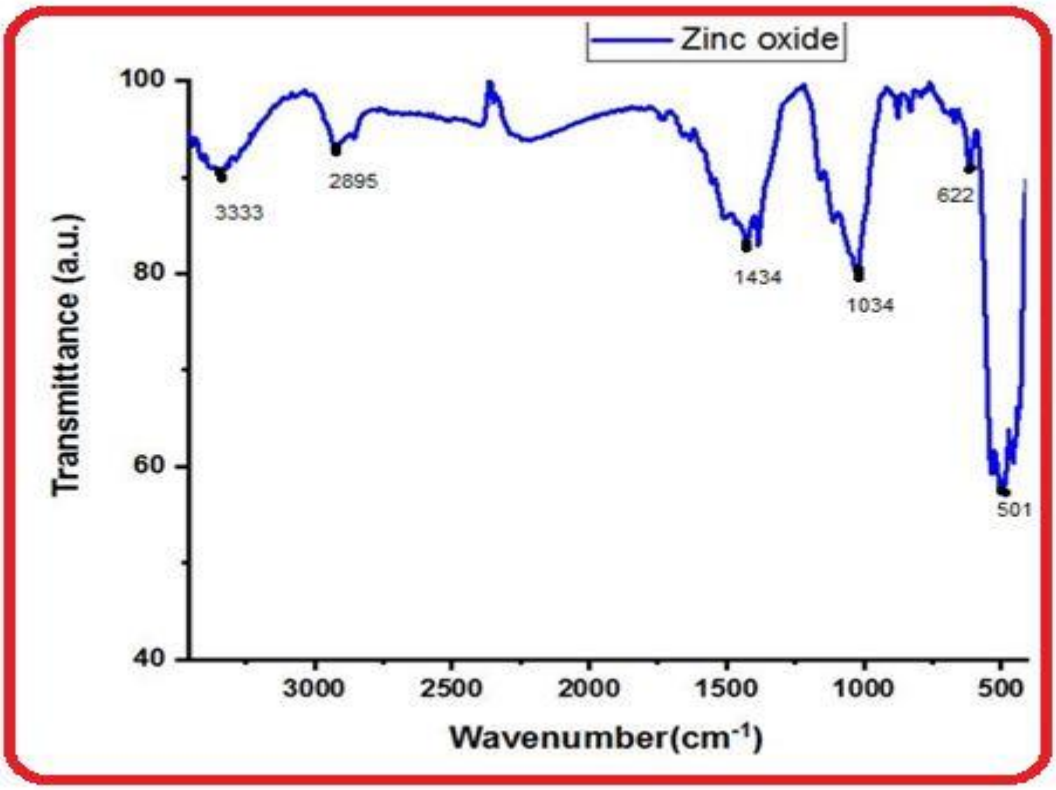

Fig . (3-4) : FTIR patterns of synthesized Zinc Oxide .

3-1-4-2- Fourier- Transform Infrared Spectroscopy synthesized Graphene oxide:

Fourier- Transform Infrared Spectroscopy was used for examined the functional group of the synthesized Graphene oxide. As shown in Figure.(3-5) the spectrum consists of the peaks at (471.39,532.75,825.45,1016.16,1124.79,2349.50,2363.59,2847,2921.64,3445.68 cm^{-1}). The typical peaks of the oxygen-containing functional groups emerge in the IR spectra of GO at 1650 cm^{-1} (C=O), 1137 cm^{-1} of (C–OH) and 612 cm^{-1} of (C–O-C) groupe , respectively. and 1632 cm^{-1} due to aromatic (C=C) vibrations . The band located (C-H) at 3114cm^{-1} and band located (OH) groups at 3445 cm^{-1} , show that GO has changed structurally. (Alam et al., 2017) (Durmus et al., 2019) (Al-Rawashdeh et al., 2020) .

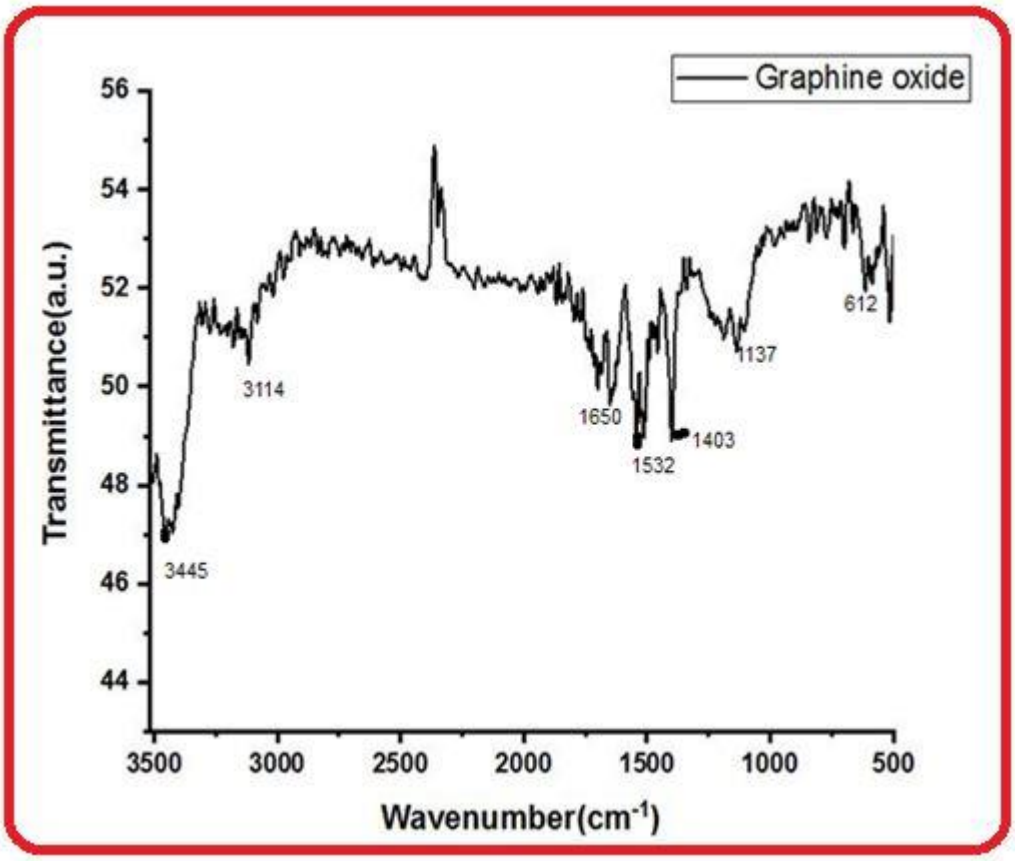

Fig. (3-5) : FTIR patterns synthesized Graphene oxide

3-1-4-3- Fourier- Transform Infrared Spectroscopy synthesized GO/ZnO nanocomposite .

For the GO/ZnO nanocomposite consists of the peaks at (471.39,532.75,825.45,1016.16,1124.79,2349.50,2363.59,2847,2921.64,3445.68 cm^{-1}).

The absorption peak was appear at 3407 cm^{-1} represent to the stretching vibrations of the (OH) groups. The band located at 2922 cm^{-1} represent (CO_2) groups. The band located at 1582 cm^{-1} represent (C=O) symmetric groups .The peak at 1049 cm^{-1} can be attributed to the (C-O) bond and 1414 cm^{-1} (C=C)) . The band located (C-O-C) at 680 cm^{-1} and 485.48 cm^{-1} of Zn-O. (Mohamed et al., 2019) Allresults are in Figure. (3-6) **.**

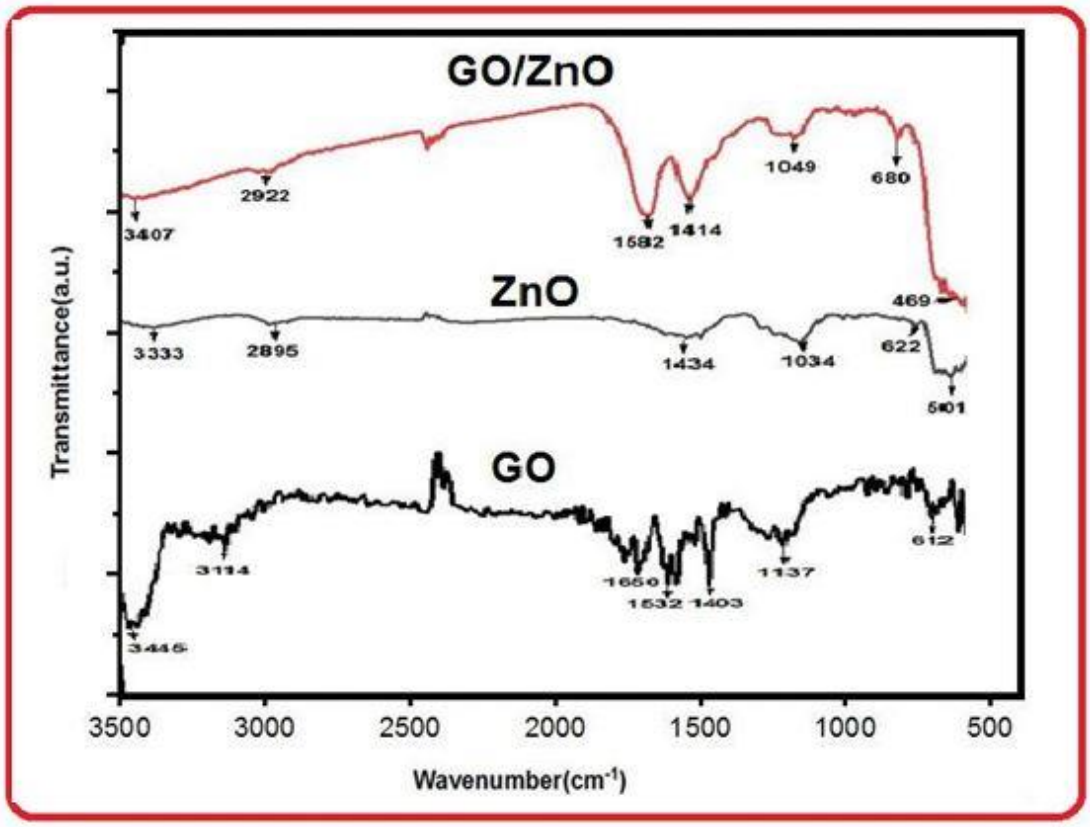

Fig. (3-6) : FTIR GO/ZnO nanocomposite.

3-1-5- Scanning Electron Microscopy (SEM) for synthesized GO/ZnO nanocomposites .

Scanning Electron Microscopy techniques was used to study the morphology of GO/ZnO nanocomposites in order to obtained useful information about the structure of the synthesized GO/ZnO nanocomposite by using SEM, Zeiss , Germany. SEM images, Gaussian and histogram of GO/ZnO nanocomposites are illustrated in Figure.(3-7).SEM micrograph analysis was appeared as irregular distributed aggregated along with aspherical shape. The average grain size measured from histogram was in the range of (40-60nm) ,and the grain size equal (48.75 nm) from Gaussian (Chen et al., 2020) (Ainali et al., 2021).

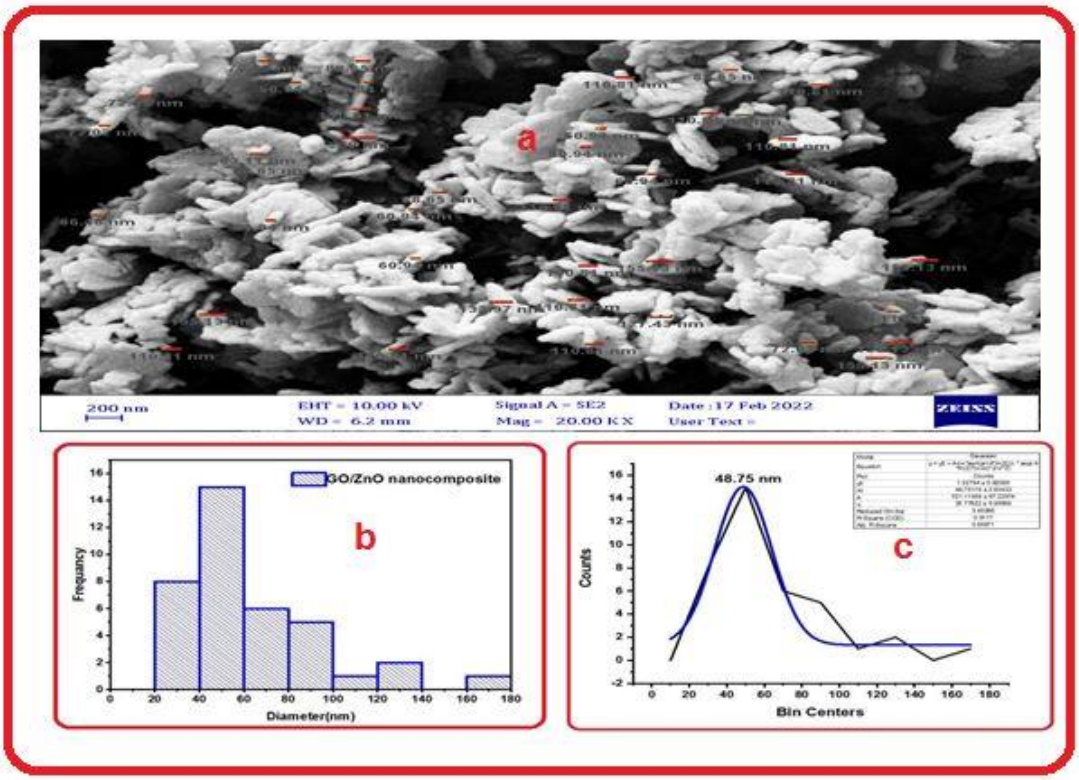

Fig . (3-7) : SEM pattern of GO/ZnO nanocomposite.

3-1-6 Energy Dispersive X-ray spectroscopy (EDX) of GO/ZnO nanocomposites:

Energy dispersive x-ray spectroscopy (EDX) analysis was carried out to determine the composition of the prepared GO/ZnO nanocomposite. The EDX spectrum in Fig.(3-8) indicates that the particles in the synthesized GO/ZnOnanocomposite consisting of (C, O, and Zn) elements confirming successfully prepared of nanocomposite. The atomic percentage of O is (14.3%) , C is (43.20) and Zn is (42.50 %) , respectively. (Azim et al., 2018) (Yaqoob et al., 2021)

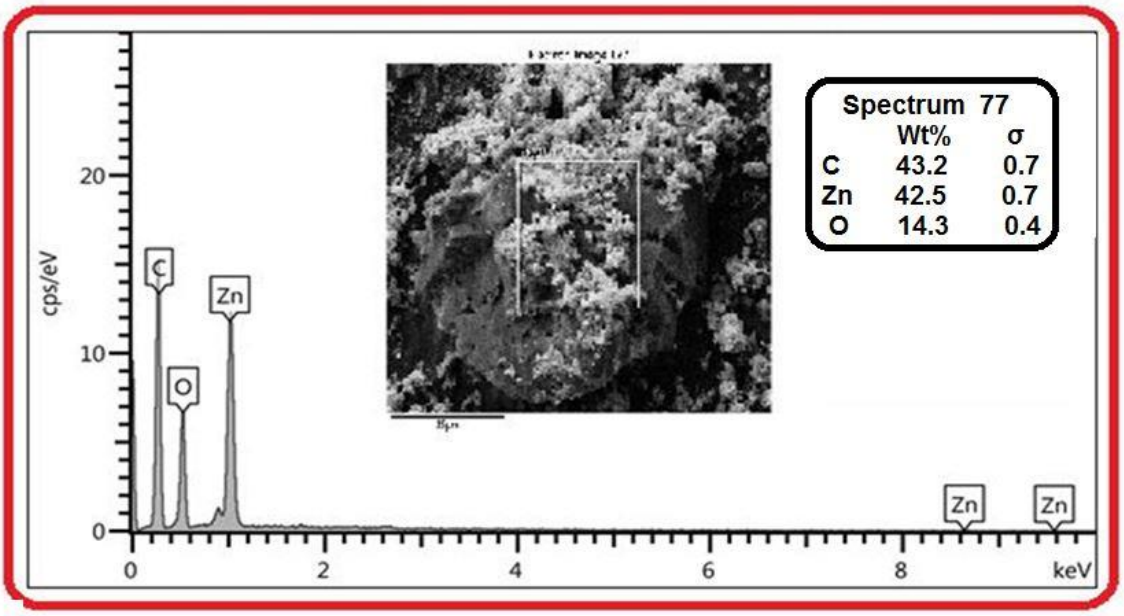

Fig. (3-8) : EDX spectrum of GO/ZnO nanocomposites .

3-1-7 Brunauer–Emmett–Teller (BET) Surface Area of the prepared GO/ZnO nanocomposite:

Brunauer–Emmett–Teller method was used for determine the surface area of a prepared GO/ZnO nanocomposite, was investigated by using nitrogen adsorption-desorption isotherm , as shown in Figure. (3-10). From the results a specific surface area and pore volume were obtained as (220.23 m^2 /g) and (0.111 cm^3 /g), respectively. As found in the literature the specific surface area of the commercial ZnO catalyst has been calculated as (64.4 m^2 /g).Thus synthesized GO/ZnO nanocomposite with larger surface area may provide active sites for photocatalytic degradation of pollutants (Sun et al., 2020).

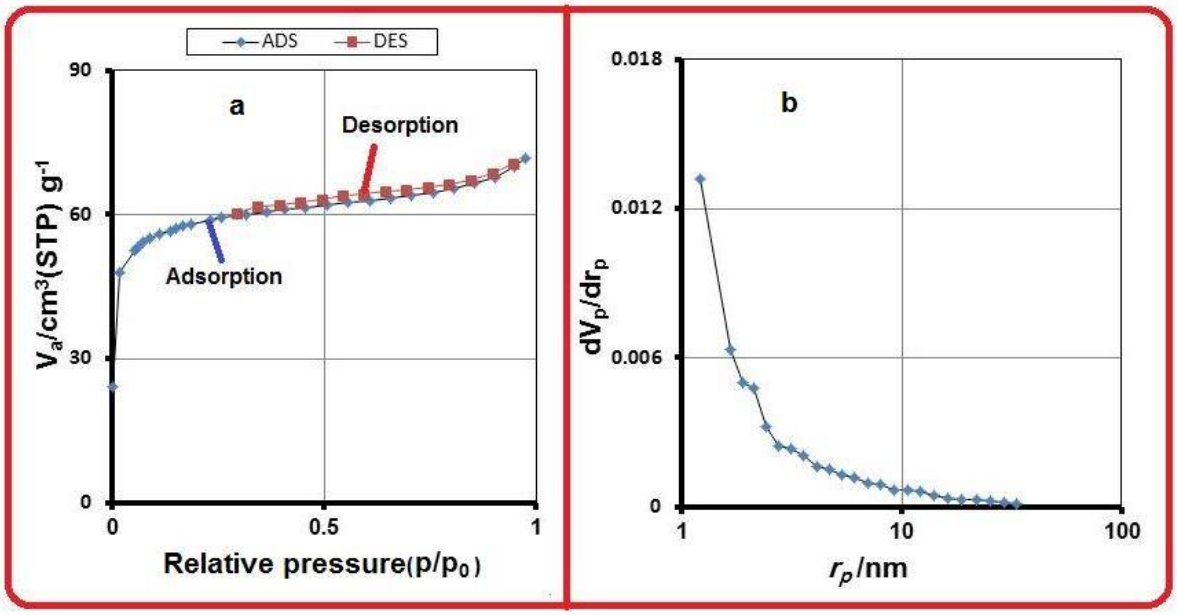

Fig.(3-9) : a- Nitrogen adsorption-desorption isotherm of prepared GO/ZnOnanocomposite , b- Pore size distribution curves of nanostructured catalysts .

3-1-8 Thermo Gravimetric Analysis (TGA) for GO/ZnO nanocomposite :

TGA is an analytical technique was used to determine the temperature decomposition of metal precursors using the NETZSCH STA 2500 TGADTA setup, which operates at room temperatures up to (800 °C) (Nayl et al., 2019). Thermal properties of GO/ZnO nanocomposite were investigated using Thermogravimetric analysis(TGA), the sample weighed approximately (10 mg) and was placed inside a platinum crucible with air or nitrogen flowing at a rate of (20 cm^3 min^{-1}). As clear in the Figure.(3-11) , a major weight loss (3.300 mg) was observed in the range (250 – 580°C), this weigh loss was about (65.609 %) for GO/ZnO nanocomposite is contributed by destruction of the carbon dioxide, or the removal of impurities, and unreacted monomers of omposite (Badvi et al., 2021).

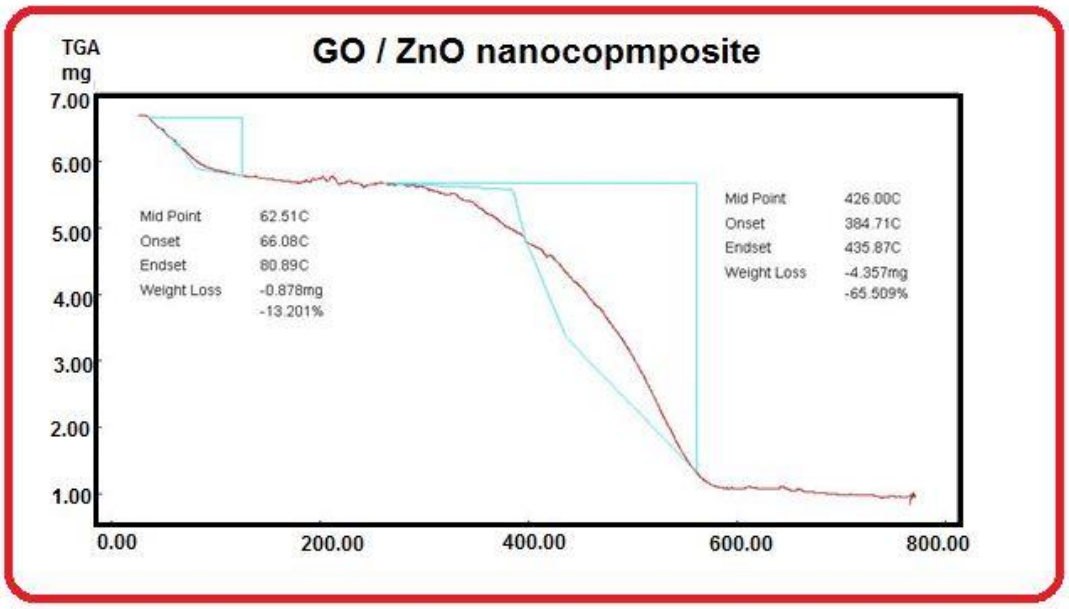

Fig.(3-10):Thermogravimetric analysis (TGA) of GO/ZnO nanocomposite .

3-2 Photocatalytic degradation of orange G dye

3-2-1 Preliminary experiments

Many experiments were performed to reach the optimum conditions of the photocatalytic degradation processes. The first reaction has been done using (10mg/L) of orange G dye with the addition of (0.15 g/100mL) of GO/ZnO nanocomposite under solar lamp and(10ml/min) flow rate of air at room temperature (25°C) and (pH=8.7) (photocatalytic process). The second reaction has been carried out using (10mg/L) of dye in the dark using (0.15 g/100mL) of GO/ZnO nanocomposite and (10ml/min) flow rate of air at room temperature (25°C) and (pH=8.7) (adsorption). The third reaction was performed using the same solution but without addition of GO/ZnO nanocomposite under solar lamp(photolysis). The results are plotted Figure. (3-11) .The experiments showed in the presence of solar irradiation wihout addtion GO/ZnO nanocomposite, the degradation of

orange G dye by (16.18%) . The addition of catalysts to suspension aqueous solution , without solar irradiation, decreases the pollutant degradation of orange G dye. However, the efficiency was (32.94 %) when employed GO/ZnO alone (adsorption process) (Abdel-Khalek etal ., 2018) . Furthermore, presence of GO/ZnO nanocomposite with solar lamp enhanced photocatalytic degradation of orange G dye**,** the photocatalytic degradation efficiency was estimated by examining the photo degradation of orange G dyeand was compared to 90.69% (Nenavathu et al., 2018).

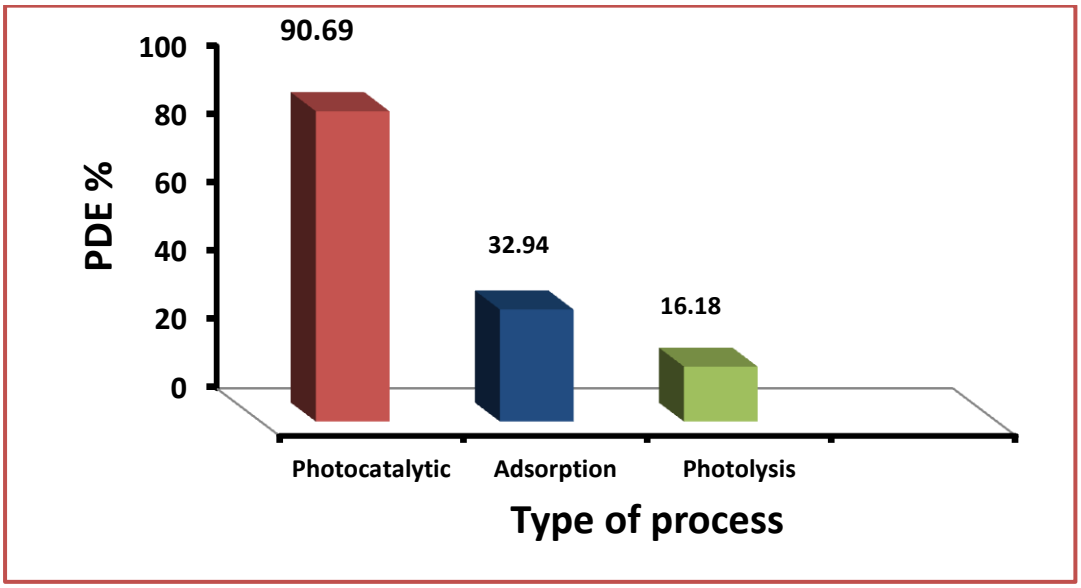

Fig.(3-11) : The variation of PDE% of orange G dye with type of process .

3-2-2 Effect of different process on the photo-catalytic-degradation for orange G dye.

photocatalytic degradation of different types of pollutants such as organic dyes is reactions occurs on the surface of the semiconductors (TiO_2, ZnO, and many prepared nanocomposite) , The parameter that will affect the surface properties of semiconductors will have an impact on the photocatalytic degradation efficiency. In this part reviews different kind of parameters that was reported to affect the photocatalytic degradation efficiency of dyes (Niu et al ., 2020) (Rashid et al., 2016).

3-2-2-1 Effect of the mass of GO/ZnO nanocomposite on photo catalytic degradation of the orange G dye

The effect of mass of GO/ZnO nanocomposite on Photocatalytic degradation of orange G dye, was studied using (10 mg/L) of dye, flow rate of air (10mL/min), temperature (25°C) and (pH=8.7). When the masses of GO/ZnO nanocomposite increases until reach to the mass (0.15g/100mL) photo catalytic degradation of orange G dye, gradually increases, then gradually decreases. When the mass of GO/ZnO nanocomposite (0.15g /100mL) the semiconductor can be provide the highest absorpption of light. The decrease in the efficiency of photo degradation process at the masses of GO/ZnO nanocomposite higher than (0.15 g/100 mL) due to the light absorption will be limited only to the first layers of orange G dye and the other layers of solution do not receive photons.Moreover light scattering at high GO/ZnO nanocomposite loading , this lead to decrease the photon intensity, therefor the strong absorption of light through the first successive layers of solution and prevent light from passing through all other layers in the reaction vessel . Table (3-4) and Figure.(3-12).Many workers studied this effect , At the loading mass of GO/ZnO nanocomposite below the

optimum value (0.15 g/100 mL) the rate of photo degradation of orange G dyealso decrease due to the quantity of mass of GO/ZnO nanocomposite decrease that mean the surface area decrease which lead to decrease of light absorption of light by GO/ZnO nanocomposite which cause lower photo degradation rate of orange G (Alshehri et al., 2020) (Jamil et al., 2020).

Table (3-4):The chang in A_t/A_0 with irradiation time on different masses of GO/ZnO nanocomposite .

Catalyst mass of (GO/ ZnO) g/100ml	**0.01**	**0.03**	**0.06**	**0.15**	**0.7**
Irradiation Time/min	**At/A0**				
0	**1**	**1**	**1**	**1**	**1**
10	**0.86**	**0.82**	**0.74**	**0.58**	**0.96**
20	**0.69**	**0.61**	**0.51**	**0.32**	**0.89**
30	**0.57**	**0.47**	**0.32**	**0.12**	**0.81**
40	**0.44**	**0.35**	**0.19**	**0.07**	**0.76**
50	**0.34**	**0.26**	**0.14**	**0.05**	**0.72**
60	**0.30**	**0.23**	**0.12**	**0.04**	**0.67**
70	**0.27**	**0.20**	**0.10**	**0.04**	**0.65**
80	**0.25**	**0.17**	**0.07**	**0.03**	**0.63**

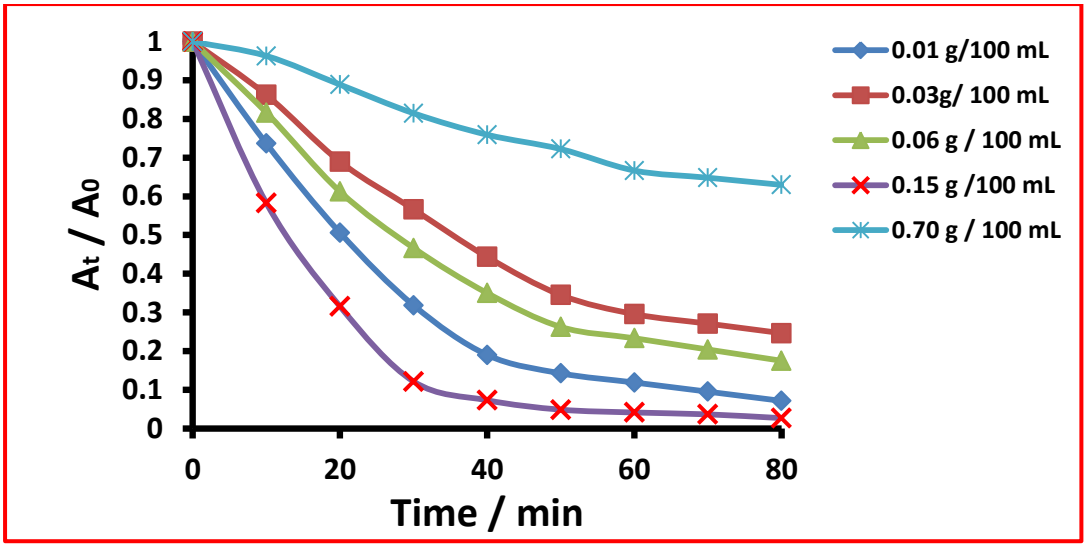

Fig.(3-12) : Variation in (A_t / A_0) with irradiation time at (10 mg/L) of the prepared dye.

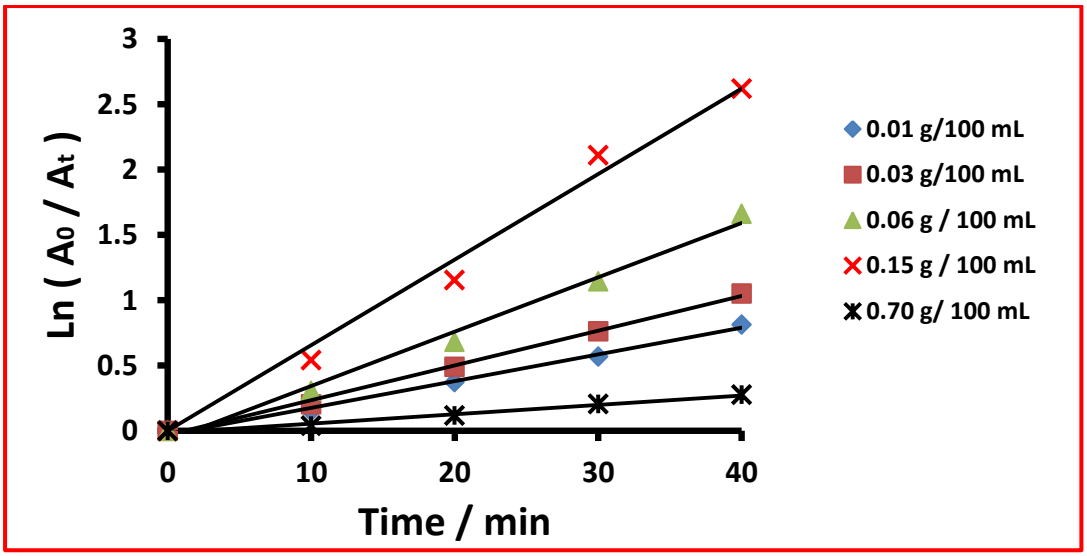

Fig.(3-13) : Chang in Ln (A_0 / A_t) through irradiation-time at different of the mass of GO/ZnO nanocomposite using UV radiation .

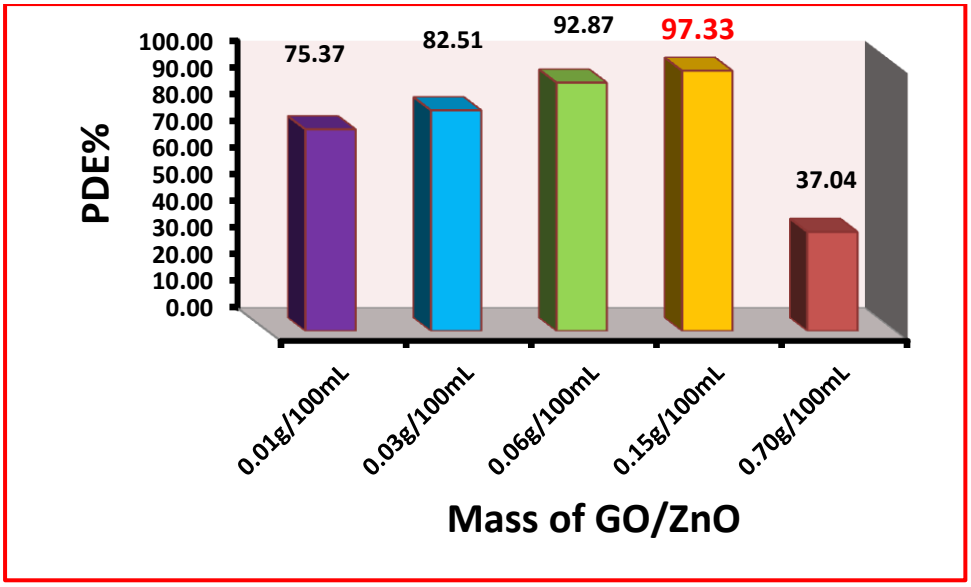

Fig. (3-14) : Photocatalytic degradation efficiency using (10mg/L) of orange G against mass of GO/ ZnO nanocomposite .

3-2-2-2 Effect of orange G dye initial concentration on the photocatalytic degradation process

The effect of orange G dye concentration solution in the photocatalytic degradation processes in the range (10-50 mg/L) was tested by keeping all the other experimental conditions constant at temperature (25°C), flow rate of air (10mL/min), (pH=8.7) and mass of GO/ZnO (0.15g/100mL).The results are plotted in Table(3-5) and Figure.(3-15).These result indicate the rate of Photocatalytic degradation reduced with the increasing of initial dye concentration . As initial orange G dye concentration decreases, the path length of the photon entering the solution increase so the number of photons reaching to catalyst surface increase and hence rate of formation hydroxyl radicals and super oxide ions are increases thereby increasing rate of degradation (ALjeboree et al., 2019) (Mondol et al., 2021).

Table (3-5): chang of A_t/A_0 through irradiation-time on different-concentration for orange G dye .

Concentration of orange G dye (mg/L)	10	20	30	40	50
Iradiation Time min	A_t/A_0				
0	1	1	1	1	1
10	0.73	0.84	0.92	0.97	0.99
20	0.49	0.69	0.80	0.88	0.95
30	0.31	0.50	0.72	0.81	0.90
40	0.20	0.31	0.57	0.74	0.84
50	0.12	0.21	0.46	0.65	0.74
60	0.05	0.18	0.36	0.53	0.63
70	0.04	0.16	0.27	0.48	0.58
80	0.03	0.13	0.27	0.47	0.57

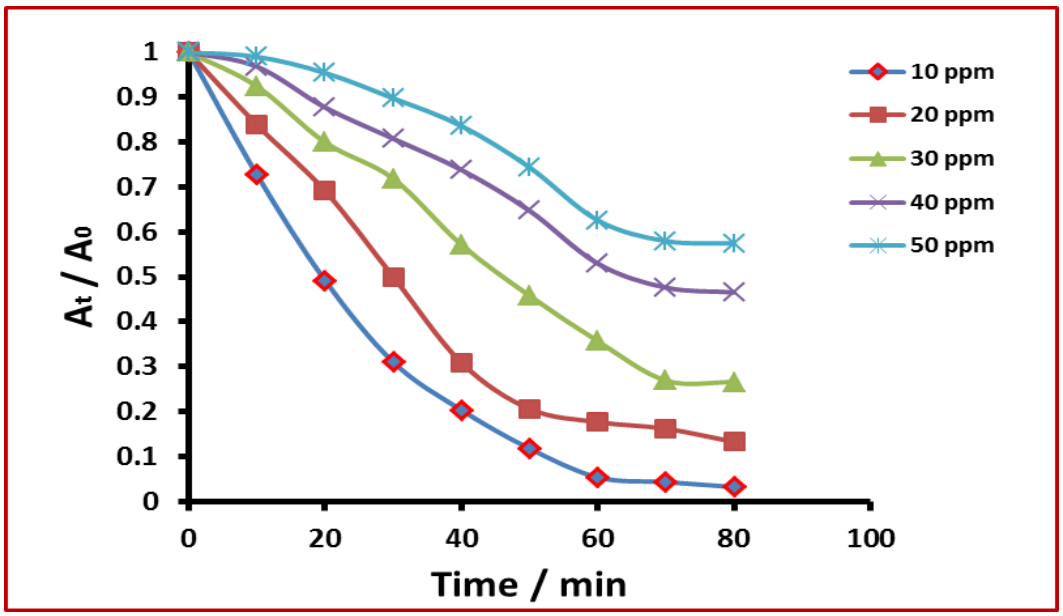

Fig. (3-15) : Variation in (A_t / A_0)with irradiation time at different concentrations of dye

Langmuir–Hinshelwood rate expression has been successfully used for heterogeneous photocatalytic degradation to determine the relationship between the initial degradation rate and the initial concentration of the organicsubstrate. The Langmuir–Hinshelwood model is expressed as Eq. (2-4)and (2-5).

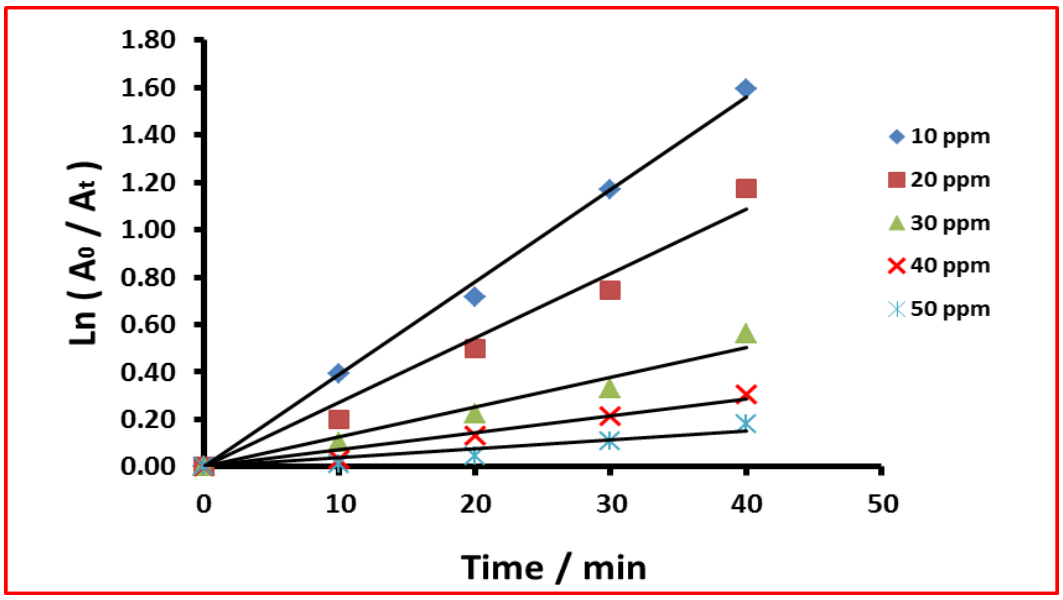

Fig.(3-16): Linear variation of $\ln(A_0 / A_t)$ versus time for the photocatalytic degradation of orange G dye at different initial concentrations.

The results showed that the kinetics of photocatalytic reaction fit the Langmiur– Hinshelwood kinetics model well. Therefore, the absorption of orange G on the thin film surface is the controlling step in the whole degradation process.

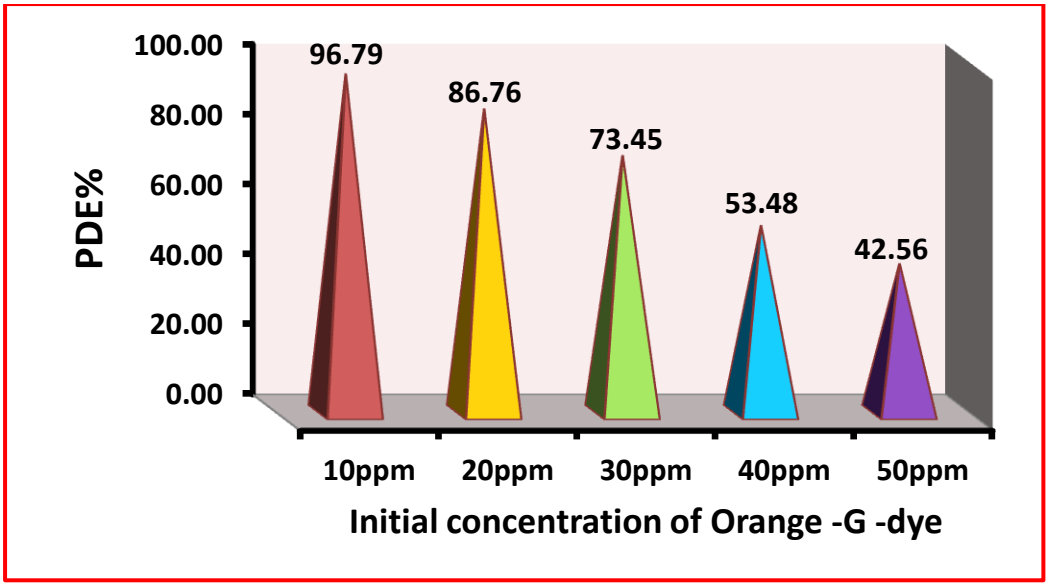

Fig. (3-17) : Photocatalytic degradation efficiency using 0.15 g / 100 mL GO/ ZnO nanocomposite against different concentration of orange G dye .

3-2-2-3 The effect of light intensity on photodegradation of orange G dye using GO/ZnO nanocomposite

Different experiments were accomplished for studding the influence of light intensity on photocatalytic degradation of orange G dyein range (1 – 9 mW/cm^2) .By conservation other experimental conditions apply constant at initial Orange G dye concentration of (10 mg/L), prepared GO/ZnO catalyst dosage was (0.15 g /100mL) , (10 mL/min) flow rate of an air bubble at temperature (25°C), (pH=8.7).The results in Table(3-6) and Figure.(3-18) show that the degradation process of dye progressively increased with increase in the light intensity (Ebrahimi et al., 2020) (Siong et al., 2019). This may be attributed to the increased photons formation required for the electron transfer from the valence band to the conduction band of catalyst.

Table(3-6):The change of A_t/A_0 through irradiation-time on different light intensity.

Light-intensity / m W/cm^2	1	3	5	7	9
Iradiation Time min	A_t/A_0				
0	1	1	1	1	1
10	0.69	0.81	0.88	0.92	0.94
20	0.46	0.65	0.76	0.81	0.92
30	0.33	0.52	0.65	0.70	0.77
40	0.17	0.39	0.52	0.58	0.67
50	0.08	0.26	0.41	0.49	0.59
60	0.06	0.17	0.35	0.40	0.51
70	0.04	0.11	0.29	0.36	0.40
80	0.02	0.09	0.24	0.28	0.33

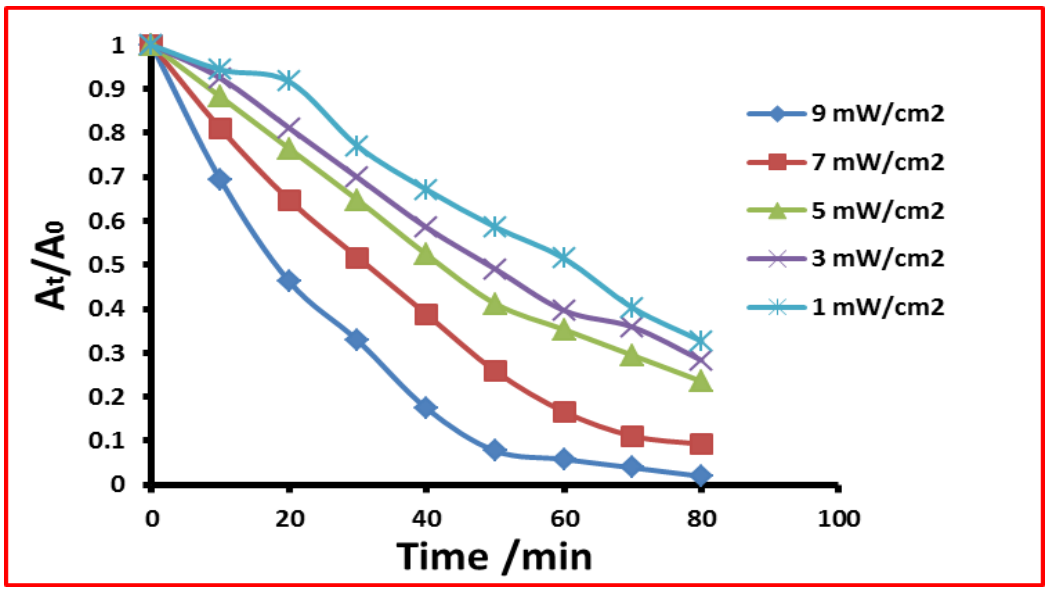

Fig. (3-18) : Variation in (A_t / A_0)with irradiation time at different light intensity.

3-2-2-4 Effect of pH on photocatalytic degradation of orange G dye:

A set of works was performed to investigate the effect of initial pH of suspension solution on the ability photocatalytic degradation of orange G dyeover (0.15 g /100mL) of GO/ZnO nanocomposite ,(10mg/L) of orange G dye concentration, (10 mL/min) flow rate of an air bubble at temperature (25°C). The practical experiments was carried out under pH solution (3.76 , 5.62 , 8.74 and 10.32). As shown in the Table (3-7) and Figure.(3-19) the optimum value of degradation orange G dye, was determined at (pH=8.74).At pH in the acidic medium the surface of catalyst become acidic this lead to increase repulsion of dye molecules with catalyst surface, and hence decreases photocatalytic degradation efficiency (Abilarasu et al., 2021). While at higher pH function in the basic medium increase the attractive force between molecular dye and catalyst surface and hence increase photocatalytic degradation efficiency(Kurniawan et al ., 2020).

Table (3-7): chang for A_t/A_0 through irradiation-time on diffrent pH value .

Initial-pH solution	3.76	5.62	8.74	10.32
Iradiation Time /min	A_t/A_o			
0	1	1	1	1
10	0.98	0.98	0.97	0.98
20	0.97	0.97	0.92	0.95
30	0.95	0.94	0.87	0.91
40	0.95	0.93	0.86	0.89
50	0.94	0.91	0.80	0.83
60	0.94	0.90	0.71	0.76
70	0.92	0.87	0.68	0.71
80	0.92	0.85	0.66	0.65

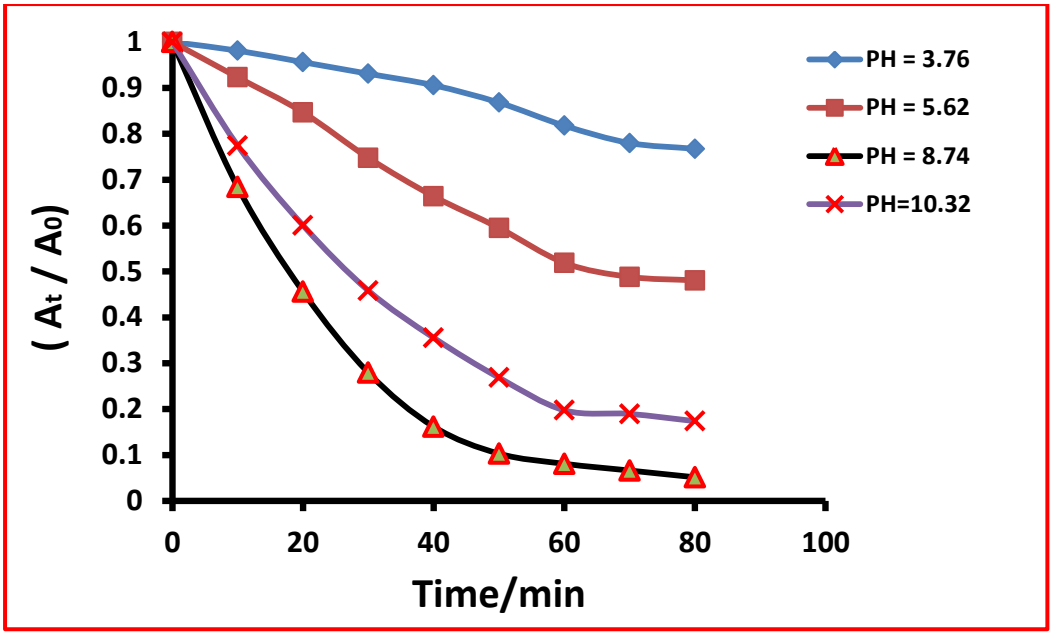

Fig.(3-19) : Variation in (A_t / A_0)with irradiation time at different initial pH solution .

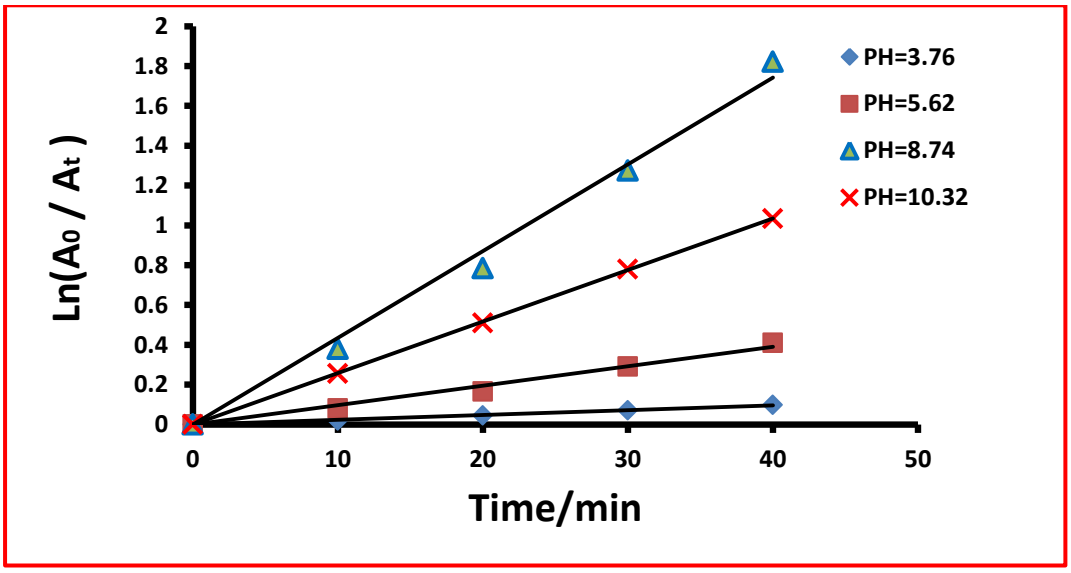

Fig.(3-20) : Chang in Ln (A_0 / A_t) through irradiation-time at different pH using UV radiation, initial orange G dye .

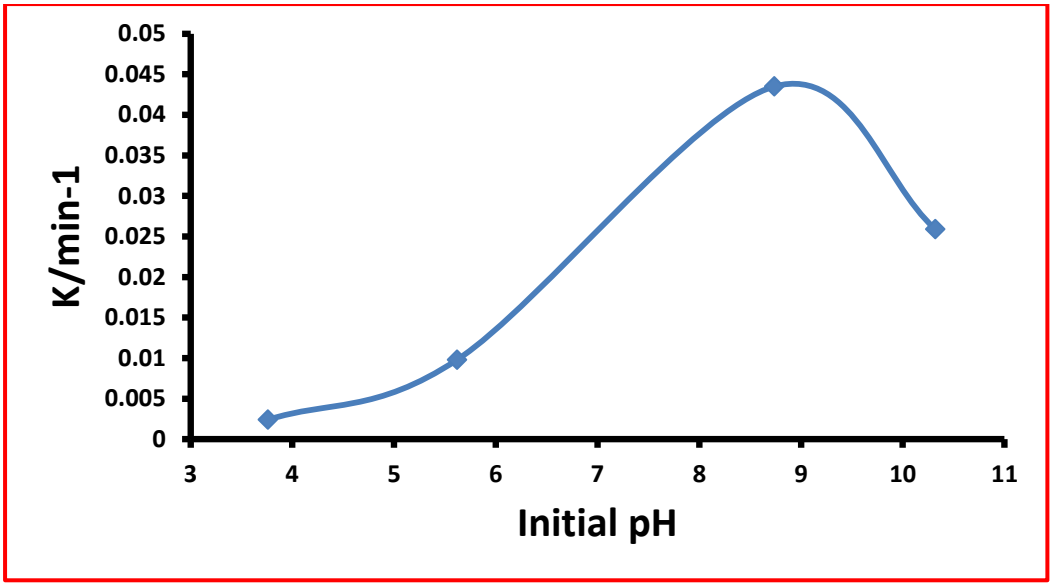

Fig. (3-21) : Effect of pH on photo degradation rate constants

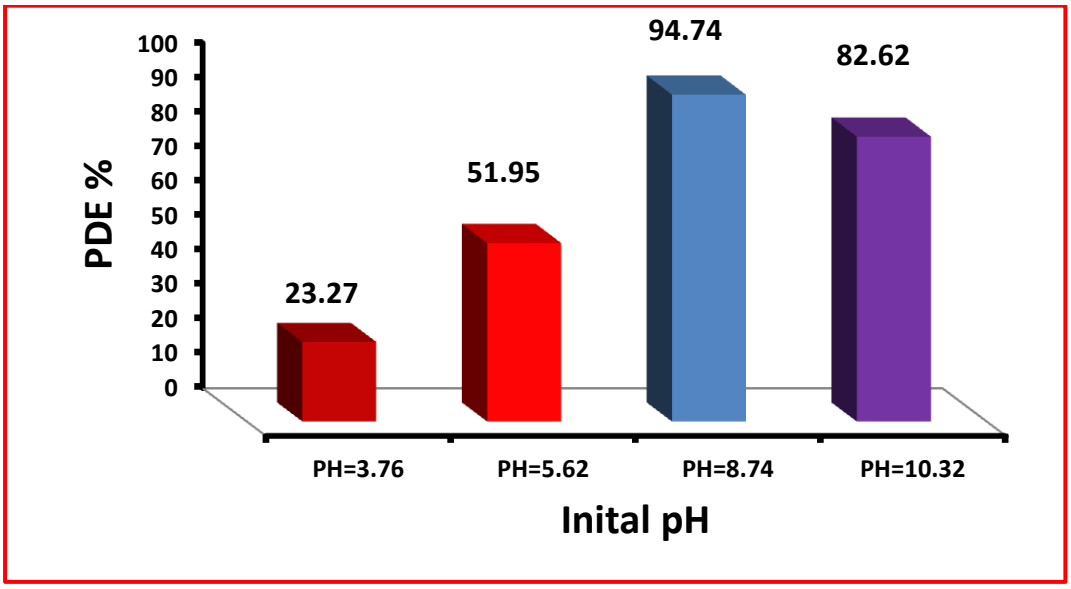

Fig.(3-22) : Photocatalytic degradation efficiency using (0.15g / 100 mL) GO/ZnO nanocomposite and (10 mg/L) of orange G dye for different initial pH.

3.2.2.5 : Effect of the hydrogen Peroxide

Deferent experiments were performed to study the effect of the initial hydrogen peroxide concentration range (0.3 ,1.5, 3.0, 3.9 and 4.5 %) on the photocatalytic degradation of dye by GO/ZnO naocomposite was investigated at initial (pH 8.74), catalyst dosage (0.15 g/100 mL), and initial concentration of orange G dye (10 mg/L), (10 mL/min) flow rate of an air bubble at temperature (25°C) for different time intervals. Figure.(3-23) shows the effect of the hydrogen peroxide concentration on photocatalytic degradation of dye . Figure. (3-26) shows the degradation efficiency enhanced from (71.83 to 96.32%) by increasing the initial hydrogen peroxide concentration from (0.3,1.5,3.0,3.9 and 4.5%). The increased photocatalytic degradation efficiency of orange G after the addition of hydrogen peroxide can be explained by the increased reaction between hydrogen peroxide and electron in the conduction band of orange G. According to , hydrogen peroxide can effectively inhibit the electron–hole recombination. Since hydrogen peroxide is a better electron acceptor than dissolved oxygen, it could act as an alternative electron acceptor to oxygen.At low concentration of hydrogen peroxide, inhibition of the electron–hole recombination is effectively contributed to the photocatalytic degradation of orange G dye. However, further increase in hydrogen peroxide concentration above (3%) caused lower degradation of orange G due to an inhibitive effect on the reaction between orange G and electron in the conduction band of GO/ZnO nanocomposite. The other reason for the inhibition effect can also be explained in terms of scavenging of positive holes by adsorbed H_2O_2 on the surface of GO/ZnO nanocomposite (Danyliuk et al., 2021) (Aziztyana et al., 2019) (Sharma et al ., 2021). The added H_2O_2 could accelerate the reaction by

producing hydroxyl radicals from scavenging the electrons and absorption of UV-light by the following reactions :

$$H_2O_2 + e^-_{(c.b.)} \rightarrow {}^{\bullet}OH + {}^{-}OH \quad (3\text{-}3)$$

$$H_2O_2 + O_2{}^{\bullet -} \rightarrow {}^{\bullet}OH + {}^{-}OH + O_2 \quad (3\text{-}4)$$

$$H_2O_2 + h\nu \rightarrow 2{}^{\bullet}OH \quad (3\text{-}5)$$

By addition of excess H_2O_2, it acts as hydroxyal radical or hole scavenger to form the perhydroxyl radicals $(HO_2^{\bullet})$ which is a much weaker oxidant than hydroxyl radicals **:**

$$H_2O_2 + {\bullet}OH \rightarrow H_2O + HO_2^{\bullet} \quad (3\text{-}6)$$

$$H_2O_2 + h^+ \rightarrow H^+ + HO_2{}^{\bullet} \quad (3\text{-}7)$$

Table (3-8): chang for A_t/A_0 through irradiation-time on diffrent initial H_2O_2 solution value .

initial hydrogen Peroxide solution % v/v	0.3	1.5	3	3.9	4.5
Iradiation Time min	A_t/A_o				
0	1	1	1	1	1
10	0.45	0.60	0.89	0.93	0.96
20	0.32	0.51	0.80	0.88	0.92
30	0.22	0.50	0.74	0.78	0.87
40	0.16	0.41	0.63	0.70	0.79
50	0.09	0.31	0.56	0.63	0.70
60	0.06	0.26	0.52	0.56	0.68
70	0.04	0.10	0.46	0.50	0.60
80	0.03	0.06	0.42	0.46	0.52

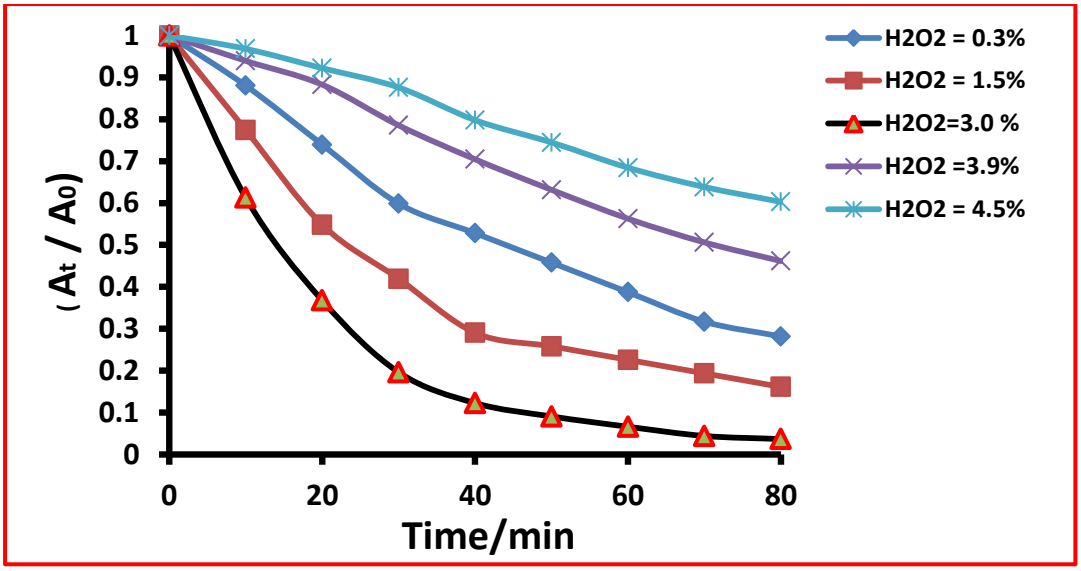

Fig. (3-23) : Variation in (A_t / A_0)with irradiation time at different initial H_2O_2 solution.

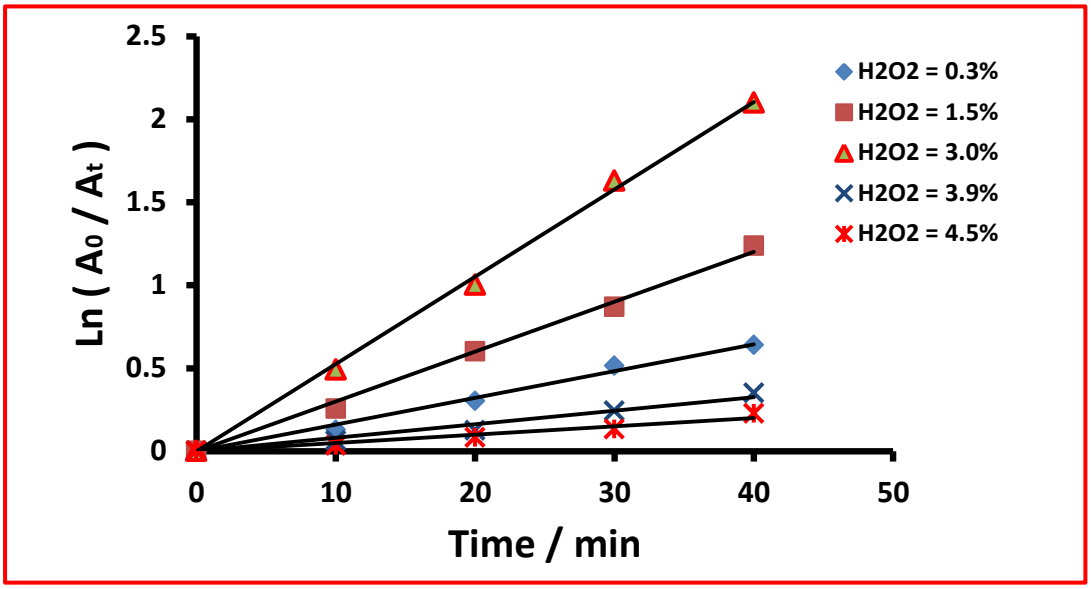

Fig.(3-24) : Chang in Ln (A_0 / A_t) through irradiation-time at different-H_2O_2 using UV radiation, initial orange G dye.

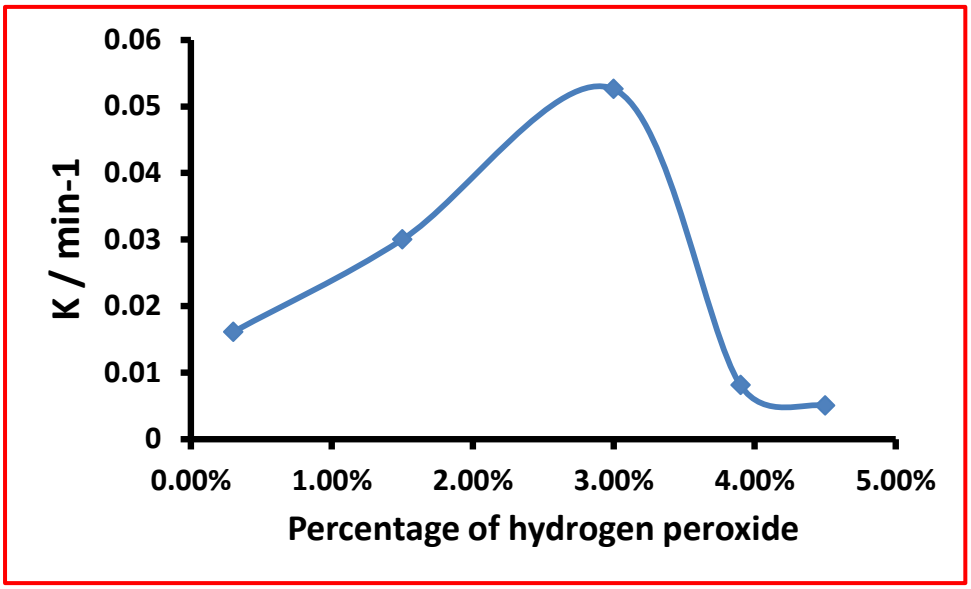

Fig. (3-25) . Effect of H_2O_2 on photo degradation rate constants

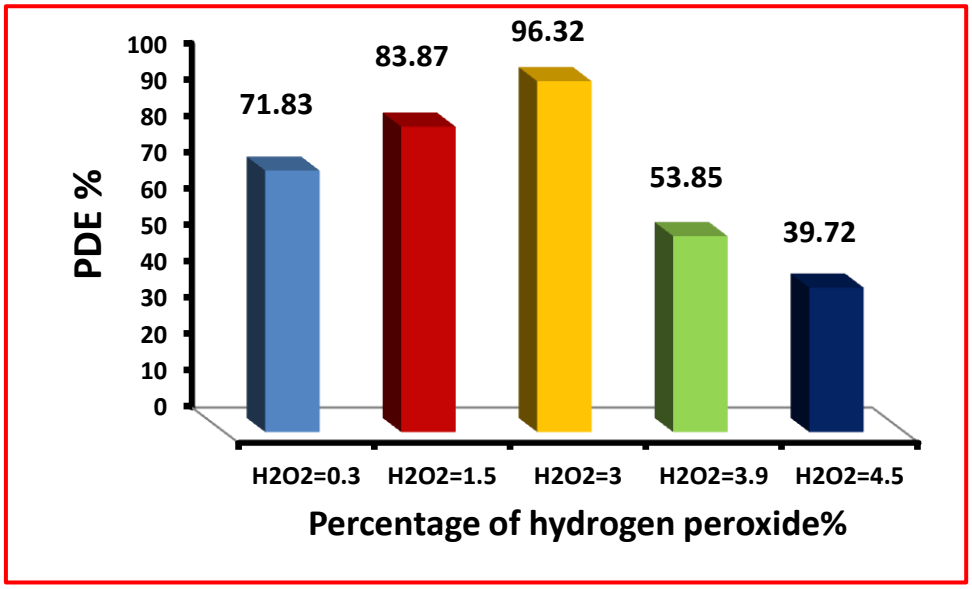

Fig. (3-26) . Photocatalytic degradation efficiency using (0.15g / 100 mL) GO/ZnO nanocomposite and (10 mg/L) of orange G dye for different H_2O_2 concentrations.

3-2-2-6 Effect of addition of ethanol

A few experiments were performed to test the influence of the ethanol concentration range **(** 3 , 7 , 11, 17 , and 21 %) on the photocatalytic degradation of dye by GO/ZnO naocomposite was investigated at initial (pH 8.7), catalyst dosage (0.15 g/100mL), and initial concentration of orange G dye (10 mg/L), (10 mL/min) flow rate of an air bubble at temperature (25°C) for different time intervals. Alcohols such as ethanol are commonly used to quench hydroxyl radicals. It was observed that small amounts of ethanol inhibited the photocatalytic degradation of dye . Figure. (3-27) shows that addition of ethanol inhibits the photo oxidative degradation of dye. The effect of ethanol in this system can be explained by •OH competitive reactions with dye and ethanol. Adding extra amount of ethanol leads to a mild increase in the process efficiency due to the formation of ethoxy radicals ($C_2H_5O^{\bullet}$) from direct photocatalytic oxidation of ethanol (Zhang et al., 2020, Saien et al., 2010, Alahiane et al., 2014)**.**

Table (3-9): chang for A_t/A_0 through irradiation-time on diffrent initial ethanol solution value .

initial ethanol solution % v/v	3	7	11	17	21
Iradiation Time min	A_t/A_o				
0	1	1	1	1	1
10	0.99	0.97	0.93	0.90	0.84
20	0.95	0.88	0.82	0.76	0.65
30	0.88	0.81	0.72	0.63	0.49
40	0.80	0.70	0.57	0.49	0.30
50	0.72	0.59	0.46	0.35	0.17
60	0.61	0.49	0.38	0.31	0.15
70	0.59	0.47	0.36	0.28	0.14
80	0.57	0.45	0.33	0.25	0.13

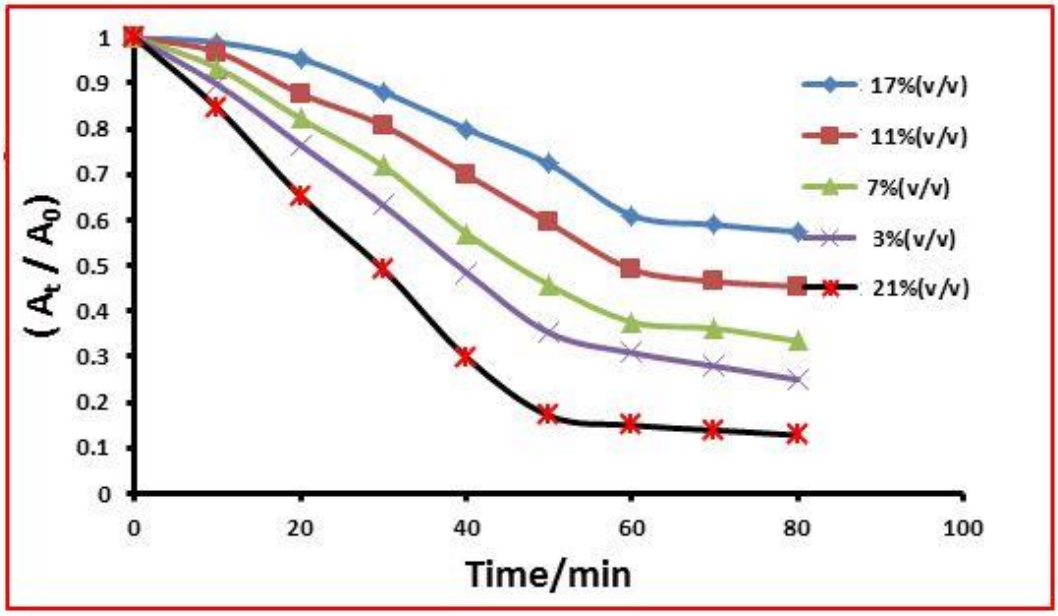

Fig. (3-27) . Variation in (A_t / A_0)with irradiation time at different initial ethanol solution.

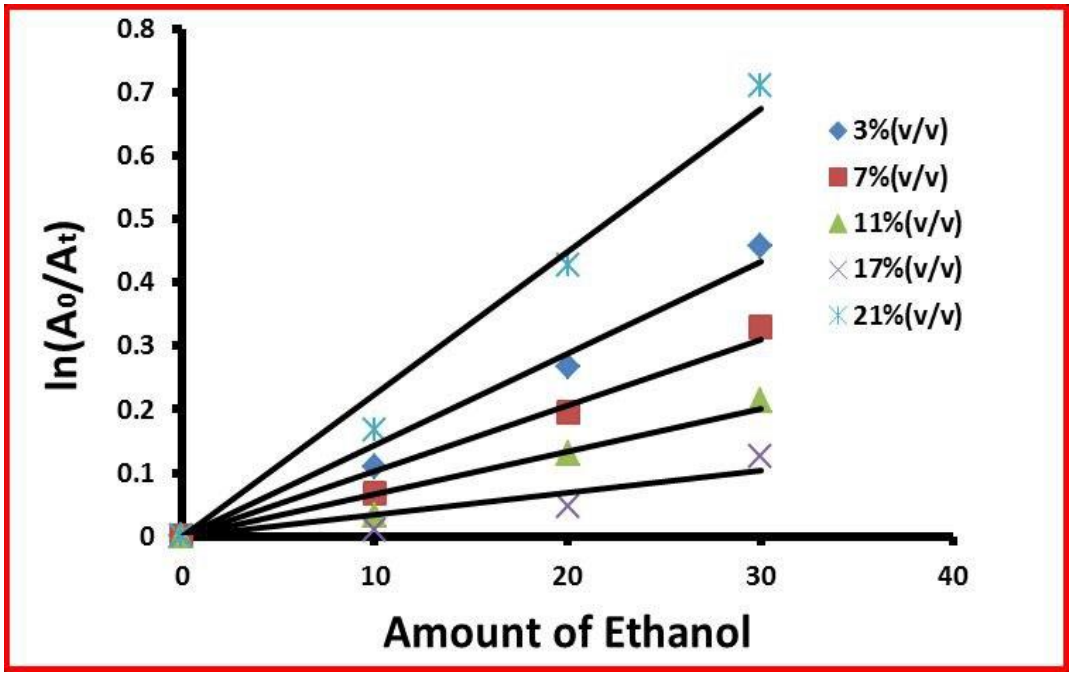

Fig.(3-28) : Chang in Ln (A_0 / A_t) through irradiation-time at different initial ethanol solution using UV radiation, initial orange G dye.

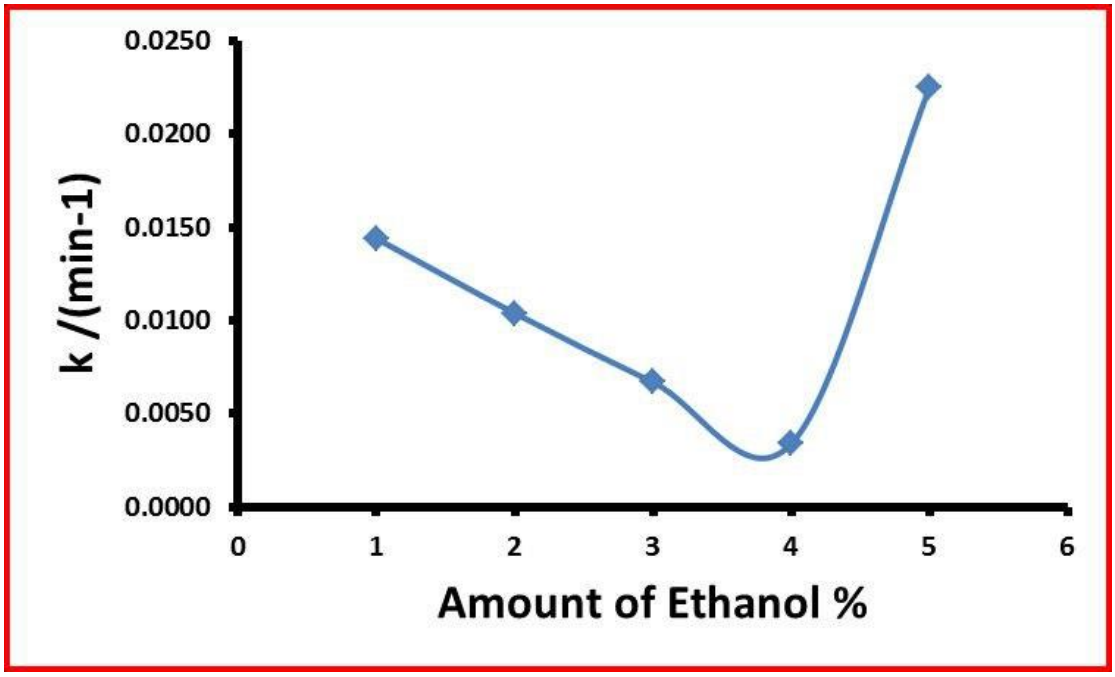

Fig. (3-29) . Effect of CH_3OH on photo degradation rate constants

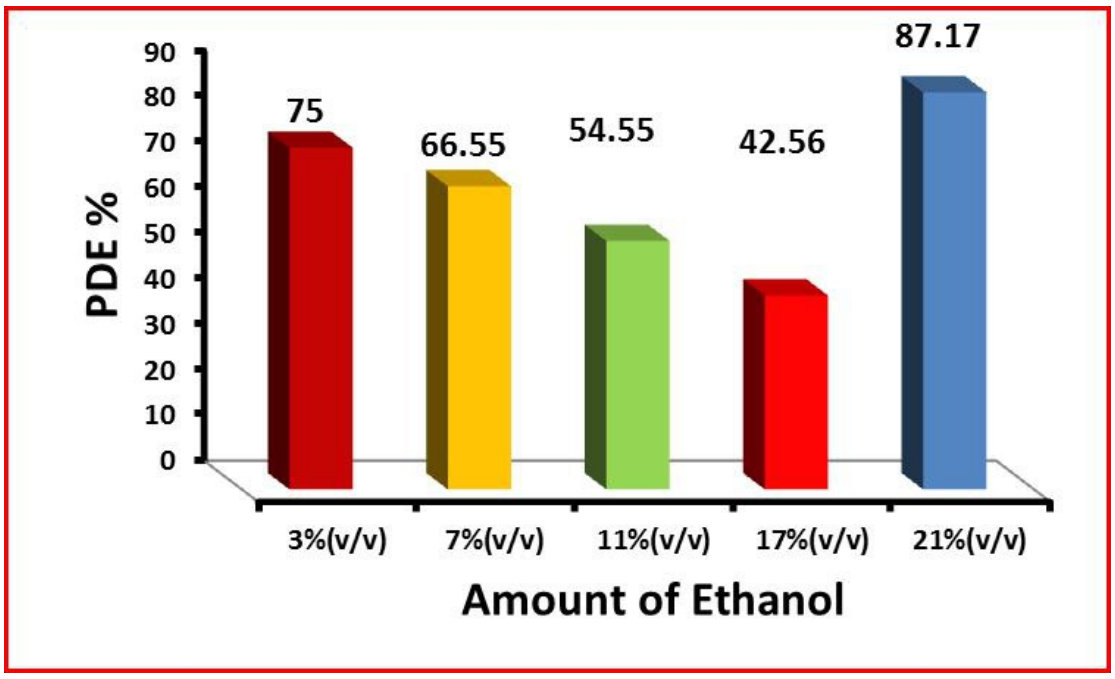

Fig.(3-30) : Photocatalytic degradation efficiency using (0.15g / 100 mL) GO/ZnO nanocomposite and (10 mg/L) of orange G dye for different amount of ethanol .

3-2-2-7 Temperature effect of on photo-catalytic-degradation for orange G dye :

A series of experiments were done for studding the influence of temperature on photocatalytic degradation of orange G dye in range (285 – 311) k. By conservation other experimental conditions apply constant at initial orange G dye concentration of (10 mg/L), prepared GO/ZnO catalyst dosage was (0.15 g /100mL), (10 mL/min) flow rate of an air bubble and (pH=8.7) .The results in Table (3-10) and figure.(3-31) show that the degradation process of dye progressively increased with increase in the temperature,this may be due to the increased reactive hydroxyl radical obstetrics (Mardiroosi et al.,2017) (Singh et al., 2021). The activation energy associated with the photodegrdation of dye was calculated according to the Arrhenius equation (2-7).

By plot of In k versus 1/T . From the Figure.(3-34) the activation energy which gives 35.35. ±1 $kJ.mol^{-1}$.

Table (3-10): Change of A_t/A_0 through irradiation-time of different-temperature.

Temperature K	285	298	303	311
Iradiation Time min	A_t/ A_0			
0	1	1	1	1
10	0.94	0.86	0.81	0.73
20	0.79	0.70	0.60	0.44
30	0.69	0.52	0.41	0.29
40	0.56	0.35	0.17	0.07
50	0.50	0.29	0.13	0.06
60	0.38	0.23	0.11	0.05
70	0.34	0.17	0.09	0.04
80	0.32	0.11	0.07	0.03

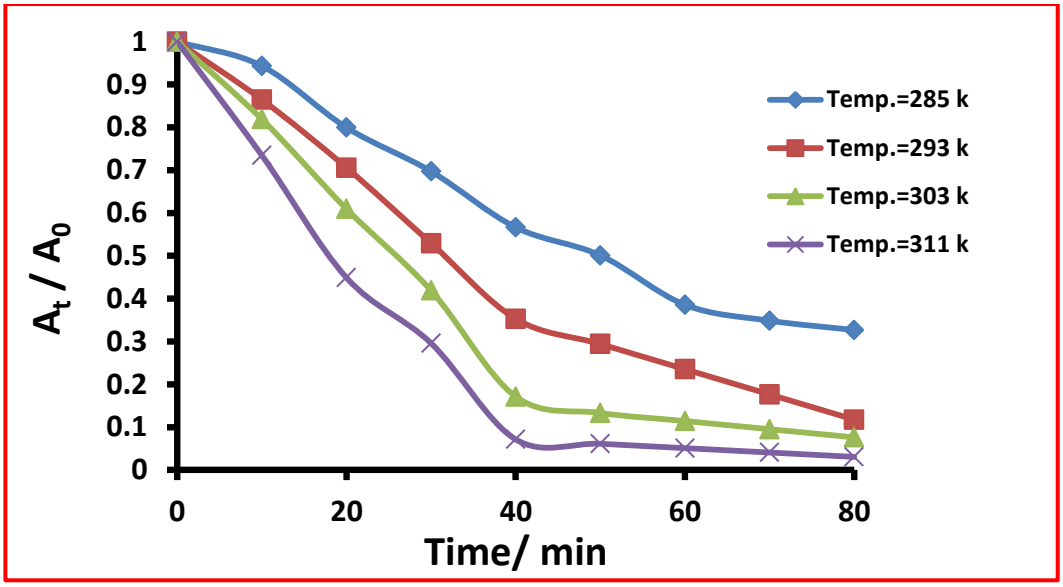

Fig. (3-31) . Variation in (A_t / A_0)with irradiation time at different temperature.

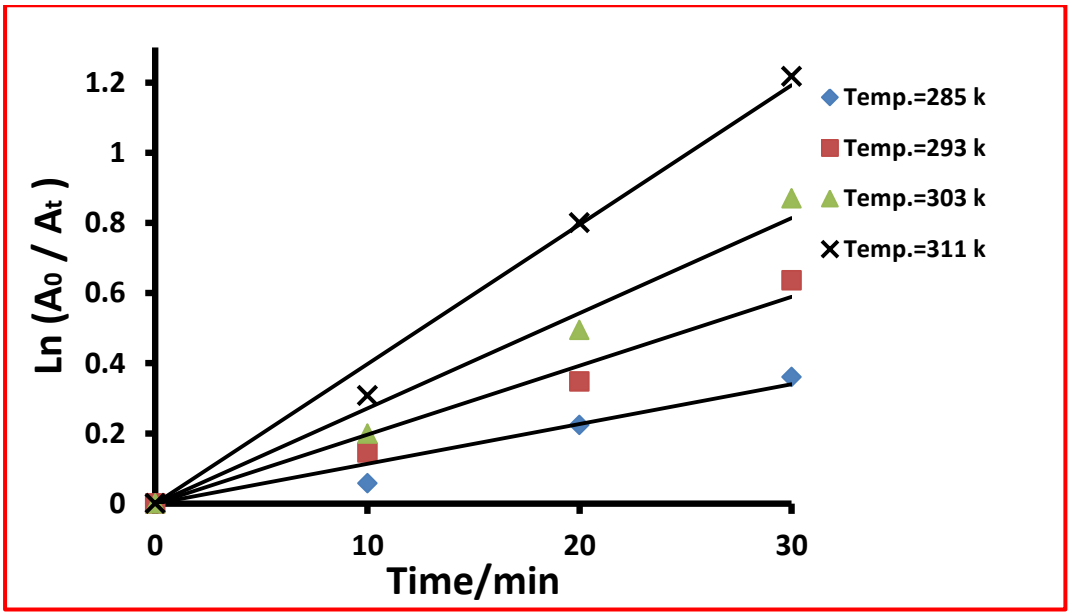

Fig.(3-32) : Chang in Ln (A_0 / A_t) through irradiation-time at different-temperature using UV radiation, (10 mg/L) of orange G dye and (0.15g / 100 mL) GO/ZnO nanocomposite.

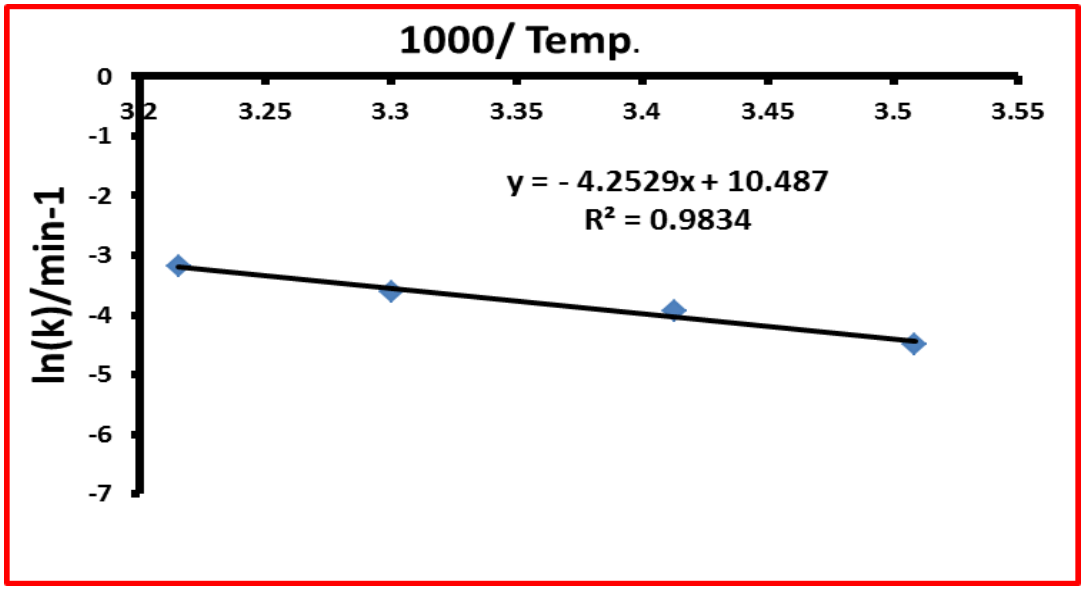

Fig. (3-33) : Arrhenius plot of orange G dye .

In order to calculate thermodynamic functions such as ΔH(Change Enthalpy of activation**)** and ΔS(Change Entropy of activation**)**, Figure (3-34) was shown a linear relationship fitting the graph of Eyring equation (2-8).

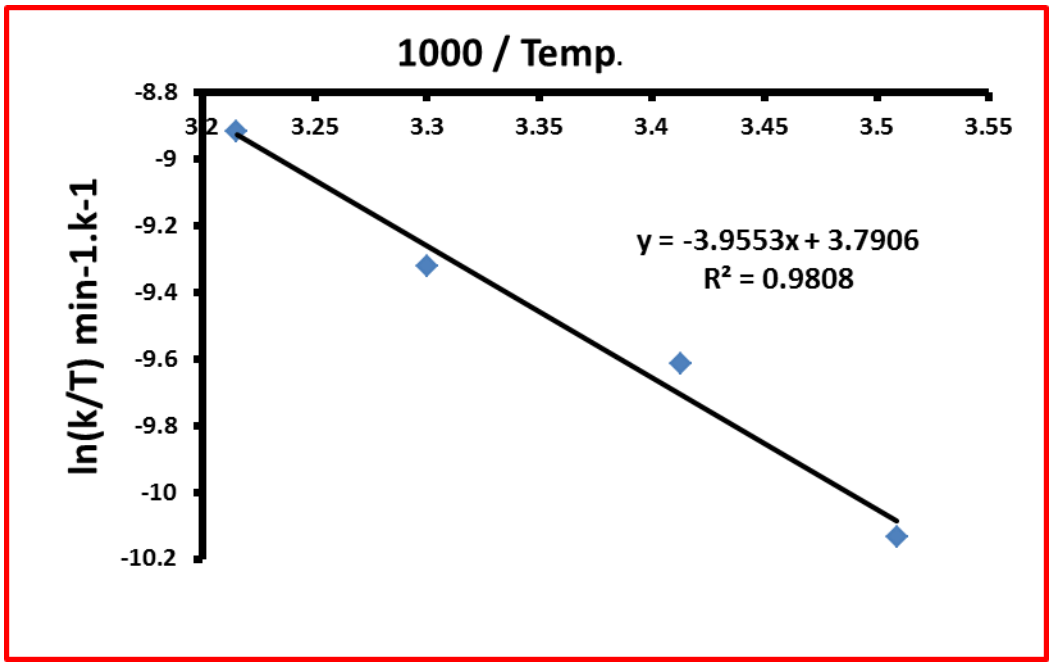

Fig. (3-34) : Eyring equation plot ln(k/T) against 1000/T for orange G dye .

According to the equation (2-8) , a plot of ln(k/T) versus 1/T produces a straight line and the value of Enthalpy of activation can be calculated from the slop of this line ($\Delta H = 32.88$ kJ/mol) . And from the y-intercept the Entropy of activation value ($\Delta S = -0.164$k J/ mol.k).

The positive value of Enthalpy of activation refer to endothermic reaction . In the present case the value of Entropy of activation is negative as in Table (3-11), so that the prodect formed is more ordered than the reactants.

The Gibbs' free energy ΔG can be calculated from the equation (2-9) and equal (81.75 kJ/mol) . The positive values of ΔG for the reaction indicate the non-spontaneous nature of photocatalytic degradation of orange G dye.

Table (3-11): The thermodynamic parameters of the photocatalytic degradation of dye .

Temperature/ k	Enthalpy of activation/ $KJ.mol^{-1}$	Entropy of activation/ $KJ.mol^{-1}.k^{-1}$	Gibbs' free energy/ $kJ.mol^{-1}$
298	**32.88**	**- 0.164**	**81.75**

3.3 . Degradation kinetics

The rate of reaction has been studied using the effect of initial dye rang (10, 20, 30.40, and 50 mg/L) with constant catalyst loading .a series of experiments has been performed to determine the rate of reaction. Pseudo first order and pseudo second order kinetic expressions were widely used by majority of the researchers today to describe the

photocatalytic oxidation of pollutant . These models are expressed by the equations (2-10)and (2-11):

The relationship between the initial concentration of orange g dye and the illumination time . The degradation rate is directly proportional to the probability of formation of hydroxyl radicals (˙OH) on the catalyst surface and theprobability of hydroxyl radicals reacting with the dye molecules. The interaction of (˙OH) radical with dye decreases as the initial concentration of the dye increases. Furthermore, the increase in dye concentration also reduces the relative formation of both hydroxyl radicals and super oxide radical anions due to the reduced light penetration to the solution, leading to the decrease in photo degradation efficiency (Długosz et al., 2021) . Best fitting kinetic model was chosen using linear regression method . Figures.(3-35) and (3.36) depict the kinetics of orange G degradation under UV catalytic activities by the GO/ZnO photocatalysts.

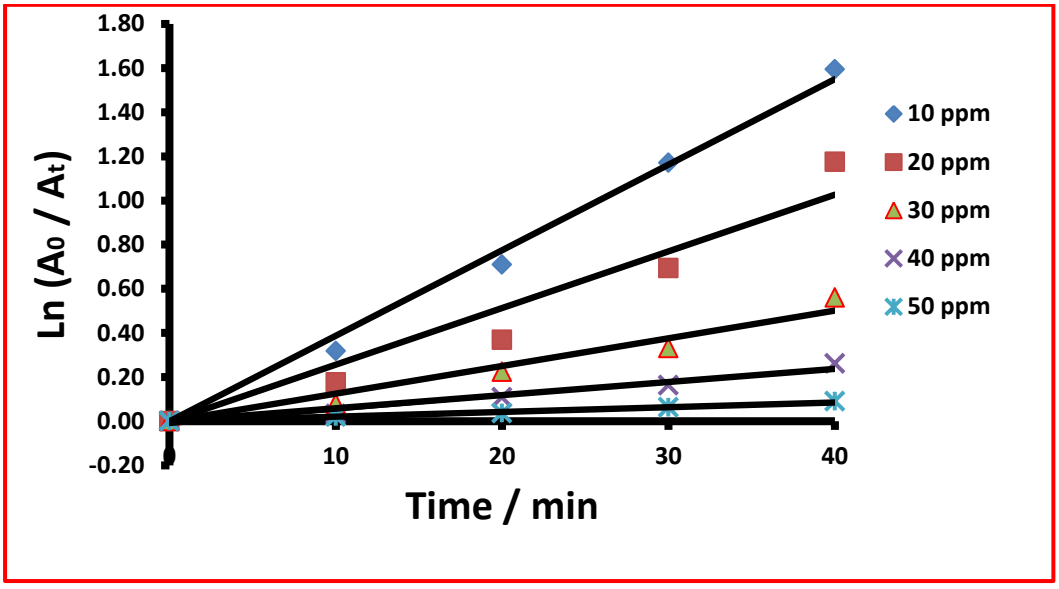

Fig. (3-35) . The plots of ln(A_0 /A_t) versus irradiation time at different initial orange G concentrations.

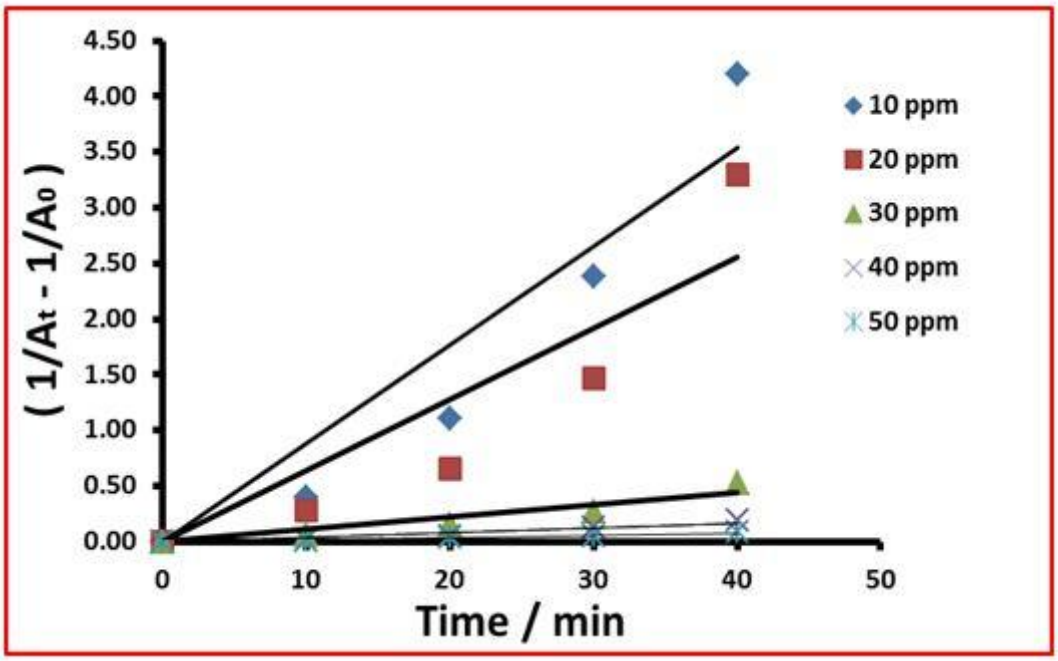

Fig . (3-36) : Orange G dye photooxidation GO/ ZnO nanocomposite photo catalysts – second order reaction kinetics.

Table (3-12) Kinetics of dye photo catalytic degradation by deferent concentration.

Concentration/ (mg/L)	First order		Second order	
	k_1	R^2	k_2	R^2
10	0.0387	0.9933	0.0884	0.898
20	0.0256	0.9362	0.0639	0.8213
30	0.0125	0.9572	0.0109	0.8972
40	0.0059	0.9618	0.0041	0.8962
50	0.0021	0.9865	0.0017	0.9378

3-4 Conclusions

1- Prepearation of GO by modified hummer method.
2- Graphite oxide/Zince Oxide (GO/ZnO) nanocomposite was prepared using sonocatalysis method.

3-The mean crystallite size for the prepared GO/ZnOnanocomposite were calculated using Scherer equation, and the results showed that the average crystallite size and average particle size of all photocatalysts were 23.769nm according to XRD.

4- The photocatalytic degradation processes of orange G dye depended on the amount of catalyst dosage and the optimum value equal (0.15 g / 100 mL) of GO/ZnO nanocomposite. The best removal percentage of orange G dye (97.33%) .

5- The effect of dye concentration has been studied the optimum value of orange G dye (10mg/L) dye . The photocatalytic degradation of orange G decrease with increase concentration of dye due to the decrease of the concentration OH^{-} adsorbed on the catalyst surface.

6- The light intensity 9mW/cm2. The photocatalytic degradation increased with increase in light intensity.

7- The activation energy has been calculated when used orange G dye = 35.35 $kJ.mol^{-1}$

8- Using Eyring equation thermodynamic parameters (ΔH, ΔS) for orange G dye were calculated (32.88 kJ/mol and (- 0.164 kJ/mol.k) respectively, from the results the reaction is endothermic with low randomness. ΔG (81.75 kJ/mol)was calculated and the reaction is non-spontaneous.

9- Alcohols such as ethanol are commonly used to quench hydroxyl radicals. The effect of ethanol in this system can be explained by $^{\bullet}OH$ competitive reactions with dye and ethanol. Adding extra amount of ethanol leads to a mild increase in the process efficiency due to the formation of ethoxy radicals ($C_2H_5O^{\bullet}$) from direct photocatalytic oxidation of ethanol.

10- Effect addation of the hydrogen peroxide concentration on photocatalytic degradation of dye.The increased photocatalytic degradation efficiency of orange G after the addition of hydrogen peroxide can be explained by the increased reaction between hydrogen peroxide and electron in the conduction band of orange G. According to , hydrogen peroxide can effectively inhibit the electron–hole recombination. The other reason for the inhibition effect can also be explained in terms of scavenging of positive holes by adsorbed H_2O_2 on the surface of GO/ZnO nanocomposite.

3-5 Recommendations

1. Modification the surface of Zinc Oxide with Au nanoparticle.

2. Synthesized new nanocomposite by using green method.

3. Studying the biological activity of prepared nanocomposite.

4.Studying the effect of added hydrogen peroxide and ethanol.

References

References

Aljeboree, A. M., Al-Gubury, H. Y., Bader, A. T., & Alkaim, A. F. (2020). Adsorption of Textile Dyes in the Presence Either Clay or Activated Carbon as a Technological Models: A Review. J. Crit. Rev, 7, 620-626.

Almutairi, F. M., El Rabey, H. A., Alalawy, A. I., Salama, A. A., Tayel, A. A., Mohammed, G. M., ... & Zayed, M. M. (2021). Application of Chitosan/Alginate Nanocomposite Incorporated with Phycosynthesized Iron Nanoparticles for Efficient Remediation of Chromium. Polymers, 13(15), 2481.

Adya, A. K., & Canetta, E. (2020). Nanotechnology and its applications to animal biotechnology. In Animal Biotechnology (pp. 309-326). Academic Press.

Al-Gubury, H. Y., Altameme, H. J., & Ali, M. M. (2018). SIGNIFICANT ENHANCEMENT OF PHOTOCATALYTIC ACTIVITY OF ZINC OXIDE BY EXTRACTED ANTHOCYANIN PIGMENT AND SOLAR LIGHT. Plant Archives, 18(2), 2723-2726.

Alamdari, S., Ghamsari, M. S., Afarideh, H., Mohammadi, A., Geranmayeh, S., Tafreshi, M. J., & Ehsani, M. H. (2019). Preparation and characterization of GO-ZnO nanocomposite for UV detection application. Optical Materials, 92, 243-250.

Ameen, S., Akhtar, M. S., Seo, H. K., & Shin, H. S. (2013). Advanced ZnO–graphene oxide nanohybrid and its photocatalytic applications. Materials Letters, 100, 261-265.

Alshamsi, H. A., & Ali, S. K. (2016). Kinetics of green reduction of graphene oxide via Hibiscus sabdarriffa L aqueous solution. International Journal of ChemTech Research, 9(9), 321-331.

References

Abbasi, S., Ahmadpoor, F., Imani, M., & Ekrami-Kakhki, M. S. (2020). Synthesis of magnetic Fe_3O_4@ ZnO@ graphene oxide nanocomposite for photodegradation of organic dye pollutant. International Journal of Environmental Analytical Chemistry, 100(2), 225-240.

Anjum, F., Asiri, A. M., Khan, M. A., Khan, M. I., Khan, S. B., Akhtar, Chakraborty, S. (2021). Photo-degradation, thermodynamic and kinetic study of carcinogenic dyes via zinc oxide/graphene oxide nanocomposites. Journal of Materials Research and Technology, 15, 3171-3191.

Al-Mamun, M. R., Islam, M. S., Hossain, M. R., Kader, S., Islam, M. S., & Khan, M. Z. H. (2021). A novel and highly efficient Ag and GO co-synthesized ZnO nano photocatalyst for methylene blue dye degradation under UV irradiation. Environmental Nanotechnology, Monitoring & Management, 16, 100495.

Aqeel, M., Anjum, S., Imran, M., Ikram, M., Majeed, H., Naz, M. Ahmad, M. 2. (2019). TiO_2@ RGO (reduced graphene oxide) doped nanoparticles demonstrated improved photocatalytic activity. Materials Research Express, 6(8), 086215.

Alam, S. N., Sharma, N., & Kumar, L. (2017). Synthesis of graphene oxide (GO) by modified hummers method and its thermal reduction to obtain reduced graphene oxide (rGO). Graphene, 6(1), 1-18.

Al-Rawashdeh, N. A., Allabadi, O. Aljarrah, M. T. (2020). Photocatalytic activity of graphene oxide/zinc oxide nanocomposites with embedded metal nanoparticles for the degradation of organic dyes. ACS omega, 5(43), 28046-28055.

References

Ainali, N. M., Kalaronis, D., Evgenidou, E., Bikiaris, D. N. Lambropoulou, D. A. (2021). Insights into biodegradable polymer-supported titanium dioxide photocatalysts for environmental remediation. Macromol, 1(3), 201-233.

Azim, M. B., Tanim, I. A., Rezaul, R. M., Tareq, R., Rahul, A. H., Kurny, A. S. Gulshan, F. (2018). Degradation of methylene blue using graphene oxide-tin oxide nanocomposite as photocatalyst. arXiv preprint arXiv:1806.06481.

Abdel-Khalek, A. A., Mahmoud, S. A., & Zaki, A. H. (2018). Visible light assisted photocatalytic degradation of crystal violet, bromophenol blue and eosin Y dyes using AgBr-ZnO nanocomposite. Environmental Nanotechnology, Monitoring & Management, 9, 164-173.

Alshehri, A., Narasimharao, K. (2020). PtOx-TiO_2 anatase nanomaterials for photocatalytic reformation of methanol to hydrogen: effect of TiO_2 morphology. Journal of Materials Research and Technology, 9(6), 14907-14921.

ALjeboree, A. M., ALshirfi, A. N., ALkaim, A. F. (2019). Removal of pharmaceutical amoxicillin drug by using (Cnt) decorated clay/Fe_2 O_3 micro/nanocomposite as effective adsorbent: Process optimization for ultrasound-assisted adsorption. International Journal of Pharmaceutical Research, 11(4), 80-86.

Abilarasu, A., Kumar, P. S., Vo, D. V. N., Krithika, D., Ngueagni, P. T., Joshiba, G. J., Prasannamedha, G. (2021). Enhanced photocatalytic degradation of diclofenac by SnO. 15MnO. 85Fe_2O_4 catalyst under solar light. Journal of Environmental Chemical Engineering, 9(1), 104875.

References

Aziztyana, A. P., Wardhani, S., Prananto, Y. P., Purwonugroho, D. (2019, June). Optimisation of methyl orange photodegradation using TiO2-zeolite photocatalyst and H_2O_2 in acid condition. In IOP Conference Series: Materials Science and Engineering (Vol. 546, No. 4, p. 042047). IOP Publishing.

Ahmad, M., Ahmed, E., Hong, Z. L., Ahmed, W., Elhissi, A., & Khalid, N. R. (2014). Photocatalytic, sonocatalytic and sonophotocatalytic degradation of Rhodamine B using ZnO/CNTs composites photocatalysts. Ultrasonics sonochemistry, 21(2), 761-773.

Alahiane, S., Qourzal, S., El Ouardi, M., Abaamrane, A., & Assabbane, A. (2014). Factors influencing the photocatalytic degradation of reactive yellow 145 by TiO_2-coated non-woven fibers. American Journal of Analytical Chemistry, 2014.

Barhoum, A., García-Betancourt, M. L., Jeevanandam, J., Hussien, E. A., Mekkawy, S. A., Mostafa, M., Bechelany, M. (2022). Review on natural, incidental, bioinspired, and engineered nanomaterials: history, definitions, classifications, synthesis, properties, market, toxicities, risks, and regulations. Nanomaterials, 12(2), 177.

Benkhaya, S., M'rabet, S., El Harfi, A. (2020). A review on classifications, recent synthesis and applications of textile dyes. Inorganic Chemistry Communications, 115, 107891.

Badvi, K., Javanbakht, V. (2021). Enhanced photocatalytic degradation of dye contaminants with TiO2 immobilized on ZSM-5 zeolite modified with nickel nanoparticles. Journal of Cleaner Production, 280, 124518.

Cai, M., Su, J., Zhu, Y., Wei, X., Jin, M., Zhang, H., Wei, Z. (2016). Decolorization of azo dyes Orange G using hydrodynamic cavitation

coupled with heterogeneous Fenton process. Ultrasonics sonochemistry, 28, 302-310.

Chen, Y. L., Zhang, C. E., Deng, C., Fei, P., Zhong, M., Su, B. T. (2013). Preparation of ZnO/GO composite material with highly photocatalytic performance via an improved two-step method. Chinese Chemical Letters, 24(6), 518-520.

Chiu, Y. H., Chang, T. F. M., Chen, C. Y., Sone, M., Hsu, Y. J. (2019). Mechanistic insights into photodegradation of organic dyes using heterostructure photocatalysts. Catalysts, 9(5), 430.

Chen, L., Batchelor-McAuley, C., Rasche, B., Johnston, C., Hindle, N., Compton, R. G. (2020). Surface area measurements of graphene and graphene oxide samples: Dopamine adsorption as a complement or alternative to methylene blue. Applied Materials Today, 18, 100506.

Darshita, M. N., Sood, R. (2021). Review on synthesis and applications of zinc oxide nanoparticles.

Dhatwalia, J., Kumari, A., Chauhan, A., Mansi, K., Thakur, S., Saini, R. V., Kumar, R. (2022). Rubus ellipticus Sm. Fruit Extract Mediated Zinc Oxide Nanoparticles: A Green Approach for Dye Degradation and Biomedical Applications. Materials, 15(10), 3470.

Dewil, R., Mantzavinos, D., Poulios, I., Rodrigo, M. A. (2017). New perspectives for advanced oxidation processes. Journal of environmental management, 195, 93-99.

Di, X., Guo, F., Zhu, Z., Xu, Z., Qian, Z., Zhang, Q. (2019). In situ synthesis of ZnO–GO/CGH composites for visible light photocatalytic degradation of methylene blue. RSC Advances, 9(70), 41209-41217.

References

Danyliuk, N., Tatarchuk, T., Shyichuk, A. (2020). Estimation of photocatalytic degradation rate using smartphone based analysis. Physics and Chemistry of Solid State, 21(4), 727-736.

Durmus, Z., Kurt, B. Z., Durmus, A. (2019). Synthesis and characterization of graphene oxide/zinc oxide (GO/ZnO) nanocomposite and its utilization for photocatalytic degradation of basic fuchsin dye. ChemistrySelect, 4(1), 271-278.

Danyliuk, N., Tatarchuk, T., Kannan, K., Shyichuk, A. (2021). Optimization of TiO_2-P25 photocatalyst dose and H_2O_2 concentration for advanced photo-oxidation using smartphone-based colorimetry. Water Science and Technology, 84(2), 469-483.

Długosz, O., Szostak, K., Krupiński, M., Banach, M. (2021). Synthesis of Fe_3O_4/ZnO nanoparticles and their application for the photodegradation of anionic and cationic dyes. International Journal of Environmental Science and Technology, 18(3), 561-574.

Erol, O., Uyan, I., Hatip, M., Yilmaz, C., Tekinay, A. B., Guler, M. O. (2018). Recent advances in bioactive 1D and 2D carbon nanomaterials for biomedical applications. Nanomedicine: Nanotechnology, Biology and Medicine, 14(7), 2433-2454.

Ebrahimi, R., Mohammadi, M., Maleki, A., Jafari, A., Shahmoradi, B., Rezaee, R., Puttaiah, S. H. (2020). Photocatalytic degradation of 2, 4-dichlorophenoxyacetic acid in aqueous solution using Mn-doped ZnO/graphene nanocomposite under LED radiation. Journal of Inorganic and Organometallic Polymers and Materials, 30(3), 923-934.

References

Farghali, A. A., Zaki, A. H., Khedr, M. H. (2016). Control of selectivity in heterogeneous photocatalysis by tuning TiO_2 morphology for water treatment applications. Nanomaterials and Nanotechnology, 6, 12.

Fu, J., Chen, Z., Wang, M., Liu, S., Zhang, J., Zhang, J., Xu, Q. (2015). Adsorption of methylene blue by a high-efficiency adsorbent (polydopamine microspheres): kinetics, isotherm, thermodynamics and mechanism analysis. Chemical Engineering Journal, 259, 53-61.

Giovannetti, R., Rommozzi, E., Zannotti, M., D'Amato, C. A. (2017). Recent advances in graphene based TiO_2 nanocomposites (GTiO2Ns) for photocatalytic degradation of synthetic dyes. Catalysts, 7(10), 305.

Gharagozlou, M., Naghibi, S., Olya, M. E. (2018). Preparing and Investigation a New Nanofluid for Employing in Machining Process: Synthesis and Characterization of Graphene Oxide Nanoparticles. JOURNAL OF ADVANCED MATERIALS AND PROCESSING (JOURNAL OF MATERIALS SCIENCE), , 6(2), 3-11.

Gholami, M., Shirzad-Siboni, M., Farzadkia, M., Yang, J. K. (2016). Synthesis, characterization, and application of ZnO/TiO_2 nanocomposite for photocatalysis of a herbicide (Bentazon). Desalination and water treatment, 57(29), 13632-13644.

Hasnidawani, J. N., Azlina, H. N., Norita, H., Bonnia, N. N., Ratim, S., & Ali, E. S. (2016). Synthesis of ZnO nanostructures using sol-gel method. Procedia Chemistry, 19, 211-216.

Hayat, K., Gondal, M. A., Khaled, M. M., Ahmed, S., Shemsi, A. M. (2011). Nano ZnO synthesis by modified sol gel method and its application in heterogeneous photocatalytic removal of phenol from water. Applied Catalysis A: General, 393(1-2), 122-129.

References

Irshad, S., Salamat, A., Anjum, A. A., Sana, S., Saleem, R. S., Naheed, A., Iqbal, A. (2018). Green tea leaves mediated ZnO nanoparticles and its antimicrobial activity. Cogent Chemistry, 4(1), 1469207.

Imran, M., Riaz, S., Shah, S. M. H., Batool, T., Khan, H. N., Sabri, A. N., Naseem, S. (2020). In-vitro hemolytic activity and free radical scavenging by sol-gel synthesized Fe_3O_4 stabilized ZrO_2 nanoparticles. Arabian Journal of Chemistry, 13(11), 7598-7608.

Jamkhande, P. G., Ghule, N. W., Bamer, A. H., Kalaskar, M. G. (2019). Metal nanoparticles synthesis: An overview on methods of preparation, advantages and disadvantages, and applications. Journal of drug delivery science and technology, 53, 101174.

Jadhav, A. S., Urkude, R. P., Jangam, S. S. (2021). CURRENT REVIEW ON NANOPARTICLES: PROPERTIES, APPLICATION AND TOXICITY.

Jiang, G., Lin, Z., Chen, C., Zhu, L., Chang, Q., Wang, N., Tang, H. (2011). TiO_2 nanoparticles assembled on graphene oxide nanosheets with high photocatalytic activity for removal of pollutants. Carbon, 49(8), 2693-2701.

Jayachandiran, J., Yesuraj, J., Arivanandhan, M., Raja, A., Suthanthiraraj, S. A., Jayavel, R., Nedumaran, D. J. J. O. I. (2018). Synthesis and electrochemical studies of rGO/ZnO nanocomposite for supercapacitor application. Journal of Inorganic and Organometallic Polymers and Materials, 28(5), 2046-2055.

Jamil, A., Bokhari, T. H., Javed, T., Mustafa, R., Sajid, M., Noreen, S., Jilani, M. I. (2020). Photocatalytic degradation of disperse dye Violet-26

using TiO_2 and ZnO nanomaterials and process variable optimization. Journal of Materials Research and Technology, 9(1), 1119-1128.

Khan, I., Saeed, K., Khan, I. (2019). Nanoparticles: Properties, applications and toxicities. Arabian journal of chemistry, 12(7), 908-931.

Kamakshi, T., Sundari, G. S., Erothu, H., Rao, T. (2018). Synthesis and characterization of graphene based iron oxide (Fe_3O_4) nanocomposites. Rasayan Journal of Chemistry, 11(3), 1113-1119.

Karim, S. A., Al-Gubury, H. Y., Abd Alrazzak, N. (2019, September). The synthesis of a novel azo dyes and study of photocatalytic degradation. In Journal of Physics: Conference Series (Vol. 1294, No. 5, p. 052054). IOP Publishing.

Karthikeyan, C., Arunachalam, P., Ramachandran, K., Al-Mayouf, A. M., Karuppuchamy, S. (2020). Recent advances in semiconductor metal oxides with enhanced methods for solar photocatalytic applications. Journal of Alloys and Compounds, 828, 154281.

Kołodziejczak-Radzimska, A., Jesionowski, T. (2014). Zinc oxide—from synthesis to application: a review. Materials, 7(4), 2833-2881.

Khan, I., Saeed, K., Ali, N., Khan, I., Zhang, B., Sadiq, M. (2020). Heterogeneous photodegradation of industrial dyes: an insight to different mechanisms and rate affecting parameters. Journal of environmental chemical engineering, 8(5), 104364.

Kashinath, L., Namratha, K., Byrappa, K. (2015). Microwave assisted facile hydrothermal synthesis and characterization of zinc oxide flower grown on graphene oxide sheets for enhanced photodegradation of dyes. Applied Surface Science, 357, 1849-1856.

References

Kashinath, L., Namratha, K., Byrappa, K. (2016). Microwave assisted synthesis and characterization of nanostructure zinc oxide-graphene oxide and photo degradation of brilliant blue. Materials Today: Proceedings, 3(1), 74-83.

Kumaresan, N., Ramamurthi, K., Babu, R. R., Sethuraman, K., Babu, S. M. (2017). Hydrothermally grown ZnO nanoparticles for effective photocatalytic activity. Applied Surface Science, 418, 138-146 .

Kzar, K. O., Mohammed, Z. F., Saeed, S. I., Ahmed, L. M., Kareem, D. I., Hadyi, H., Kadhim, A. J. (2019). Heterogeneous photo-decolourization of cobaltous phthalocyaninate dye (Reactive green dye) catalyzed by ZnO. In AIP Conference Proceedings (Vol. 2144, No. 1, p. 020004). AIP Publishing LLC.

Kumar, R., Janbandhu, S. Y., Sukhadeve, G. K., Gedam, R. S. (2022). Visible-light assisted surface plasmon resonance triggered Ag/ZnO nanocomposites: synthesis and performance towards degradation of indigo carmine dye.

Kong, D., He, L., Li, H., Song, Z. (2021). Preparation and characterization of graphene oxide/chitosan composite aerogel with high adsorption performance for Cr (VI) by a new crosslinking route. Colloids and Surfaces A: Physicochemical and Engineering Aspects, 625, 126832.

Krishnan, T., Mansor, W. S. W. (2020). Photocatalytic Degradation of Dyes by TiO_2 Process in Batch Photoreactor. Letters in Applied NanoBioScience, 9, 1502-1512.

Kumar, S., Kaushik, R. D., Purohit, L. P. (2021). Novel ZnO tetrapod-reduced graphene oxide nanocomposites for enhanced photocatalytic

degradation of phenolic compounds and MB dye. Journal of Molecular Liquids, 327, 114814.

Kathiresan, G., Vijayakumar, K., Sundarrajan, A. P., Kim, H. S., Adaikalam, K. (2021). Photocatalytic degradation efficiency of ZnO, GO and PVA nanoadsorbents for crystal violet, methylene blue and trypan blue dyes. Optik, 238, 166671.

Kurniawan, T. A., Mengting, Z., Fu, D., Yeap, S. K., Othman, M. H. D., Avtar, R., Ouyang, T. (2020). Functionalizing TiO2 with graphene oxide for enhancing photocatalytic degradation of methylene blue (MB) in contaminated wastewater. Journal of environmental management, 270, 110871.

Krishnakumar, B., Swaminathan, M. (2011). Influence of operational parameters on photocatalytic degradation of a genotoxic azo dye Acid Violet 7 in aqueous ZnO suspensions. Spectrochimica Acta Part A: Molecular and Biomolecular Spectroscopy, 81(1), 739-744.

Li, T., Shang, D., Gao, S., Wang, B., Kong, H., Yang, G., Wei, G. (2022). Two-dimensional material-based electrochemical sensors/biosensors for food safety and biomolecular detection. Biosensors, 12(5), 314.

Lee, S. C., Jeong, Y., Kim, Y. J., Kim, H., Lee, H. U., Lee, Y. C., Lee, G. (2018). Hierarchically three-dimensional (3D) nanotubular sea urchin-shaped iron oxide and its application in heavy metal removal and solar-induced photocatalytic degradation. Journal of hazardous materials, 354, 283-292.

Lin, Y., Hong, R., Chen, H., Zhang, D., Xu, J. (2020). Green synthesis of ZnO-GO composites for the photocatalytic degradation of methylene blue. Journal of Nanomaterials.

References

Moorthy, S. K., Viswanathan, C., Ponpandian, N. (2017). Facile approach for synthesis of GO/ZnO nanocomposite for highly efficient photocatalytic degradation of organic dyes under visible light. In Nano Hybrids and Composites (Vol. 17, pp. 121-126). Trans Tech Publications Ltd.

Moezzi, A., McDonagh, A. M., Cortie, M. B. (2012). Zinc oxide particles: Synthesis, properties and applications. Chemical engineering journal, 185, 1-22.

Madhavan, J., Grieser, F., Ashokkumar, M. (2010). Degradation of orange-G by advanced oxidation processes. Ultrasonics sonochemistry, 17(2), 338-343.

Meetani, M. A., Rauf, M. A., Hisaindee, S., Khaleel, A., AlZamly, A., Ahmad, A. (2011). Mechanistic studies of photoinduced degradation of Orange G using LC/MS. Rsc Advances, 1(3), 490-497.

Masuda, K., Kobayashi, S. (2020). Direct and quantitative monitoring of catalytic organic reactions under heterogeneous conditions using direct analysis in real time mass spectrometry. Chemical science, 11(19), 5105-5112.

Marco, C., Giulio, F., Alberto, T., Minella, M., Vione, D. V. (2021). Advanced oxidation processes in the removal of organic substances from produced water: Potential, configurations, and research needs.

Maruthupandy, M., Qin, P., Muneeswaran, T., Rajivgandhi, G., Quero, F., Song, J. M. (2020). Graphene-zinc oxide nanocomposites (G-ZnO NCs): Synthesis, characterization and their photocatalytic degradation of dye molecules. Materials Science and Engineering: B, 254, 114516.

References

Meva, F. E. A., Ntoumba, A. A., Kedi, P. B. E., Tchoumbi, E., Schmitz, A., Schmolke, L., Janiak, C. (2019). Silver and palladium nanoparticles produced using a plant extract as reducing agent, stabilized with an ionic liquid: sizing by X-ray powder diffraction and dynamic light scattering. Journal of Materials Research and Technology, 8(2), 1991-2000.

Mishra, V., Sharma, R. (2015). Green synthesis of zinc oxide nanoparticles using fresh peels extract of Punica granatum and its antimicrobial activities. International Journal of Pharma Research and Health Sciences, 3(3), 694-699.

Mohammad, E. J., Lafta, A. J., Kahdem, S. H., & Alkaim, A. F. (2016). Enhancement the photocatalytic activity of zinc oxide surface by combination with functionalized and non-functionalized activated carbon. Int J ChemTech Res, 9(12), 656.

Maddu, A., Meliafatmah, R., Rustami, E. (2021). Enhancing Photocatalytic Degradation of Methylene Blue Using ZnO/Carbon Dots Nanocomposite Derived From Coffee Grounds. Polish Journal of Environmental Studies, 30(1).

Munawaroh, H., Sari, P. L., Wahyuningsih, S., & Ramelan, A. H. (2018, September). The photocatalytic degradation of methylene blue using graphene oxide (GO)/ZnO nanodrums. In AIP Conference Proceedings (Vol. 2014, No. 1, p. 020119). AIP Publishing LLC.

Mahdavi, R., Talesh, S. S. A. (2021). Enhanced selective photocatalytic and sonocatalytic degradation in mixed dye aqueous solution by ZnO/GO nanocomposites: Response surface methodology. Materials Chemistry and Physics, 267, 124581.

References

Margaret, S. M., Paul Winston, A. J. P., Muthupandi, S., Shobha, P., Sagayaraj, P. (2021). Enhanced Photocatalytic Degradation of Phenol Using Urchin-Like ZnO Microrod-Reduced Graphene Oxide Composite under Visible-Light Irradiation. Journal of Nanomaterials, 2021.

Mohamed, M. M., Ghanem, M. A., Khairy, M., Naguib, E., & Alotaibi, N. H. (2019). Zinc oxide incorporated carbon nanotubes or graphene oxide nanohybrids for enhanced sonophotocatalytic degradation of methylene blue dye. Applied Surface Science, 487, 539-549.

Mohsin, D. H., Juda, A. M., Mashkour, M. M. S. (2013). Thermodynamic and kinetic study for aromatic rings effect on the photooxidation rate. Int. J. Eng. Technol, 13, 34-41.

Mondol, B., Sarker, A., Shareque, A. M., Dey, S. C., Islam, M. T., Das, A. K., Sarker, M. (2021). Preparation of activated carbon/TiO_2 nanohybrids for photodegradation of reactive red-35 dye using sunlight. Photochem, 1(1), 54-66.

Mardiroosi, A., Mahjoub, A. R., Fakhri, H. (2017). Efficient visible light photocatalytic activity based on magnetic graphene oxide decorated ZnO/NiO. Journal of Materials Science: Materials in Electronics, 28(16), 11722-11732.

Nasrollahzadeh, M., Sajjadi, M., Soufi, G. J., Iravani, S., Varma, R. S. (2020). Nanomaterials and nanotechnology-associated innovations against viral infections with a focus on coronaviruses. Nanomaterials, 10(6), 1072.

Neto, J. S. G., Satyro, S., Saggioro, E. M., Dezotti, M. (2021). Investigation of mechanism and kinetics in the TiO2 photocatalytic degradation of Indigo Carmine dye using radical scavengers.

International Journal of Environmental Science and Technology, 18(1), 163-172.

Noman, M. T., Amor, N., Petru, M. (2022). Synthesis and applications of ZnO nanostructures (ZONSs): A review. Critical Reviews in Solid State and Materials Sciences, 47(2), 99-141.

Nayl, A. A., Abd-Elhamid, A. I., El-Shanshory, A. A., Soliman, H. M., Kenawy, E. R., Aly, H. F. (2019). Development of sponge/graphene oxide composite as eco-friendly filter to remove methylene blue from aqueous media. Applied Surface Science, 496, 143676.

Niculescu, A. G., Grumezescu, A. M. (2022). Applications of Chitosan-Alginate-Based Nanoparticles—An Up-to-Date Review. Nanomaterials, 12(2), 186.

Nguyen, C. H., Fu, C. C., Juang, R. S. (2018). Degradation of methylene blue and methyl orange by palladium-doped TiO_2 photocatalysis for water reuse: Efficiency and degradation pathways. Journal of Cleaner Production, 202, 413-427.

Nenavathu, B. P., Kandula, S. Verma, S. 2018. Visible-light-driven photocatalytic degradation of safranin-T dye using functionalized graphene oxide nanosheet (FGS)/ZnO nanocomposites. RSC advances, 8, 19659-19667.

Niu, B., Wu, D., Wang, J., Wang, L., Zhang, W. (2020). Salt-sealing-pyrolysis derived Ag/ZnO@ C hollow structures towards efficient photo-oxidation of organic dye and water-born bacteria. Applied Surface Science, 528, 146965.

References

Olajire, A. A., Olajide, A. J. (2014). Kinetic study of decolorization of methylene blue with sodium sulphite in aqueous media: influence of transition metal ions.

Oppong, S. O. B., Opoku, F., Anku, W. W., Govender, P. P. (2021). Insights into the complementary behaviour of Gd doping in GO/Gd/ZnO composites as an efficient candidate towards photocatalytic degradation of indigo carmine dye. Journal of Materials Science, 56(14), 8511-8527.

Oun, A., Tahri, N., Mahouche-Chergui, S., Carbonnier, B., Majumdar, S., Sarkar, S., Amar, R. B. (2017). Tubular ultrafiltration ceramic membrane based on titania nanoparticles immobilized on macroporous clay-alumina support: elaboration, characterization and application to dye removal. Separation and Purification Technology, 188, 126-133.

Paul, S. K., Dutta, H., Sarkar, S., Sethi, L. N., Ghosh, S. K. (2019). Nanosized Zinc Oxide: Super-functionalities, present scenario of application, safety issues, and future prospects in food processing and allied industries. Food Reviews International, 35(6), 505-535.

Puneetha, J., Kottam, N., Rathna, A. (2021). Investigation of photocatalytic degradation of crystal violet and its correlation with bandgap in ZnO and ZnO/GO nanohybrid. Inorganic Chemistry Communications, 125, 108460.

Pop, E., Varshney, V., Roy, A. K. (2012). Thermal properties of graphene: Fundamentals and applications. MRS bulletin, 37(12), 1273-1281.

Peter, C. N., Anku, W. W., Sharma, R., Joshi, G. M., Shukla, S. K., Govender, P. P. (2019). N-doped ZnO/graphene oxide: a photostable

photocatalyst for improved mineralization and photodegradation of organic dye under visible light. Ionics, 25(1), 327-339.

Rhazouani, A., Gamrani, H., El Achaby, M., Aziz, K., Gebrati, L., Uddin, M. S., Aziz, F. (2021). Synthesis and toxicity of graphene oxide nanoparticles: A literature review of in vitro and in vivo studies. BioMed Research International, 2021.

Rana, A., Qanungo, K. (2021). Orange G dye removal from aqueous-solution using various adsorbents: A mini review. Materials Today: Proceedings.

Rong, X., Qiu, F., Rong, J., Zhu, X., Yan, J., Yang, D. (2016). Enhanced visible light photocatalytic activity of W-doped porous g-C3N4 and effect of H_2O_2. Materials Letters, 164, 127-131.

Rajamanickam, D., Shanthi, M. (2016). Photocatalytic degradation of an organic pollutant by zinc oxide–solar process. Arabian Journal of Chemistry, 9, S1858-S1868.

Rabieh, S., Nassimi, K., Bagheri, M. (2016). Synthesis of hierarchical ZnO–reduced graphene oxide nanocomposites with enhanced adsorption–photocatalytic performance. Materials Letters, 162, 28-31.

Raliya, R., Avery, C., Chakrabarti, S., Biswas, P. (2017). Photocatalytic degradation of methyl orange dye by pristine titanium dioxide, zinc oxide, and graphene oxide nanostructures and their composites under visible light irradiation. Applied Nanoscience, 7(5), 253-259.

Ravi, K., Mohan, B. S., Sree, G. S., Raju, I. M., Basavaiah, K., Rao, B. V. (2018). ZnO/RGO nanocomposite via hydrothermal route for photocatalytic degradation of dyes in presence of visible light. Int J Chem Stud, 6(6), 20-26.

References

Rajput, V. D., Minkina, T., Fedorenko, A., Chernikova, N., Hassan, T., Mandzhieva, S., Burachevskaya, M. (2021). Effects of zinc oxide nanoparticles on physiological and anatomical indices in spring barley tissues. Nanomaterials, 11(7), 1722.

Resmi, R., Yoonus, J., Beena, B. (2021). A novel greener synthesis of ZnO nanoparticles from Nilgiriantusciliantus leaf extract and evaluation of its biomedical applications. Materials Today: Proceedings, 46, 3062-3068.

Rashid, A., Bhatti, H. N., Iqbal, M., Noreen, S. (2016). Fungal biomass composite with bentonite efficiency for nickel and zinc adsorption: a mechanistic study. Ecological engineering, 91, 459-471.

Siddiqi, K. S., ur Rahman, A., & Husen, A. (2018). Properties of zinc oxide nanoparticles and their activity against microbes. Nanoscale research letters, 13(1), 1-13.

Shahriari, S., Sastry, M., Panjikar, S., Raman, R. S. (2021). Graphene and Graphene Oxide as a Support for Biomolecules in the Development of Biosensors. Nanotechnology, Science and Applications, 14, 197.

Smith, A. T., LaChance, A. M., Zeng, S., Liu, B., Sun, L. (2019). Synthesis, properties, and applications of graphene oxide/reduced graphene oxide and their nanocomposites. Nano Materials Science, 1(1), 31-47.

Song, J., Wang, X., Chang, C. T. (2014). Preparation and characterization of graphene oxide. Journal of Nanomaterials, 2014.

Saratale, R. G., Saratale, G. D., Chang, J. S., & Govindwar, S. P. (2011). Bacterial decolorization and degradation of azo dyes: a review. Journal of the Taiwan institute of Chemical Engineers, 42(1), 138-157.

References

Sharma, A., Ahmad, J., Flora, S. J. S. (2018). Application of advanced oxidation processes and toxicity assessment of transformation products. Environmental research, 167, 223-233.

Shanmugasundaram, A., Boppella, R., Jeong, Y. J., Park, J., Kim, Y. B., Choi, B., Lee, D. W. (2018). Facile in-situ formation of rGO/ZnO nanocomposite: Photocatalytic remediation of organic pollutants under solar illumination. Materials Chemistry and Physics, 218, 218-228.

Shukla, P., Shukla, J. K. (2019). Fabrication of graphene-supported palladium nanoparticles-decorated zinc oxide nanorods for potential application. Journal of Superconductivity and Novel Magnetism, 32(3), 721-728.

Saratale, R. G., Saratale, G. D., Chang, J. S., & Govindwar, S. P. (2011). Bacterial decolorization and degradation of azo dyes: a review. Journal of the Taiwan institute of Chemical Engineers, 42(1), 138-157.

Sharma, M., Sondhi, H., Krishna, R., Srivastava, S. K., Rajput, P., Nigam, S., Joshi, M. (2020). Assessment of GO/ZnO nanocomposite for solar-assisted photocatalytic degradation of industrial dye and textile effluent. Environmental Science and Pollution Research, 27(25), 32076-32087.

Samsudin, E. M., Goh, S. N., Wu, T. Y., Ling, T. T., Hamid, S. A., Juan, J. C. (2015). Evaluation on the photocatalytic degradation activity of reactive blue 4 using pure anatase nano-TiO_2. Sains Malaysiana, 44(7), 1011-1019.

Sun, Q., Li, K., Wu, S., Han, B., Sui, L., Dong, L. (2020). Remarkable improvement of TiO_2 for dye photocatalytic degradation by a facile post-treatment. New Journal of Chemistry, 44(5), 1942-1952.

References

Siong, V. L. E., Lee, K. M., Juan, J. C., Lai, C. W., Tai, X. H., & Khe, C. S. (2019). Removal of methylene blue dye by solvothermally reduced graphene oxide: a metal-free adsorption and photodegradation method. RSC Advances, 9(64), 37686-37695.

Salhi, A., Tahiri, S., Khamliche, L., Aarfane, A., Jouali, A., Bensitel, M., & Krati, M. E. (2019). Photo-catalytic degradation of methylene blue in aqueous solution using TiO**2** supported on bovine bone powder by-product. Desalination and Water Treatment, 159, 356-364.

Sharma, P. K., & Pandey, O. P. (2021). Effect of processing parameters on structural and optical properties of CeO2 nanoparticles for the removal of crystal violet dye. Journal of Sol-Gel Science and Technology, 99(1), 75-91.

Singh, A., Chahal, S., Dahiya, H., Goswami, A., & Nain, S. (2021). Synthesis of Ag nanoparticle supported graphene/multi-walled carbon nanotube based nanohybrids for photodegradation of toxic dyes. Materials Express, 11(6), 936-946.

Saien, J., Delavari, H., & Solymani, A. R. (2010). Sono-assisted photocatalytic degradation of styrene-acrylic acid copolymer in aqueous media with nano titania particles and kinetic studies. Journal of Hazardous Materials, 177(1-3), 1031-1038.

Wang, Z., Hu, T., Liang, R., & Wei, M. (2020). Application of zero-dimensional nanomaterials in biosensing. Frontiers in Chemistry, 8, 320.

Wu, H., Lin, S., Chen, C., Liang, W., Liu, X., & Yang, H. (2016). A new ZnO/rGO/polyaniline ternary nanocomposite as photocatalyst with improved photocatalytic activity. Materials Research Bulletin, 83, 434-441.

References

Xiang, Q., Yu, J., & Jaroniec, M. (2012). Graphene-based semiconductor photocatalysts. Chemical Society Reviews, 41(2), 782-796.

Yu, Y., Huang, F., He, Y., Liu, X., Song, C., Xu, Y., & Zhang, Y. (2019). Heterogeneous fenton-like degradation of ofloxacin over sludge derived carbon as catalysts: Mechanism and performance. Science of the Total Environment, 654, 942-947.

Yaqoob, A. A., Umar, K., Adnan, R., Ibrahim, M. N. M., & Rashid, M. (2021). Graphene oxide–ZnO nanocomposite: An efficient visible light photocatalyst for degradation of rhodamine B. Applied Nanoscience, 11(4), 1291-1302.

Zhou, Q., Wen, J. Z., Zhao, P., & Anderson, W. A. (2017). Synthesis of vertically-aligned zinc oxide nanowires and their application as a photocatalyst. Nanomaterials, 7(1), 9.

Zhou, X., Shi, T., & Zhou, H. (2012). Hydrothermal preparation of ZnO-reduced graphene oxide hybrid with high performance in photocatalytic degradation. Applied surface science, 258(17), 6204-6211.

Zhang, L., Du, L., Yu, X., Tan, S., Cai, X., Yang, P., ... & Mai, W. (2014). Significantly enhanced photocatalytic activities and charge separation mechanism of Pd-decorated ZnO–graphene oxide nanocomposites. ACS applied materials & interfaces, 6(5), 3623-3629.

Zaaba, N. I., Foo, K. L., Hashim, U., Tan, S. J., Liu, W. W., & Voon, C. H. (2017). Synthesis of graphene oxide using modified hummers method: solvent influence. Procedia engineering, 184, 469-477.

Zhang, D., Dai, F., Zhang, P., An, Z., Zhao, Y., & Chen, L. (2019). The photodegradation of methylene blue in water with PVDF/GO/ZnO

composite membrane. Materials Science and Engineering: C, 96, 684-692.

Zhang, J., Su, C., Xie, X., Liu, P., & Huq, M. E. (2020). Enhanced visible light photocatalytic degradation of dyes in aqueous solution activated by HKUST-1: performance and mechanism. RSC advances, 10(61), 37028-37034.

الخلاصة :

يحتوي هذا العمل على جزأين رئيسيين:

يتضمن الجزء الأول تحضير أكسيد الجرافين (GO) بطريقة هامر المعدلة ، وتحضير جزيئات أكسيد الزنك (ZnO) النانوية بطريقة sol-gel وتحضير GO / ZnO nanocomposite بطريقة التحفيز الصوتي. دراسة خصائص المركبات النانوية باستخدام تقنيات مختلفة مثل حيود الأشعة السينية (XRD) ، وتحويل فورييه للأشعة تحت الحمراء (FTIR) ، والتحليل الطيفي للأشعة السينية المشتتة للطاقة (EDX) ، والمسح المجهري الإلكتروني (SEM) ، ومساحة السطح المحددة (BET) والحرارة تحليل الجاذبية (TGA). تم حساب حجم الجسيم للمركب النانوي المركب GO / ZnO باستخدام معادلة شيرر (23.769 نانومتر).

الجزء الثاني يتضمن دراسة النشاط التحفيزي الضوئي لمركب النانو المحضر باستخدام صبغة G البرتقالية. يتأثر معدل عملية التحلل الضوئي بمعلمات مختلفة مثل التركيز الأولي للصبغة ، وتأثير كتلة المحفز ، ودرجة الحموضة الأولية للمحلول ، وتأثير درجة الحرارة ، وتأثير شدة الضوء ، وتأثير CH3OH و H2O2. تم إجراء جميع التجارب تحت الظروف المثلى من (0.15 جم / 100 مل) من GO / ZnO nanocomposite، 10) مل / دقيقة) معدل تدفق الهواء. أفضل نسبة إزالة لصبغ البرتقال 97.33) G٪). تم دراسة تأثير تركيز الصبغة على القيمة المثلى لصبغة البرتقال G (10 مجم / لتر). شدة الضوء 9 ميجا واط / سم 2. الرقم الهيدروجيني = 8.7 ودرجة الحرارة 25 درجة مئوية وفي ظروف المختبر لصبغ البرتقال G. تم حساب طاقة التنشيط لعملية التحلل الضوئي باستخدام معادلة أرينيوس حيث كانت تساوي (35.35 كيلوجول/ مول) ويمكن تقدير الانتالبي والانتروبيا للتفعيل والطاقة الحرة للتنشيط وفقًا لمعادلة ايرنك. تم حساب المعلمات الديناميكية الحرارية (ΔH، ΔS) لصبغة G البرتقالية (32.88 كيلوجول / مول و - 0.164 كيلوجول / مول. كلفن)على التوالي ، من النتائج يكون التفاعل ماصًا للحرارة مع عشوائية منخفضة. تم حسابΔG (81.75 كيلوجول / مول) وكان التفاعل غير تلقائي.

جمهورية العراق
وزارة التعليم العالي والبحث العلمي
جامعة بابل / كلية العلوم للبنات
قسم الكيمياء

إزالة صبغة G البرتقالية باستخدام المتراكب النانوي GO / ZnO المحضر كمحفز ضوئي تحت إشعاع الضوء الشمسي

رساله

مقدمة الى مجلس كلية العلوم للبنات - جامعة بابل

كجزء من متطلبات نيل درجة الماجستير في العلوم / الكيمياء

تقدمت بها

هبة رزاق كاظم علوان

بأشراف

الاستاذ المساعد الدكتور حازم يحيى محمد علي

1444ه **2022م**